AD-A147 778 AFRRI (ARMED FORCES RADIOBIOLOGY RESEARCH INSTITUTE) ANNUAL RESEARCH REPO..(U) ARMED FORCES RADIOBIOLOGY RESEARCH INST BETHESDA MD 30 SEP 83 AFRRI-ARR-17 1/2

UNCLASSIFIED F/G 6/18 NL

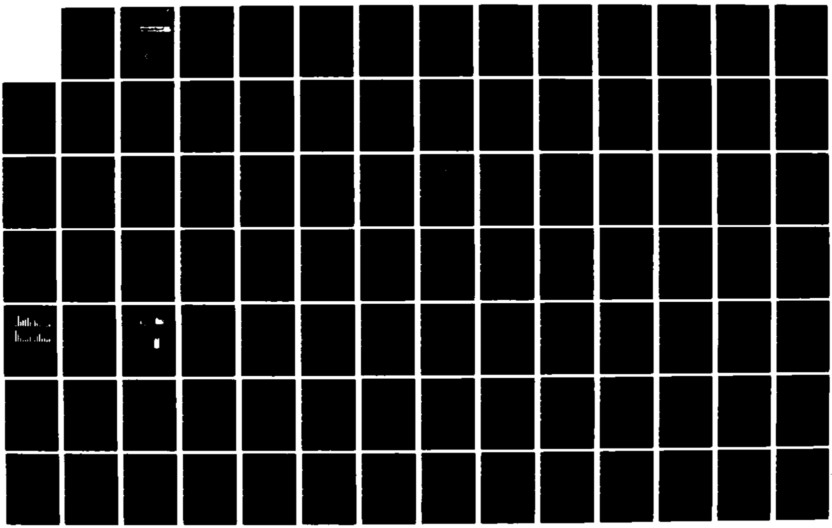

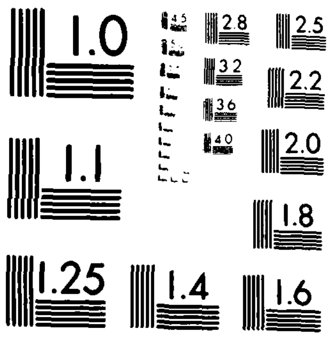

MICROCOPY RESOLUTION TEST CHART
NATIONAL BUREAU OF STANDARDS-1963-A

12

AD-A147 778

AFRRI

Annual Research Report

ARMED FORCES RADIOBIOLOGY RESEARCH INSTITUTE
DEFENSE NUCLEAR AGENCY

Approved for public release; distribution unlimited

UNCLASSIFIED

SECURITY CLASSIFICATION OF THIS PAGE (When Data Entered)

REPORT DOCUMENTATION PAGE	READ INSTRUCTIONS BEFORE COMPLETING FORM
1. REPORT NUMBER: ARR-17 — 2. GOVT ACCESSION NO.: AD-A149778	3. RECIPIENT'S CATALOG NUMBER
4. TITLE (and Subtitle): ANNUAL RESEARCH REPORT 1 October 1982 - 30 September 1983	5. TYPE OF REPORT & PERIOD COVERED
	6. PERFORMING ORG. REPORT NUMBER
7. AUTHOR(s)	8. CONTRACT OR GRANT NUMBER(s)
9. PERFORMING ORGANIZATION NAME AND ADDRESS: Armed Forces Radiobiology Research Institute (AFRRI) Defense Nuclear Agency Bethesda, Maryland 20814	10. PROGRAM ELEMENT, PROJECT, TASK AREA & WORK UNIT NUMBERS
11. CONTROLLING OFFICE NAME AND ADDRESS: Director Defense Nuclear Agency (DNA) Washington, DC 20305	12. REPORT DATE
	13. NUMBER OF PAGES: 190
14. MONITORING AGENCY NAME & ADDRESS (if different from Controlling Office)	15. SECURITY CLASS. (of this report): UNCLASSIFIED
	15a. DECLASSIFICATION DOWNGRADING SCHEDULE

16. DISTRIBUTION STATEMENT (of this Report)

Approved for public release; distribution unlimited.

17. DISTRIBUTION STATEMENT (of the abstract entered in Block 20, if different from Report)

18. SUPPLEMENTARY NOTES

19. KEY WORDS (Continue on reverse side if necessary and identify by block number)

20. ABSTRACT (Continue on reverse side if necessary and identify by block number)

This report contains a summary of the research projects of the Armed Forces Radiobiology Research Institute for the period 1 October 1982 through 30 September 1983.

CONTENTS

Introduction	1
Behavioral Sciences Department	5
Biochemistry Department	19
Experimental Hematology Department	65
Physiology Department	105
Radiation Sciences Department	129
Index to Principal Investigators	189

INTRODUCTION

The Armed Forces Radiobiology Research Institute was established in 1961 as a subordinate command of the Defense Nuclear Agency. It is the primary Department of Defense facility for scientific research in the field of radiobiology and related matters. It conducts applied and basic research that is essential for the operational and medical support of the Department of Defense. The work is carried out by five scientific departments as listed below:

Behavioral Sciences: Effects of ionizing radiation, chemicals, and drugs on performance.

Biochemistry: Elucidation of mechanisms of injury, repair, and protection from the effects of ionizing radiation alone or in combination with other agents; development of improved methods to detect and quantify the severity of radiation injury.

Experimental Hematology: Investigation of radiation injury of bone marrow; development of therapy for damage from intermediate radiation doses; determination and treatment of injuries caused by combined effects of radiation, blast, and burns.

Physiology: Research on cellular, tissue, and whole-animal models to determine physiological and biophysical changes resulting from radiation either alone or in combination with drugs or other chemicals.

Radiation Sciences: Operation, maintenance, and quality control of all AFRRI radiation sources; radiation dosimetry and estimation of tissue doses at various depths in different kinds of tissues; development and use of nuclear medicine and magnetic spectroscopic techniques for determining radiation damage in animals and model systems.

The results of this broad multidisciplinary program are summarized in this report. In addition, much of the work is published in the scientific literature, where it contributes significantly to the body of radiobiological knowledge, as well as in AFRRI scientific and technical reports.

BEHAVIORAL SCIENCES DEPARTMENT

The Behavioral Sciences Department conducts investigations assessing the effects of ionizing radiation, chemicals, and drugs on combat performance. This program encompasses a spectrum of multidisciplinary approaches in experimental animal models, ranging from operant conditioning techniques to methods used in physiological psychology, neurochemistry, and neurophysiology. The Department addresses the specific behavioral consequences of exposure to ionizing radiation, and explores the biological mechanisms responsible for radiation-induced behavioral decrements. Collaborative efforts are being pursued with other AFRRI departments, the Naval Research and Development Command, and the National Institutes of Health.

The Department has two Divisions: Experimental Psychology and Physiological Psychology. The Experimental Psychology Division uses behavioral and electrophysiological models to determine conditions under which ionizing radiation and militarily relevant chemicals can degrade combat performance. Behavioral tasks that model specific aspects of cognitive and physical combat performance are used to determine the radiation levels that affect combat effectiveness. The information from these studies is compiled into a data base that provides rapid retrieval, overall summary analyses, and development of extrapolated models applicable to battlefield conditions. Research in behavioral toxicology quantitates the changes in behavioral and neurophysiological capabilities due to exposure to chemicals and radiations that may be present in the military environment. This work uses a battery of tests designed to provide information on toxic dose levels and or mechanisms by which these environmental hazards affect behavior.

The Physiological Psychology Division explores the mechanisms by which ionizing radiation and chemical toxins disrupt behavior. Behavioral, physiological, and neurochemical approaches are predominant. This information can be used to develop methods of preventing performance decrement.

The results obtained from the research of this Department are disseminated to the military services and appropriate Government agencies by means of informal reports, committee assignments, working groups, and correspondence. Information is also transmitted through publication in the open scientific literature and through presentation at scientific meetings.

CHARACTERISTICS OF RADIATION-INDUCED PERFORMANCE DECREMENT USING A COMPLEX TWO-LEVER SHOCK AVOIDANCE TASK

Principal Investigators: W. F. Burghardt, Jr., and W. A. Hunt

Considerable interest has been expressed in defining the specific behavioral deficits caused by exposure to ionizing radiation in terms of the relative contributions of inability to physically perform a task, effect of task complexity, ability to correctly detect and use informational aids, and relative motivation to complete a task, and in terms of formulating a more useful definition of behavioral decrement. The following work suggests that the ability to perform coordinated movements after irradiation is often maintained in the absence of adequate task performance, whereas the number of responses made on different tasks may differ as a function of the particular task and the dose of radiation. Animal subjects can detect and use auditory and tactile stimulation as cues for responding, when these are provided, but will not anticipate their presentation.

Rats were trained on a two-lever task. Responding on the avoidance lever delayed the onset of electrical footshock for 20 sec for each response. Responding on the warning lever turned on a light for 60 sec, during which the task on the avoidance lever was changed from unsignalled avoidance to signalled avoidance. After 10,000 rads of cobalt-60 irradiation, subjects showed a decreased ability to avoid shock, which recovered only partially. The response rate on the avoidance lever remained at or above control rates, whereas the response rate on the warning lever showed an initial increase, followed by a decrease below baseline.

The data suggest that a subject will neither respond appropriately to avoid shock nor acquire cues that can facilitate the avoidance task in this situation. However, this does not reflect an inability to perform the required movements; instead, it reflects the demands of the tasks associated with each lever.

EFFECTS OF PROPYLENEGLYCOL DINITRATE ON MOTOR PERFORMANCE OF RATS

Principal Investigators: V. Bogo and J. Nold, *AFRRI*
F. A. Hill, *Naval Medical Research Institute, Bethesda, Maryland*

Propyleneglycol dinitrate (PGDN), a major constituent of the liquid propellant Otto Fuel II, is reported to cause incoordination, headaches, and impairment of balance in humans. This study was conducted to evaluate the rat as a model of PGDN-produced motor performance decrement, and to determine if direct application of PGDN onto neural tissue is a useful alternative to inhalation exposure.

PGDN was injected into the cisterna magna of adult Sprague-Dawley rats that had been trained to perform a test of motor coordination, the accelerod. Three groups of 13-14 male rats each received a single dose of either 5 or 10 microliters (µl) of PGDN or 25 µl of sterile saline (control) while anesthetized with halothane. Sufficient saline was added to the PGDN injection to produce a total volume of 25 µl. Performance on the accelerod was measured 12 min after recovery from anesthesia, then hourly for 6 hr, and again at 24 hr. Each injection was evaluated against a five-step screening criterion to eliminate grossly traumatized subjects, to verify the accuracy of the injection, and to determine the extent of mechanical damage.

Eighteen out of 41 subjects met the screening criterion. A significant decrease in performance was seen during the first 2 hr following the injection of 10 µl PGDN (Figure 1). These data confirm the previous findings of PGDN-produced changes in human motor performance, and they suggest that the rat may be a useful model for further PGDN neurobehavioral assessment. They also indicate that intracisternal injection is a reasonable alternative to inhalation exposure, if an evaluation screen is in force.

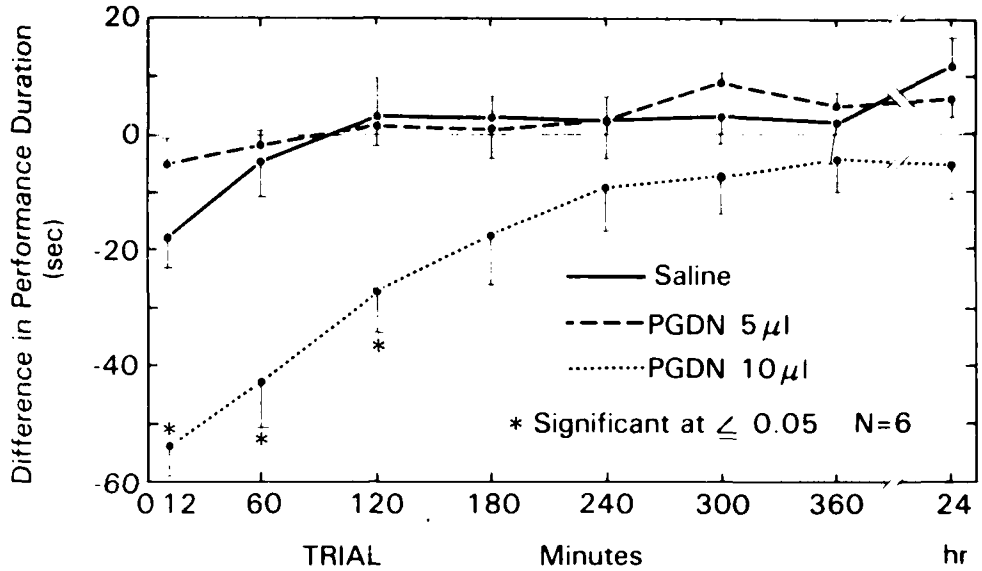

Figure 1. Performance of subjects treated with intracisternal injections of PDGN or saline. Decrement profiles are mean ± SE of difference between pre- and posttreatment performance duration. *Significant effects ($p < 0.05$).

EVIDENCE FOR ENDORPHIN-MEDIATED CROSS-TOLERANCE BETWEEN CHRONIC STRESS AND THE BEHAVIORAL EFFECTS OF IONIZING RADIATION

Principal Investigators: G. A. Mickley, *U. S. Air Force Academy, Colorado Springs, Colorado*
G. R. Sessions, V. Bogo, and K. H. Chantry, *AFRRI*

C57BL/6J mice exhibit a naloxone-reversible locomotor hyperactivity after exposure to ionizing radiation. These data implicate endogenous opiates in this radiogenic behavioral change. Similarly, endorphins mediate the analgesia produced by chronic stress (e.g., foot shock or restraint), and levels of plasma beta-endorphin are elevated following exposure to acute stress. Therefore, the present study sought to determine if behavioral cross-tolerance could be obtained between endorphin-producing stressors and radiation exposure.

Repeated pretreatment with foot shock or restraint subsequently inhibited the locomotor-activating effects of radiation (Figure 1). These data are consistent with the hypothesis that cross-tolerance develops between the effects of stress-induced endogenous opiate release and the radiation-induced release of endorphins.

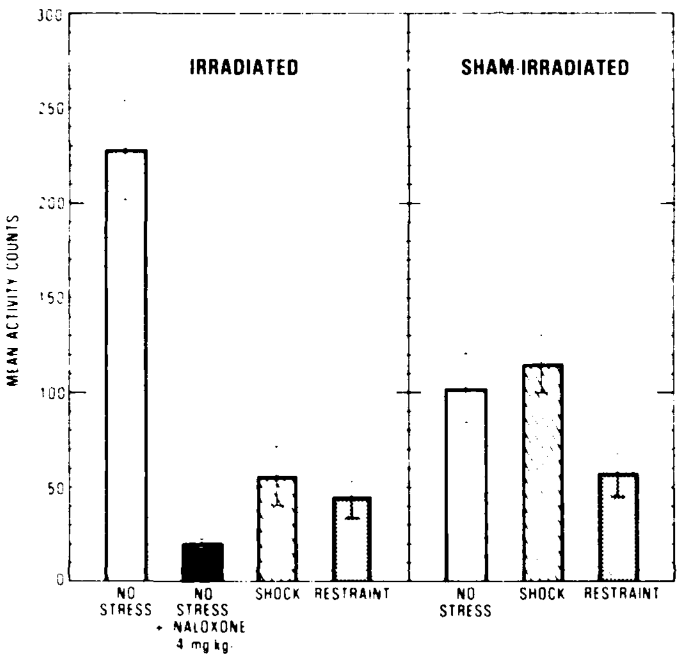

Figure 1. Mean cumulative locomotor activity counts in first and third 10-min time periods after irradiation or sham exposure. Variance indicators are SE of mean.

REDUCTION IN DOPAMINE METABOLISM IN THE CAUDATE NUCLEUS AFTER A HIGH DOSE OF IONIZING RADIATION

Principal Investigators: W. A. Hunt and T. K. Dalton

Behavioral decrement induced by ionizing radiation is expressed as reduced motor activity, lethargy, disorientation, ataxia, and an inability to avoid shock. Previous evidence from our laboratory has suggested that the reduced motor activity might be related to alterations in the activity of dopaminergic fibers in the caudate nucleus in the brain. Potassium-stimulated dopamine release from slices of caudate nucleus was increased during a period in which motor decrement is observed after exposure to ionizing radiation.

To gain further information on what occurs in dopaminergic neurons after irradiation, experiments were undertaken to determine whether the metabolism of dopamine was changed. Such measurements are an index of neuronal activity. Using a newly developed automated high-performance liquid chromatographic method, dopamine and its metabolites were quantified in several areas of the brain.

A 10-krad dose of high-energy electrons significantly reduced the metabolites of dopamine by 30 min after irradiation, specifically in the caudate nucleus. The effect was transient, with control values observed at 60 min after irradiation. The metabolism of norepinephrine and serotonin was unaltered in any of the brain areas studied.

These data suggest that the electrical activity of dopaminergic pathways in the caudate nucleus is reduced after exposure to ionizing radiation. This effect may play a role in the behavioral decrement that occurs under these experimental conditions.

ROLE OF THE AREA POSTREMA IN RADIATION-INDUCED TASTE AVERSION LEARNING

Principal Investigators: B. M. Rabin and W. A. Hunt
Technical Assistance: J. F. Lee

This work has utilized the conditioned taste aversion (CTA), which is produced by pairing a novel preferred solution with a toxic unconditioned stimulus so that the animal will avoid further ingestion of that solution at a subsequent presentation. This will serve as a behavioral marker to provide a means for understanding how exposure to sublethal levels of radiation (approximately 100 rads) can produce changes in behavior. Previous research (1) indicated that destruction of the area postrema, the chemoreceptive trigger zone for emesis, produces a significant attenuation of the CTA produced by exposure to ionizing radiation. Since these lesions also disrupt the emetic response to systemic toxins, two additional experiments were run to further clarify the role of the area postrema in mediating the behavioral changes resulting from exposure to nonlethal levels of ionizing radiation.

The first experiment of the series looked at the effects of area postrema lesions on the acquisition of taste aversions produced by partial-body exposures to ionizing radiation. The results indicated that body-only exposure to 100 and 200 rads produced significant aversions to a novel sucrose solution and that lesions of the area postrema prevented the acquisition of the aversion. Head-only exposures did not produce an aversion at a dose of 100 rads, but did produce a CTA at doses of 200 rads and 300 rads. In contrast to the body-only exposures, lesions of the area postrema in rats given head-only exposures resulted in only a partial attenuation of the CTA; the rats still showed a preference for the sucrose solution, but the preference was significantly reduced. These results were interpreted as indicating that (a) the acquisition of a CTA following body-only exposure is mediated by the area postrema, and (b) CTA learning following head-only exposure is mediated by both the area postrema and a mechanism that is independent of the area postrema.

In the second experiment, rats were given CTA training with the area postrema intact, and were tested for the recall of the CTA after lesions had been made in the area postrema. The results indicated that lesions of the area postrema had no effect on the recall of the previously acquired CTA. These results were interpreted as being consistent with the hypothesis that the role of the area postrema in CTA learning is to monitor blood and cerebrospinal fluid for potential toxins and to transmit that information to the central nervous system. This is consistent with the hypothesized role of the area postrema in emesis, since lesions here disrupt the emetic response to systemic toxins, but do not interfere with the emetic response to gastric irritation or to stimulation of the brain-stem emetic center.

REFERENCE

1. Rabin, B. M., Hunt, W. A., and Lee, J. Attenuation of radiation- and drug-induced conditioned taste aversions following area postrema lesions in the rat. Radiation Research 93: 388-394, 1983.

IONIZING RADIATION ALTERS FUNCTIONAL PROPERTIES OF VOLTAGE-SENSITIVE SODIUM CHANNELS

Principal Investigators: M. J. Mullin and W. A. Hunt
Technical Assistance: T. K. Dalton

An important mechanism in the control of neuronal excitability is the regulation of ion movements at the level of the excitable membrane. During excitation, sodium ions move into excitable cells through voltage-sensitive sodium channels. Fortunately, a number of neurotoxins exist that can be used as tools to study the structure and function of sodium channels. By measuring the rate of sodium ($^{22}Na^+$) influx in the presence of various neurotoxins, the functional properties of sodium channels can be assessed.

Previous work in our laboratory has shown that the influx of sodium ions caused by the toxin veratridine (VER) was significantly reduced by low doses of ionizing radiation (1). When whole-rat-brain synaptosomes were exposed to 100-10,000 rads of high-energy electrons, the VER-stimulated sodium influx was reduced in a dose-dependent fashion. Gamma radiation also reduced VER-stimulated sodium influx. The inhibitory effect of ionizing radiation appeared to be due to a reduction in the maximum effect of VER (2).

High-energy electrons (100-10,000 rads) did not significantly affect the scorpion venom-induced enhancement of VER-stimulated sodium influx (2). In addition, the inhibitory potency of tetrodotoxin to reduce toxin-stimulated sodium influx was unchanged by irradiation of synaptosomes. These results indicate that distinct sites in the sodium channels of synaptosomes differ in sensitivity to the effects of ionizing radiation. The central nervous system may be more sensitive to the direct effects of radiation than previously believed.

REFERENCES

1. Wixon, H. N., and Hunt, W. A. Ionizing radiation decreases veratridine stimulated uptake of sodium in rat brain synaptosomes. Science 220: 1073-1074, 1983.

2. Hunt, W. A., Wixon, H. N., and Mullin, M. J. Veratridine stimulated sodium uptake in rat brain synaptosomes is reduced by low doses of ionizing radiation. Seventh International Congress of Radiation Research, 1983, abstr. B1-09.

MILITARY APPLICATIONS ANALYSIS OF MONKEY INCAPACITATION DATA FROM THE BHS PRIMATE DATA BASE

Principal Investigators: R. W. Young, *Science and Technology Biomedical Effects Directorate, Defense Nuclear Agency*
S. G. Levin, C. G. Franz, and W. E. Jackson, *AFRRI*

In order to meet current requirements for input to the Army combat simulation models, incapacitation must be described by functional relationships that permit performance profiles to be determined over time postirradiation for a range of doses, neutron-to-gamma ratios, and physical task demands. To simulate the radiation environment on a battlefield, the AFRRI TRIGA reactor was used to deliver a single-millisecond dose between 1,000 and 18,000 rads in a field having a neutron-to-gamma ratio of either 4:10 or 3:1. The physical demands of the task were modeled using monkey performance of either a visual discrimination task or a physical activity wheel task. The data for this analysis were from 232 rhesus monkeys retrieved from the Behavioral Sciences Department (BHS) Primate Data Base.

Analysis of these data was accomplished by a four-step process. First, a postirradiation performance history was determined for each animal. Second, a probit line was fit for each minute postexposure for all groups. Third, curves for selected dose levels were further

analyzed, using a method of mathematical decomposition into distribution parameters for time of performance and incapacitation. Fourth, the distributions obtained from the decomposition were then used in a Monte Carlo analysis to produce typical postirradiation life histories for individuals exposed to a given dose. In this analysis, the probit fits provided the estimate of the relationship of dose to incapacitation as well as the statistical confidence for any predicted value of percent incapacitated. The probit fits also provided a means of calculating the curves of percent incapacitated versus time for any specific dose.

One result of the decomposition is a smoothed family of curves of percent incapacitated versus time (Figure 1). These families of curves provide estimates of the expected percentage of individuals incapable of performing their tasks due to behavioral incapacitation at a given dose and time postexposure. These curves can be used to define the times after irradiation when individuals would be incapacitated for various combat tasks. Combined with the individual profiles of performance decrement due to radiation sickness, these data can be used to provide a complete postirradiation history for each combat task.

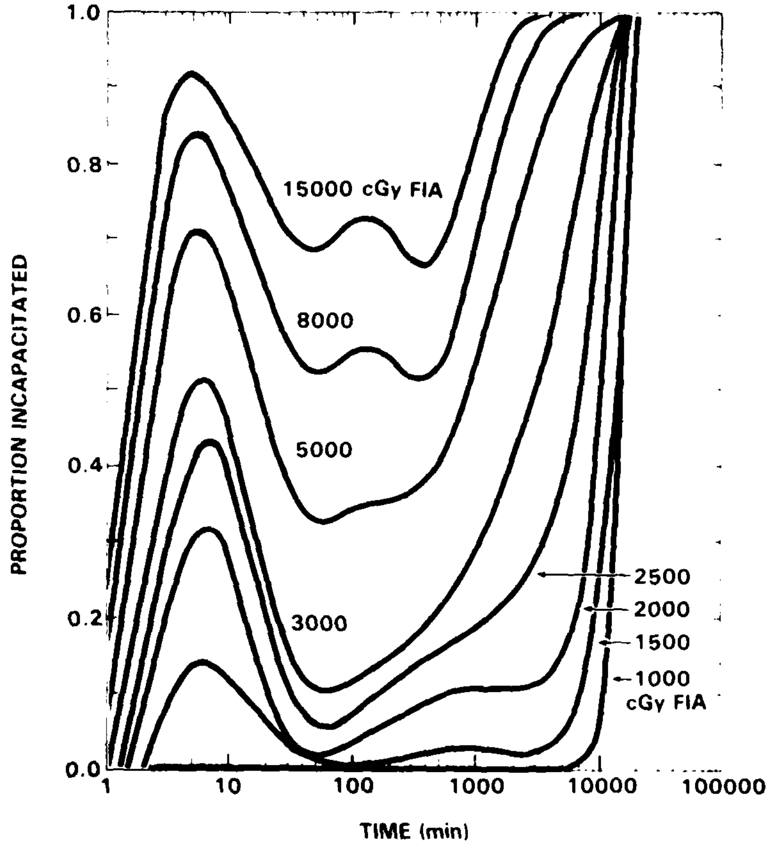

Figure 1. Smoothed proportion incapacitated versus time (min postirradiation) for visual discrimination task at 1000, 1500, 2000, 2500, 3000, 5000, 8000, and 15000 cGy free in air in the neutron/gamma = 4:10 field

BIOCHEMISTRY DEPARTMENT

The primary objectives of the Biochemistry Department have been (a) to develop an understanding of the biochemical interactions involved in the injury, repair, and protection mechanisms of mammalian systems exposed to radiation and other toxic agents, and (b) to develop reliable, sensitive, and easy-to-perform techniques to detect and assay the extent of radiation injury.

The Biochemistry Department is composed of the Physiological Chemistry Division, the Molecular Biology Division, and the Immunological Chemistry Division.

The Physiological Chemistry Division is primarily concerned with the identification and development of biochemical indicators of radiation injury. Major emphasis is placed on ascertaining the changes in serum glycoproteins, trace metals, and lipid peroxidation in response to radiation and chemical modifiers of radiation injury. The effects of radiation on the immune response also have been under investigation. The role of various immunostimulants alone or in combination with radioprotectant drugs in alleviating or preventing radiation-induced injury has been under extensive investigation. Various dietary adjuvants, such as vitamins E, C, and A, are being tested for their radioprotective properties. Experiments to assess the effects of ionizing radiation on bone and bone marrow formation also are under way.

The research objective of the Molecular Biology Division is the elucidation of the biochemical mechanisms of injury induced by toxic agents such as ionizing radiation either alone or in combination with toxic chemicals, with emphasis on commercially available anticholinesterase. Methods for more effective protection of the mammalian organism from the effects of these agents are under extensive investigation. Also under investigation are identification of the sequence of biochemical events leading to radiation-induced damage to cellular membranes and the role of various radioprotectants in preventing or alleviating this damage. Emphasis has been placed on the isolation and identification of natural radioprotectants. The effects of radiation on histamine and prostaglandin release and the mechanisms responsible for this release are being systematically investigated.

The Immunological Chemistry Division is concerned with the isolation of hematopoietic and progenitor cells and the measurement of their potential as a modifier of radiation-induced injury. The nature of interaction of stromal tissue with hematopoietic cells and its importance in postirradiation hematopoietic regeneration have also been investigated.

EFFECT OF SUBLETHAL DOSES OF ENHANCED NEUTRON IRRADIATION ON THE HEMATOPOIETIC SYSTEM OF THE RHESUS MONKEY

Principal Investigators: G. N. Catravas, R. L. Monroy, T. J. MacVittie, and J. H. Darden, *AFRRI*
L. Court, P. Gourmelon, and J. C. Mestries, *Centre de Recherches du Service de Santé des Armées, Clamart, France*

Exposure to ionizing radiation results in significant alterations of biochemical and physiologic parameters in the living organism. Previous experiments (1) have shown that the direction and magnitude of radiation-induced changes in brain cell constituents depend on the quality of radiation administered to the animal. As part of a study in which the effects of enhanced neutron radiation on the autonomic nervous system of the nonhuman primate was investigated following whole-body irradiation, a systematic study was performed to determine the radiation-induced damage and the rate of recovery of blood and bone marrow components.

Eighteen male rhesus monkeys, weighing between 3 and 3.5 kilograms, were used in this study. Following implantation of chronic electrodes in various regions of the brain to obtain an electroencephalogram, measure of cerebral blood flow, and other physiologic measurements, the subjects were allowed a 2-week period for recovery from surgery. Then the animals were exposed to whole-body radiation from the AFRRI TRIGA reactor at doses ranging from 0.5 to 4.5 grays (Gy), midline thorax dose. The neutron-to-gamma ratio was approximately 12 to 1 as measured by two 0.5-cubic-centimeter (cc) monitor ionization chambers calibrated by means of tissue-equivalent 50-cc plastic chambers using the pair-chamber method. Radiation doses were verified using sulfur activation analysis.

Prior to blood and bone marrow withdrawal, the animals were anesthetized with 0.5 ml (50 milligrams) ketamine (intramuscular) and 0.5 ml (20 mg) sodium thiamylal (intravenous). Blood was withdrawn from the leg vein by means of a heparinized syringe and needle. Bone marrow was aspirated from the iliac crest, using a special "bone marrow" needle attached to a 10-ml syringe containing 0.2 ml heparin (1000 units/ml). Three parameters (level of peripheral blood

granulocytes; differential profile of the bone marrow and granulocyte-macrophage colony-forming culture *in vitro* culture activity) were used to evaluate the degree of radiation damage and the subsequent recovery of the hematopoietic system after radiation doses of 0.5 to 1.0, 1.4, and 2.8 Gy.

Results thus far indicate that peripheral blood granulocytes decrease to a nadir by day 10 postirradiation and that the rate and degree of decrease are related to the radiation dose received. The peripheral blood granulocytes during the recovery phase increased in a linear manner to levels that were normal or above preirradiation values. However, the rate of recovery was found to be inversely proportional to the radiation dose received (Figure 1). Peripheral blood white blood cells and platelets were also found to decrease to a nadir between days 4 and 8 postirradiation, and the rate and degree of decrease were related to the radiation dose received. A rapid increase in their numbers was then observed to almost normal levels by days 10 to 16 postirradiation. The bone marrow differential profile of the 1.4-Gy and 1.8-Gy dose groups showed an almost complete depletion of the immature cells of the erythroid and myeloid series and a 90% reduction of the

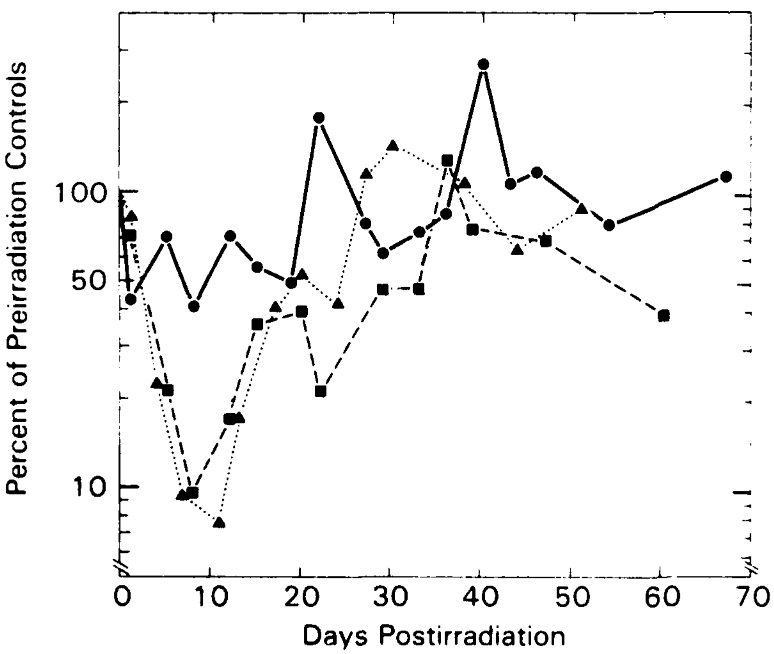

Figure 1. Recovery of peripheral blood granulocyte levels following exposure of animals to 0.58 (——), 1.40 (– – – –), or 2.80 (·······) Gy of neutron-enhanced radiation. Results are expressed as percent (%) of preirradiation controls.

lymphocyte population. In contrast, the bone marrow profile of the animals that received less than 1.0 Gy showed an increase of immature erythroid and myeloid cells to higher than the preirradiation levels. The granulocyte-macrophage colony-forming culture activity of the bone marrow, as measured on day 3-4 postirradiation, showed decreases with increasing radiation dose to 47%, 2.4%, and 0.7% of the preirradiation levels.

In the 2.8-Gy dose group, granulocyte-macrophage colony-forming culture activity was only 0.7% on day 3, but it increased to 49% by day 10. Subsequent evaluations of the bone marrow showed that the granulocyte-macrophage colony-forming culture activity decreased to 6.5% on day 20 but increased steadily to 59% by day 41 postirradiation. The observed transient increase in the granulocyte-macrophage colony-forming culture activity on day 10 preceded the observed increase in peripheral blood granulocytes (Figure 1). Preliminary evidence suggests that a similar transient activity occurred in the 1.4-Gy dose group on approximately day 5 and in the 1.0-Gy dose group on day 4. This observed transient activity in the bone marrow is reflected in the peripheral blood granulocytes and also the white blood cells and platelets. Thus, in the sublethal radiation doses, the monkey appears to meet the radiation-induced hematopoietic stress by recovering and activating its hematopoietic system. By comparing the rates of peripheral blood granulocyte recovery at different radiation doses (Figure 1), it appears that the greater the stress, the more rapid the response of the hematopoietic system to this stress.

REFERENCE

1. Catravas, G. N., and McHale, C. G. Changed activities of brain enzymes involved in neurotransmitter metabolism in rats exposed to different qualities of ionizing radiation. Journal of Neurochemistry 24: 673-676, 1975.

POSSIBLE ROLE OF HISTAMINE IN RADIATION-INDUCED HYPOTENSION IN THE RHESUS MONKEY

Principal Investigators W. A. Alter III, *Uniformed Services University of the Health Sciences, Bethesda, Maryland*
R. N. Hawkins, G. N. Catravas, T. F. Doyle, and J. K. Takenaga, *AFRRI*

To determine the possible involvement of histamine in radiation-induced hypotension, monkeys were irradiated with 4000 rads of cobalt-60. Ten chloralose-anesthetized animals (Group I) were pretreated with α-aminoquanidine (10 milligrams/kilogram) to inhibit histamine. Irradiation resulted in an immediate decrease in mean arterial pressure from 107 ± 4 to 53 ± 7 millimeters of mercury (mm Hg) within 2 min. Spectrofluorometric analysis of plasma histamine-like activity (H) indicated that irradiation resulted in an increase in H from 9.3 ± 0.8 to 187.3 ± 66.8 nanograms per milliliter (ng/ml) within 2 min. Decrease in mean arterial pressure was significantly correlated with the increase in H ($r = -0.76$).

Pretreatment of four monkeys (Group II) with 10 mg/kg of the H-receptor antagonists diphenhydramine and cimetidine did not alter preexposure values of mean arterial pressure and H.

Irradiation of Group II monkeys did not result in any immediate change in mean arterial pressure, but a dramatic increase in H to 275.9 ± 104.1 ng/ml was seen within 2 min. After a partial recovery in mean arterial pressure, a subsequent hypotensive response was recorded in Group I; however, this was not accompanied by an increase in H. Group II monkeys experienced a gradual decline in mean arterial pressure, which temporally coincided with this subsequent hypotensive response.

These results support the hypothesis that H is involved in the immediate decrease in mean aertial pressure, whereas the subsequent hypotensive response does not appear to be dependent on H.

RADIATION-INDUCED CARDIOVASCULAR DYSFUNCTION IN THE RHESUS MONKEY

Principal Investigators: R. N. Hawkins, T. F. Doyle, and G. N. Catravas, *AFRRI*
W. A. Alter III, *Uniformed Services University of the Health Sciences, Bethesda, Maryland*

Ten chloralose-anesthetized monkeys were irradiated with 4000 rads of cobalt-60. Preexposure values included mean arterial pressure of 107 ± 4 millimeters of mercury (mm Hg), heart rate of 179 ± 8 beats per minute, cardiac index of 188 ± 38 milliliters per minute per kilogram (ml/min/kg), central venous pressure of -0.38 ± 0.37 mm Hg, and total peripheral resistance (TPR) of 0.67 ± 0.12 TPR units. Preexposure values for cardiac contractility indices included left ventricular change in pressure with change in time (LVdp/dt) of 20.1 ± 1.1 and left ventricular and diastolic pressure (LVEDP) of 2.2 ± 0.6 mm Hg.

Irradiation resulted in an immediate disruption in cardiovascular function. Within 5 min, mean arterial pressure reached a minimum value of 50 ± 6 mm Hg, while cardiac index decreased to 104 ± 37 ml/min/kg, central venous pressure decreased to -1.28 ± 0.38 mm Hg, heart rate increased to 223 ± 10 beats per minute, and TPR decreased to 0.40 ± 0.10 TPR units. The contractility indices were also decreased at this time (LVdp/dt = 14.9 ± 3.8; LVEDP = -0.52 ± 0.789 mm Hg).

All parameters exhibited a transient although only partial recovery during the 15- to 45-min postirradiation period. This was followed by a subsequent decrease in all values except TPR, which returned to preexposure values and remained there for the remainder of the 90-min observation period.

Results from these experiments suggest a biphasic and differential response to irradiation by the cardiovascular system of the rhesus monkey. The immediate hypotension results from arterial vasodilation plus venous pooling. On the other hand, these data also show that the subsequent hypotensive response that begins approximately 30 min postirradiation results from venous pooling and decreased cardiac preload, while TPR remains at or near preexposure values.

PROSTAGLANDIN AND LEUKOTRIENE LEVELS IN RATS FOLLOWING COMBINED CHEMICAL AND RADIATION TREATMENT

Principal Investigators: T. L. Walden, G. N. Catravas, and L. K. Steel

The purpose of this study is to determine the effects of radiation on prostaglandins and leukotrienes in rats. In addition, this study will determine whether the effects of radiation on the leukotrienes and prostaglandins can be modulated by pretreatment with a radioprotectant (e.g., WR-2721) and a radiosensitizer (e.g., misonidazole).

Prostaglandins and leukotrienes are biological mediators for a diversity of processes, such as the contraction of smooth muscle in blood vessels and bronchial airways, and (as chemotactic factors) the attraction of white blood cells to an area during inflammation. Some of the effects of radiation on prostaglandin levels are known; however, no work has been published concerning radiation effects on leukotrienes. High-performance liquid chromatography procedures for measuring leukotrienes are available in the literature and have been adapted for use. Assay conditions were optimized late in the fiscal year 1983, and actual measurement of the treatment effects on biological samples will be conducted during 1984.

RADIOPROTECTION: VITAMINS, ENDOGENOUS PROTECTIVE SYSTEMS, AND LIPID PEROXIDATION

Principal Investigators: A. J. Jacobs and J. F. Weiss
Technical Assistance: W. A. Rankin, K. M. Hartley, and Y. Vaishnav

Vitamin E, as an integral part of the mammalian antioxidant defense system, appears to protect the body against various oxidative stresses, including chemicals, drugs, and ionizing radiation. The radioprotective role of vitamin E, particularly in relation to its antioxidant properties, has been demonstrated in cellular models or in studies on cells from animals deficient in vitamin E. Studies from our laboratory showed that the post-irradiation survival of CD2F1 male mice that had been fed a diet supplemented with three times the minimal dietary level of vitamin E was enhanced at radiation doses of 750 and 850 rads cobalt-60 (1). Investigation into the possible biochemical mechanisms of radio-protection by vitamin E included studies on hepatic enzyme systems that might be important in preventing oxidative damage resulting from radiation exposure. One of the major mechanisms for protection of cellular components from the deleterious effects of hydro-peroxides is via glutathione peroxidase. Hepatic cytosol glutathione peroxidase activity showed a reduction after irradiation, which was improved by the oral administration of a vitamin E suspension.

The nutritional relationship of vitamin E and selenium, with respect to their antioxidant activities, may be related in part to glutathione peroxidase activity and related enzymatic pathways (2). More survivors were seen in the group of CD2F1 mice allowed drinking water ad libitum containing 4 parts per million selenium as sodium selenite. However, the group of mice treated with both increased selenium and vitamin E showed a greater survival and less pronounced weight loss than groups on either treatment alone. The data suggest that vitamin E protects against glutathione peroxidase loss in the irradiated group, and that combined treat-ment appears to induce glutathione peroxidase activity and to protect against the loss of that activity (Table 1).

Table 1. Glutathione Peroxidase Activity in Tissues and Serum as Percent of Nonirradiated Control on Minimal Diet

Liver	0 rad	24 hr 900 rad	48 hr 900 rad	96 hr 900 rad
Control	-	-11	-24	-27
Vit E 10x	-26	-29	-27	-29
Vit E 3x	-12	- 8	-11	-15
Se 4 ppm	+72	+57	+56	+58
Vit E 10x, Se 4 ppm	+68	+69	+76	+76
Vit E 3x, Se 4 ppm	+65	+56	+57	+61
Kidney				
Control	-	-10	-16	-25
Vit E 10x	-11	-18	-15	-20
Vit E 3x	-13	-14	-14	-16
Se 4 ppm	+67	+55	+59	+58
Vit E 10x, Se 4 ppm	+66	+71	+70	+66
Vit E 3x, Se 4 ppm	+68	+51	+59	+55
Serum				
Control	-	-27	-24	-39
Vit E 10x	-34	-30	-32	-39
Vit E 3x	- 8	-15	-11	-19
Se 4 ppm	+19	-17	-11	-21
Vit E 10x, Se 4 ppm	+ 3	+ 9	- 4	- 3
Vit E 3x, Se 4 ppm	+14	+12	+ 7	+ 9

Current studies include the effects of dietary iron, zinc, and lithium on radiation injury. These elements, along with selenium, vitamin E, and other antioxidant vitamins, are being studied either alone or in combination with WR-2721, in an attempt to improve the radioprotective properties of WR-2721. Other current studies involve the development of *in vitro* techniques for determining the effects of antioxidants on radiation-induced lipid peroxidation, by head space analysis of volatile hydrocarbons evolved from incubating tissue homogenates.

REFERENCES

1. Srinivasan, V., Jacobs, A. J, Simpson, S. A., and Weiss, J. F. Radioprotection by vitamin E: Effects on hepatic enzymes, delayed type hypersensitivity, and postirradiation survival of mice. In: *Modulation and Mediation of Cancer by Vitamins.* Karger, Basel, 1983, pp. 119-131.

2. Jacobs, A. J., Rankin, W. A., Srinivasan, V., and Weiss, J. F. Effects of vitamin E and selenium on glutathione peroxidase activity and survival of irradiated mice. Proceedings of Seventh International Congress of Radiation Research. Broerse, J. J., Barendsen, G. W., Kal, H. B., and van der Kogel, A. J., eds. Martinus Nijhoff Publishers, Amsterdam, 1983, Abstr. No. D5-15.

RADIOPROTECTION: FREE-RADICAL INHIBITORS AND IMMUNOMODULATORS

Principal Investigators: J. F. Weiss and A. J. Jacobs
Technical Assistance: W. A. Rankin and Y. Vaishnav

Protection or stimulation of the immune system is an important aspect of radioprotection. Drugs with radioprotective properties (sulfhydryl derivatives, antioxidants) also may modulate immune responses in nonirradiated animals. Sodium diethyldithiocarbamate (DDC) is under investigation because of its immunoenhancing effects on cell-mediated responses, especially on T-lymphocyte responses.

In the present experiments, the effects of DDC on radiation-induced immunosuppression as measured by changes in delayed-type hypersensitivity and on survival of irradiated mice were compared to the protective effects of WR-2721, S-2-(3-aminopropylamino)-ethylphosphorothioic acid, which is currently the best available radioprotective drug (1). An *in vivo* method has been developed for assessing the effects of drugs on cell-mediated immunity in irradiated mice by measuring changes in delayed-type hypersensitivity to oxazolone. Mice were sensitized to oxazolone; 3 days later, the animals were treated with drugs and irradiated. Two days after irradiation, a challenge dose of oxazolone was applied to the outer side of one ear, and ear thicknesses (representing the inflammatory response due to delayed-type hypersensitivity to oxazolone) were measured at 24 and 48 hr after challenge.

Administration of either DDC or WR-2721 before irradiation resulted in increased survival of mice irradiated at doses near the $LD_{100/30}$ (lethal dose for 100% of animals after 30 days), indicating protection of hematopoietic cells. Comparison of WR-2721 and DDC at drug doses of a similar level of toxicity indicated that WR-2721 was superior in providing protection at higher radiation doses. DDC protected against radiation-induced immunosuppression as measured by the delayed-typed hypersensitivity response when administered at high doses (800 milligrams/kilogram), but protection was not as great as that afforded by WR-2721 at 200 mg/kg (Table 1). The data suggest that WR-2721 and DDC interact with cells involved in the delayed-type hypersensitivity response (lymphocytes and/or macrophages), and that these drugs may be useful in protecting against radiation-induced decrements in cell-mediated immunity.

Table 1. Effect of Diethyldithiocarbamate and WR-2721 on 24-Hour Delayed-Type Hypersensitivity Response in Mice

Treatment	Ear Thickness* (10^{-2} mm) (Mean ± S.E.)	Significance
CD2F1 (CR)†		
Nonirradiated Saline	20.3 ± 0.6 (32)§	Drug- versus saline-treated groups
WR-2721 (200 mg/kg)	20.0 ± 0.9 (16)	N.S.
WR-2721 (400 mg/kg)	19.0 ± 0.8 (16)	N.S.
DDC (200 mg/kg)	18.4 ± 0.8 (16)	N.S.
DDC (400 mg/kg)	17.7 ± 1.2 (16)	N.S.
DDC (800 mg/kg)	21.1 ± 1.0 (16)	N.S.
Irradiated (700 rad)		
Saline	8.4 ± 0.4 (32)	Drug- versus saline-treated irradiated groups
WR-2721 (200 mg/kg)	16.2 ± 0.4 (32)	$p < 0.001$
WR-2721 (400 mg/kg)	15.4 ± 0.5 (32)	$p < 0.001$
DDC (200 mg/kg)	9.9 ± 0.4 (32)	N.S.
DDC (400 mg/kg)	12.1 ± 0.4 (32)	$p < 0.001$
DDC (800 mg/kg)	13.3 ± 0.5 (32)	$p < 0.001$

* Ear thickness measurements: oxazolone-treated minus carrier-treated ears

† Data from two experiments

§ Numbers in parentheses = N

Other studies have surveyed the effects on the delayed-type hypersensitivity response of immunomodulators (C. parvum, pyran, poly ICLC, azimexon) and compounds affecting glutathione metabolism (buthionine sulfoximine, oxathiazolidine carboxylic acid). However, the greatest protective effects on the delayed-type hypersensitivity response in irradiated mice appears to be

given by a variety of sulfhydryl derivatives, and the comparative effects of equitoxic doses of potential sulfhydryl radioprotective agents is being determined. Other work involves the development of analytical methods for determining the concentrations of WR-2721 and its metabolite WR-1065 in biological fluids and tissues, using gas chromatography and gas chromatography-mass spectrometry.

REFERENCE

1. Weiss, J. F., Jacobs, A. J., and Rankin, W. A. Effects of diethyldithiocarbamate and WR-2721 on delayed-type hypersensitivity and survival of irradiated mice. Proceedings of Seventh International Congress of Radiation Research. Broerse, J. J., Barendsen, G. W., Kal, H. B., and van der Kogel, A. J., eds. Martinus Nijhoff Publishers, Amsterdam, 1983, Abstr. No. C1-37.

MECHANISMS OF RADIATION INJURY: SERUM PROTEINS AND OTHER CIRCULATING FACTORS

Principal Investigators: J. F. Weiss and A. J. Jacobs
Collaborator: P. B. Chretien
Technical Assistance: J. E. Egan, W. A. Rankin, and L. V. Seales

The consequences of acute-phase protein changes during various types of trauma have been considered (1). Evidence is increasing that host systemic immunity is the result of the interaction of circulating immune-reactive white blood cells and multiple serum factors. Serum proteins (other than immunoglobulins) change in concentration after various types of disease and injury, such as infectious diseases, inflammation, radiation injury, and malignancy. Many of these proteins have been referred to as either positive or negative acute-phase proteins or reactants, but little is known about the mechanism(s) that controls the acute-phase

response. Although specific proteins that increase or decrease in the acute-phase response have specific functions, experimental studies indicate that a general effect of acute-phase proteins is to modulate immunological responses occurring during different types of trauma. These experimental studies provide evidence that several of the acute-phase proteins may influence systemic immunity, suggesting that a more appropriate term for these proteins would be "immune-reactive proteins."

Studies on cancer patients showed that levels of certain serum proteins correlated with extent of disease, host immune status, and clinical course (2). Some of the acute-phase proteins that change to the greatest extent in cancer patients were found to correlate with parameters of cellular immunity. Serum levels of haptoglobin and α_1-acid glycoprotein correlated inversely, and α_2HS-glycoprotein correlated directly with lymphocyte reactivity to phytohemagglutinin. α_2HS-glycoprotein, and to a lesser extent prealbumin, correlated with immune status as measured by delayed-typed hypersensitivity to dinitrochlorobenzene, whereas serum levels of haptoblobin and α_1-acid glycoprotein were significantly higher in patients with abnormal skin test responses. Studies of patients undergoing radiotherapy indicated that further changes in serum proteins could occur that paralleled cellular immunosuppression. A study of effects of surgery also indicated an exacerbation of acute-phase protein changes along with a depression in lymphocyte levels due to surgical intervention. The utility of monitoring changes in proteins that parallel immunological changes has been demonstrated in human and animal studies in which immunotherapeutic measures were applied. For instance, changes in serum glycoproteins may reflect alterations in immunologic states due to treatment with thymic hormones (Figure 1).

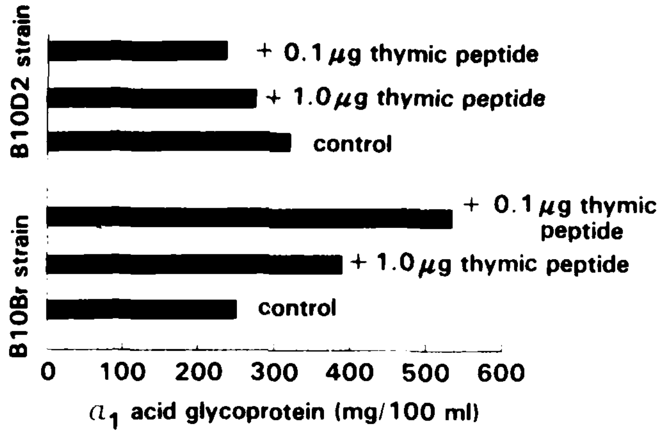

Figure 1. Effect of thymic peptide α-1 on serum α_1-acid glycoprotein in mice sensitive (B10Br) and insensitive (B10D2) to autoimmune thyroiditis

Our studies emphasize the importance of evaluating systemic immunity, compared to cellular immune parameters, for insight into clinically relevant aspects of host-disease relationships. Future studies should determine the most appropriate cellular and circulating factors that will define extent and aggressiveness of disease or injury, integrity of immunological defense capabilities, and impact of treatment for various types of trauma, including combined injury. In this regard, current studies are concentrating on changes in specific serum glycoproteins, such as α_1-acid glycoprotein, in experimental animals after radiation exposure and combined injury.

Studies on biochemical markers of radiation exposure in urine are continuing, with a concentration on changes in irradiated mice, including those treated with radioprotective drugs. Of importance to the study of biological markers is the finding that urine volumes do not increase after lethal or sublethal irradiation (cobalt-60) of mice, in contrast to the postirradiation diuresis observed with rats.

REFERENCES

1. Weiss, J. F., and Chretien, P. B. Acute-phase proteins and systemic immunity. In: Proceedings of the First International Symposium on the Pathophysiology of Combined Injury and Trauma. Walker, R. I., Gruber, D. F., MacVittie, T. J., and Conklin, J. J., eds. Kaman-Tempo, Santa Barbara, CA, in preparation.

2. Chretien, P. B., and Weiss, J. F. Clinical applications of acute phase proteins. In: Advances in Immunopharmacology 2. Hadden, J. W., Chedid, L., Dukor, P., Spreafico, F., and Willoughby, D., eds. Pergamon Press, Oxford, 1983, pp. 517-524.

PROSTAGLANDIN AND THROMBOXANE SYNTHESIS IN PARENCHYMAL LUNG TISSUES OF GUINEA PIGS EXPOSED TO AN ENHANCED NEUTRON FIELD

Principal Investigators: L. K. Steel and G. N. Catravas
Technical Assistance: I. K. Sweedler

The rationale for examining the cyclooxygenase products prostaglandin $F_{2\alpha}$ ($PGF_{2\alpha}$), prostaglandin E_2 (PGE_2), and thromboxane B_2 (TxB_2) in lung tissue postirradiation stems from earlier reports that ionizing radiation can induce lipid peroxidation (1) as well as alter arachidonic acid metabolism in a variety of animal tissues and body fluids (for review, see reference 2). Since prostaglandins are derived from arachidonic acid and have been demonstrated to participate in the regulation of pulmonary vascular and airway function as well as inflammatory reactions in tissues, alterations in the levels of these pharmacological mediators may play an important role in lung injury. Furthermore, prostaglandins may be a limiting factor in the use of whole-body irradiation for treatment of hematologic disorders, particularly in view of radiation toxicity to the pulmonary system (3).

The present investigation was undertaken to determine whether a different quality of ionizing radiation induces alteration in parenchymal lung tissue synthesis of $PGF_{2\alpha}$, PGE_2, and TxB_2, similar to that observed previously for cobalt-60 gamma radiation (1). Tissue capacity to generate prostaglandin in response to the exogenous addition of ionophore or histamine was also investigated.

Alterations were detected in prostaglandin and thromboxane synthesis in parenchymal lung tissues, resulting from a single total-body exposure to 0.5, 1.5, or 3.0 grays of neutron-enriched radiation. Tissues demonstrated radiation-induced alterations in their capacity to generate prostaglandin in response to histamine receptor stimulation or ionophore provocation of transmembrane divalent cation transport. Comparison of parenchymal lung tissue response to neutron-enhanced radiation with those observed following exposure to gamma radiation from a cobalt-60 source revealed dramatically different patterns of alteration (Figure 1). The biological response, as reflected in tissue prostaglandin synthesis, differed quantitatively and temporally for the two qualities of ionizing radiation. A radiation dose-response relationship in parenchymal lung tissue basal synthesis, previously seen with cobalt-60 exposure, was not observed following whole-body exposure to an enhanced neutron field.

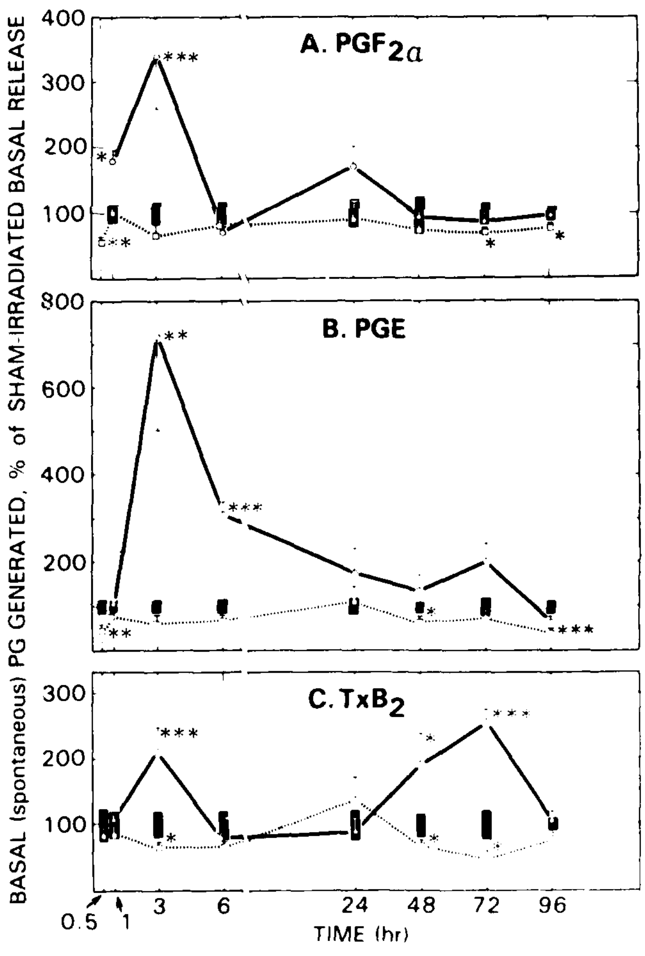

Figure 1. Basal prostaglandin and thromboxane levels in parenchymal lung tissues of guinea pigs exposed to cobalt-60 gamma radiation or neutron-enriched mixed field. Generation is expressed as percent of sham-irradiated (control) release at indicated times postirradiation. (■). Control values at each time. (—). 3.0 Gy cobalt-60 gamma radiation. (------). 3.0 Gy neutron-enriched radiation. Means ± SEM are given; SE indicated by vertical lines. Significantly different from sham controls: $^{*}p < 0.05$, $^{**}p < 0.025$, $^{***}p < 0.005$, N = 12.

A possible explanation for the differences in response observed between the two qualities of radiation could be the high density of ionization caused by neutrons when traveling through tissue, compared to that of gamma rays. Since exposure to ionizing radiation can result in secondary free radical formation, these free radicals could serve as substrates for intermediate endoperoxide formation. In fact, hydrogen peroxide has been demonstrated to stimulate cellular prostaglandin synthesis, and peroxide molecules have been shown to activate endoperoxide cyclooxygenase.

Hydroperoxide molecules have also been shown to stimulate (at low concentrations) or inhibit (at high concentrations) prostaglandin synthesis in endothelial cells and lung fibroblasts (4). Thus, we speculate that the degree of oxygen radical and peroxide formation may control prostaglandin synthesis in response to the two qualities of radiation.

REFERENCES

1. Wills, E. D., and Wilkinson, H. E. The effect of irradiation on lipid peroxide formation in subcellular fractions. Radiation Research 31: 732-747, 1967.

2. Steel, L. K., and Catravas, G. N. Radiation-induced changes in production of prostaglandins $F_{2\alpha}$, E, and thromboxane B_2 in guinea pig parenchymal lung tissues. International Journal of Radiation Biology 42: 517-530, 1982.

3. Gross, N. J. Pulmonary aspects of radiation therapy. Annals of Internal Medicine 86: 81-92, 1977.

4. Taylor, L., Monconi, M. J., and Polgar, P. The participation of hydroperoxides and oxygen radicals in the control of prostaglandin synthesis. Journal of Biological Chemistry 258: 6855-6857, 1983.

ISOLATION AND CHARACTERIZATION OF RADIOPROTECTIVE FACTORS FROM THE RADIORESISTANT ORGANISM *DEINOCOCCUS RADIODURANS*

Principal Investigators: M. R. Past and J. P. Christopher, *AFRRI*
Collaborator: D. R. Galloway, *Naval Medical Research Institute, Bethesda, Maryland*
Technical Assistance: D. Preston and J. E. Egan, *AFRRI*

A survey of the literature has revealed that several organisms are capable of surviving high doses of ionizing radiation. Among the radioresistant organisms are some members of the Deinococcus family of bacteria, including Deinococcus radiodurans. The extreme radioresistance of D. radiodurans may be due to several factors that differentiate this bacterial strain from radiosensitive strains of bacteria. Efficient deoxyribonucleic acid repair systems operate in this organism. Other investigators (1) have shown that a low-molecular-weight extract isolated from D. radiodurans conferred radioprotection on a radiosensitive strain of bacteria, Escherichia coli B/r, with a dose modification factor of 3.2. The chemical composition of the radioprotective extract has not been established.

Using a variety of techniques (including ultrafiltration, organic solvent fractionation, and Sephadex G-25 column chromatography), an extract from D. radiodurans has been resolved into a radioprotective fraction of approximately 1000 daltons. This radioprotective fraction has a spectral absorbance at 262 nanometers (nm), suggesting the presence of a nucleotide component. Studies have confirmed that this radioprotective fraction contains unidentified sulfhydryl compounds. It is known that the sulfhydryl compound coenzyme A and thioester derivatives of coenzyme A have spectral absorbances ranging from 259 to 263 nm.

Preliminary results obtained with high-performance liquid chromatography (HPLC) indicate a marked similarity in the chromatographic resolution of coenzyme A and the radioprotective fraction on a C-18 column monitored at 254 nm. However, the fraction from D. radiodurans was found to be a more effective radioprotectant than commercially available coenzyme A. Using equivalent amounts of free sulfhydryl, it was shown that the D. radiodurans fraction afforded fourfold greater protection to the E. coli B/r cells compared to coenzyme A. Studies are currently under way to specifically identify the sulfhydryl compound in

the radioprotective fraction using separation of monobromobimane derivatives of thiols on reverse-phase HPLC.

REFERENCE

1. Serianni, R. W., and Bruce, A. K. Role of sulphur in radioprotective extracts of Micrococcus radiodurans. Nature 218: 485-487, 1968.

ALTERATION IN CYCLIC AMP ACCUMULATION IN CULTURED LUNG TISSUES FROM GUINEA PIGS EXPOSED TO AN ENHANCED NEUTRON FIELD

Principal Investigators: L. K. Steel and G. N. Catravas
Technical Assistance: W. W. Wolfe

An accumulating number of *in vitro* and *in vivo* experiments suggest that cyclic nucleotides are important factors in determining the radiosensitivity of mammalian cells (1-3). Evidence indicates that the lungs may be a source of plasma cyclic adenosine-3',5'-monophosphate (cAMP) (4). The regulatory role of cAMP in the release of mediators and the magnitude of secretory responses have been amply demonstrated. Ionizing radiation alters cAMP levels in a variety of mammalian cells and tissues; however, the mechanism of radiation-induced changes as well as the relationship to expression of symptoms is unknown.

Based on our previous observations of radiation-induced alterations in prostaglandin synthesis in lung tissues and on reported findings (for review, see reference 5) of uncoupling of the relationship between prostaglandins and cAMP synthesis following exposure to ionizing radiation, we are investigating the extracellular accumulation of cAMP in cultured parenchymal lung tissues from guinea pigs exposed (whole-body) to 0.5, 1.5, or 3.0 grays of neutron-enhanced radiation.

The data suggest that increased cellular extrusion of the nucleotide is inversely correlated with radiation dose. This inverse relationship may be associated with increasing nucleotide hydrolysis secondary to increasing cyclic phosphodiesterase activity, decreasing cAMP production secondary to decreasing cyclase activity, decreasing cell membrane permeability to the nucleotide, or decreasing nucleotide substrate availability.

REFERENCES

1. Hess, D., and Prasad, K. N. Modification of radiosensitivity of mammalian cells by cyclic nucleotides. Life Sciences 29: 1-4, 1981.

2. Păusescu, E., Popescu, M., Păun, C., and Teodosiu, T. Dynamics of the changes in the tissular levels of cyclic AMP after cobalt-60 gamma irradiation. Strahlentherapie 151: 165-171, 1976.

3. Trocha, P. J., and Catravas, G. N. Variation in cyclic nucleotide levels and lysosomal enzyme activities in the irradiated rat. Radiation Research 83: 658-667, 1980.

4. Wehmann, R. E., Blonde, L., and Steiner, A. L. Sources of cyclic nucleotide in plasma. Journal of Clinical Investigation 53: 173-179, 1979.

5. Păusescu, E., Chirvasie, R., Teodosiu, T., and Păun, C. Effects of ^{60}Co gamma-radiation on the hepatic and cerebral levels of some prostaglandins. Radiation Research 65: 163-171, 1976.

POTENTIAL USE OF URINARY CYCLIC NUCLEOTIDES, PROSTAGLANDIN E_2, AND THROMBOXANE B_2 LEVELS IN EVALUATION OF ACUTE WHOLE-BODY EXPOSURE TO AN ENHANCED NEUTRON FIELD

Principal Investigators: L. K. Steel, G. N. Catravas, and
I. K. Sweedler

Whole-body exposure to gamma radiation from a cobalt-60 source was recently demonstrated to alter the urinary excretion of $PGF_{2\alpha}$, PGE_2, and TxB_2 in rats (1). The potential use of urinary constituents as non-invasive indicators of radiation exposure was extended in this study. The objectives were twofold: To determine quantitative changes in urine volume and constituents, and to correlate the measured changes with subsequent survival or death (assess their potential use as indicators of mortality) after whole-body exposure to an enhanced neutron field.

Urinary volume and radioimmunoassay measurement of urinary constituents [creatinine, cyclic nucleotides (cAMP, cGMP), PGE_2, and TxB_2] were determined on individual 24-hr collections from 32 guinea pigs, 7 days preexposure (baseline) and 7 days postexposure to 1.5 grays (Gy) neutron-enriched field (neutron-to-gamma ratio 17, gamma component less than 7%, tissue-to-air ratio 0.79, midline tissue dose 0.40 Gy/min). The surviving animals (14 of 32, more than 100 days) and those that died (18 of 32, mean survival 12.1 ± 0.7 days) had significant alterations in total (24-hr) urinary volume and PGE_2 excretion. In contrast, only those animals that ultimately died demonstrated significant changes in urinary cAMP, cGMP, and TxB_2 excretion, as well as delayed (days 6 and 7 postexposure) reductions in total urine volume. No differences were observed in urinary creatinine excretion rates.

These results support the following conclusions. In the guinea pig model, creatinine, cGMP, PGE_2, and TxB_2 excretion rates appear to be independent of urine volume, 1-7 days postexposure, regardless of animal survival. Mortality from acute, enhanced-neutron exposure is associated with the following urinary parameters: transient elevations in TxB_2 at 24 hr postexposure; transient reductions in PGE_2 (day 3) and TxB_2 (day 5) excretion; elevated urinary cGMP levels 4 days postexposure; and significantly reduced urine

volume, but elevated cAMP excretion, at 5-7 days after acute exposure to fission neutrons.

Animal survival is associated with the following urinary parameters: transient reduced urine excretion at 2 days postexposure; marked reductions in PGE_2 excretion rates at 3-5 days postexposure; and daily urinary excretion of cAMP, cGMP, and TxB_2 unaltered at 1-7 days postexposure.

These findings suggest that urinary volume, arachidonic acid metabolites, and cyclic nucleotide excretion rates may be useful indicators of morbidity resulting from acute exposure to fission neutrons, when medical intervention is not undertaken.

REFERENCE

1. Donlon, M., Steel, L., Helgeson, N., Shipp, A., and Catravas, G. N. Radiation-induced alterations in prostaglandin excretion in the rat. Life Sciences 32: 2631-2639, 1983.

INHIBITION OF DNA SYNTHESIS BY WR 2721

Principal Investigators: L. I. Giambarresi and G. N. Catravas
Technical Assistance: W. Murray

S-2-(3-aminopropylamino)-ethylphosphorothioic acid (WR 2721) is one of the most effective radioprotectants yet developed (1). However, little detail is known regarding its mechanisms of action in vivo. The regenerating rat liver is being used as an in vivo model system for gaining some insight into this mechanism. Specifically, the effect of WR 2721 on the peak of deoxyribonucleic acid (DNA) synthesis after a two-thirds partial hepatectomy was examined.

Two groups of five male F344 rats (160 grams body weight) were subjected to partial hepatectomy between the hours of 1700 and 1730. Thirteen hr after surgery, one group (Group 1) received WR 2721 by intraperitoneal (i.p.) injection at a dose of 200 milligrams per kilogram (mg/kg). The WR 2721 was dissolved in phosphate-buffered saline at a concentration of 40 mg/ml, filtered through a 0.22-micron Millipore filter, and used within 1 hr. The control group (Group 2) received i.p. injections of phosphate-buffered saline alone. An additional control group (Group 3) received neither partial hepatectomy nor injections. At 20 hr after surgery (the time point that corresponds to the peak of DNA synthesis after partial hepatectomy), all rats were given i.p. injections of tritiated thymidine at a dose of 0.1 microcurie/g body weight. Exactly 1 hr later, the rats were anesthetized with pentobarbital; the liver was removed and weighed, and a 0.5-g sample was taken from the median lobe. The samples were quickly frozen in liquid nitrogen and stored at -70°C for subsequent DNA extraction, quantitation, and determination of specific radioactivity.

As shown in Table 1, the administration of WR 2721 after partial hepatectomy resulted in a dramatic (tenfold) decrease in uptake of tritiated thymidine by liver DNA after partial hepatectomy (Group 1 versus Group 2). Indeed, a comparison of the DNA specific activities between Groups 1 and 3 indicates that WR 2721 reduced the level of DNA synthesis to almost pre-hepatectomy levels. Therefore, WR 2721 almost abolished the peak of DNA synthesis after partial hepatectomy. The liver weight of both groups of rats subjected to partial hepatectomy was found to be 33% of that in the nonhepatectomized group.

Table 1. Effect of WR 2721 on DNA Synthesis in Regenerating Rat Liver

Group	Treatment*	Body Weight (g)	Liver Weight (g)	dpm [^{3}H]/mg DNA
1	WR 2721	160.0 ± 4.5	2.25 ± 0.08	3,031 ± 1,745
2	PBS	158.4 ± 5.0	2.24 ± 0.10	32,128 ± 16,811
3	None	158.0 ± 6.3	6.78 ± 0.26	1,266 ± 400

All values expressed as means ± SEM of five rats per group.

*Treatment:

Group 1: WR 2721 in phosphate-buffered saline injected i.p. (200 mg/kg) 13 hr after partial hepatectomy

Group 2: Phosphate-buffered saline alone injected i.p. 13 hr after surgery

Group 3: Received neither partial hepatectomy nor injection

These findings are consistent with reports showing that DNA synthesis, both in vivo and in vitro, is inhibited by other sulfhydryl radioprotectants, such as cysteine, MEA, and AET (2). The data also lend support to the hypothesis that radioprotection in vivo is brought about, at least in part, by the ability of radioprotectants to reversibly inhibit DNA synthesis in order to allow a more complete repair of this critical target molecule to occur (3). This hypothesis is being examined in more detail, using the regenerating rat liver as an in vivo model system.

REFERENCES

1. Yuhas, J. M. Biological factors affecting the radioprotective efficiency of S-2-(3-amino-propylamino) ethylphosphorothioic acid (WR 2721). $LD_{50(30)}$ doses. Radiation Research 44: 621, 1970.

2. Goutier, R. Effects on cell growth processes (mitosis, synthesis of nucleic acids and of proteins). In: Sulfur Containing Radioprotective Agents, Chapter 7. Bacq, Z. M., ed. Pergamon Press, Ltd, Oxford, 1975, pp. 283-301.

3. Bacq, Z. M., and Goutier, R. Mechanisms of action of sulfur-containing radioprotectors. In: Recovery and Repair Mechanisms in Radiobiology, No. 20. Brookhaven Symposia in Biology, 1965, pp. 241-262.

ALTERATIONS IN STRUCTURE FUNCTION OF ACETYLCHOLINESTERASE INDUCED BY GAMMA RADIATION

Principal Investigators: J. P. Christopher, J. Speicher, and G. N. Catravas, *AFRRI*
D. B. Millar, *Naval Medical Research Institute, Bethesda, Maryland*

Acetylcholinesterase (AChE) is an enzyme that plays a pivotal role in nerve transmission, so its response to radiation is important to radiobiologists who are attempting to elucidate the mechanisms of performance decrement after exposure to ionizing radiation. An early report (1) indicated that bovine erythrocyte AChE was fairly radioresistant, in that more than 30% activity remained after exposure to 120,000 rads. However, this enzyme was of unknown purity. Furthermore, bovine erythrocyte AChE is an integral membrane protein and probably does not accurately reflect the situation at the synapse. Eel AChE, which is not an integral membrane protein and is available in pure form, was used in this study to evaluate its response to gamma radiation.

Solutions of eel AChE in test tubes were positioned in a 24-place plastic block with holes spaced to guarantee uniformity of absorbed dose. Samples were then exposed bilaterally at ambient temperature (22°C ± 2°) to gamma radiation from the AFRRI cobalt-60 source at a dose rate of 502 rads/min. Eel AChE exhibited a marked degree of radiosensitivity at a concentration of 1.8×10^{-8} molar (M) (5.2 nanograms/milliliter) in pH 7.3 phosphate buffer. Inactivation was essentially complete at 5000 rads, and exposure to just 250 rads under these conditions resulted in 27% loss of activity (Table 1).

Table 1. Dose Inactivation of Acetylcholinesterase

Dose (rads)	Remaining Activity (100%)
0	100.0
250	73.0
500	55.2
750	41.1
1000	29.7
2000	10.1
5000	0.6

There was no significant dependence of dose inactivation on pH in the range of 6.5 to 7.5. Variation in the ionic strength of the phosphate buffer (pH 7.3) that was used to dilute the enzyme preparation indicated that the enzyme was slightly more radiosensitive below 0.1 molar. Estimation of Michaelis constant (K_M) of maximum velocity (V_{max}) for both irradiated and control samples revealed that while V_{max} was altered, no change in K_M ($K_M = 1.4 \times 10^{-4}$ M) occurred. Molecular weight analysis of totally inactivated and control samples by sedimentation equilibrium resulted in a decrease from 315,000 daltons to 233,000 daltons in the apparent molecular weight, suggesting a fragmentation of the protein molecule. This conclusion is consistent with the initial qualitative findings of concentration gradient polyacrylamide gel electrophoresis of both samples.

Control AChE exhibited a major band at 400,000 daltons and two minor bands of lower molecular weight (less than 5%), whereas irradiated protein showed a diffuse staining pattern with a prominent area of less than 400,000 daltons and several bands of lower molecular weight. An attempt to correlate these structure/function alterations with progressive destruction of tryptophan residues, as occurs in the photodecomposition of AChE (2), showed no significant loss in content at 100,000 rads exposure but a loss of 30% tryptophan residues at 200,000 rads. This suggests that the early stages of inactivation by ionizing radiation are not dependent on the integrity of tryptophan residues.

Initial studies designed to identify the free radical species responsible for inactivation indicate that interaction of AChE with the hydroxyl radical is the most likely cause for loss of activity. These results used various combinations of nitrogen or nitrous oxide with t-butanol and oxygen with sodium formate. Finally, an indication of AChE's radiosensitivity in vitro to that in vivo was obtained by irradiating pieces of electroplax tissue and then extracting and assaying for residual activity. This approach showed that AChE in its native environment is severalfold more radioresistant than homogeneous enzyme irradiated in vitro. Specifically, greater than 80% activity remained after exposure of tissue to 200,000 rads.

These results indicate that eel AChE is more radiosensitive to gamma radiation than is bovine erythrocyte AChE in vitro. Although both enzymes appear to fragment and lose activity upon exposure, the inactivation of eel AChE can be significantly modified by its in vivo environment.

REFERENCES

1. Nayar, G. N. A., and Srinivasan, S. The effects of gamma radiation on solutions of acetylcholinesterase. Radiation Research 64: 657-661, 1975.

2. Bishop, E. H., et al. Photodestruction of acetylcholinesterase. Proceedings of the National Academy of Sciences of the United States of America 77: 1980-1982, 1980.

IDENTIFICATION OF A LOW-AFFINITY Ca,Mg-ATPase IN MAST CELL PERIGRANULAR MEMBRANES

Principal Investigators: L. M. Amende, M. A. Donlon, and G. N. Catravas
Technical Assistance: W. W. Wolfe

The mechanism by which radiation induces histamine release from mast cells in vivo remains unknown. However, increased intracellular calcium levels are sufficient stimuli to cause histamine release. Therefore, an analysis of the intracellular compartmentalization of the calcium pump enzymes was undertaken.

Perigranular membranes from rat peritoneal mast cells were isolated and analyzed for membrane marker enzymes (5'-nucleotidase, succinic dehydrogenase, monoamine oxidase, and glucose-6-phosphatase) and the calcium pump enzyme (calcium, magnesium-adenosine triphosphatase) (Ca,Mg-ATPase). Membrane marker enzyme analysis indicated minimal (3%) contamination with plasma membranes and mitochondrial membranes, with slightly higher contamination by Golgi membranes (10%). As shown in Figure 1A, the perigranular membranes were found to contain a low-affinity ATPase *maximally stimulated by 1 millimolar (mM) magnesium* or 5 mM calcium. Maximal activity (3 nanomoles inorganic phosphorus/minute/milligram protein) occurred at 1 mM ATP (Figure 1B). This enzyme activity was found to be insensitive to micromolar concentrations of vanadate, 2 mM ouabain, and 20 micrograms/milliliter oligomycin, although 5 mM n-ethylmaleimide inhibited activity by 40%.

This enzyme may function in maintaining calcium stores within the secretory granule.

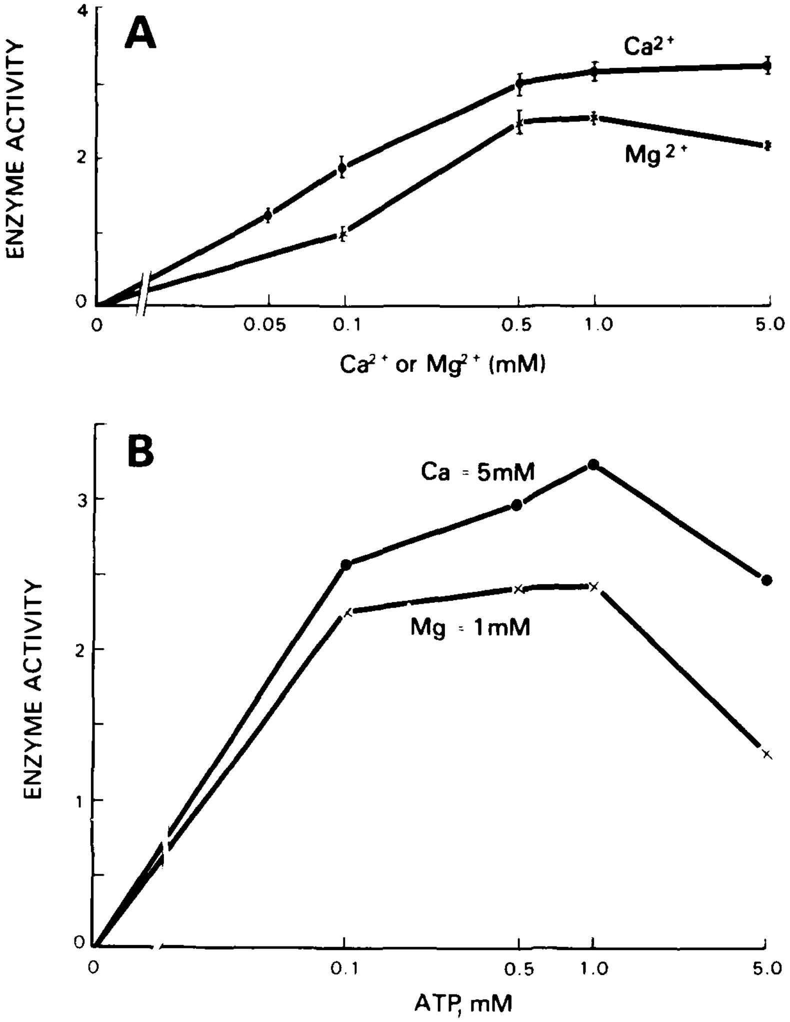

Figure 1A. Analysis of mast cell perigranular membranes for low-affinity Ca- or Mg-ATPase in presence of 1 mM ATP, 40 mM HEPES, pH 7.3. Enzyme activity in nmole/min/mg. Figure 1B. Variation in low-affinity ATPase activity of mast cell perigranular membranes with ATP concentration.

INCREASED URINARY EXCRETION OF HISTAMINE BY RATS FOLLOWING GAMMA IRRADIATION

Principal Investigators: M. A. Donlon, E. A. Helgeson, and G. N. Catravas
Technical Assistance: K. T. Lambright

Plasma histamine that circulates through the kidney is excreted intact into the urine (1). Therefore, measurement of histamine in the urine of laboratory animals can be used to monitor the fluctuations in plasma histamine that occur in response to radiation. Measurement of urinary histamine has several advantages over determining plasma histamine levels, as follows:

Stability: Histamine in the blood is rapidly degraded (half time = 0.5 min) by extremely active histaminases. Histamine in the urine is stable. It is not degraded even after incubation at 37°C, and it can be stored for long periods of time.

Elimination of biological variation: Urine from the same animal before and after irradiation can be monitored for short intervals (hourly collections postirradiation) or longer periods (up to 24 hr).

Sample size: As little as 1 milliliter is required for histamine analysis.

The effects of whole-body gamma radiation (9.0 Gy) from a cobalt-60 source on hourly and daily excretion rates of urinary histamine were monitored in female Sprague-Dawley rats. Animals were housed in individual metabolic cages. Authentic histamine (i.e., diamine oxidase degradable) was determined for each sample. The results are shown in Figure 1. Increased excretion of histamine in irradiated animals (compared to sham-irradiated) was first observed at 1 hr after irradiation. Urinary histamine levels continued to rise, with maximum excretion at 12 and 24 hr.

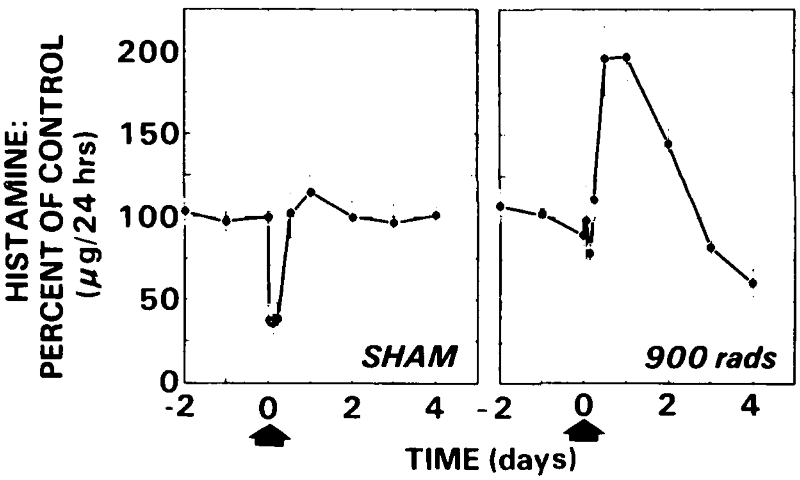

Figure 1. Urinary histamine excretion patterns in sham- and gamma-irradiated rats (n = 10)

These results demonstrate an early radiation-induced increase in excretion of urinary histamine following whole-body gamma radiation, which may reflect alterations in histamine release/metabolism in the irradiated animal.

REFERENCE

1. Myers, G., Donlon, M., and Kaliner, M. Measurement of urinary histamine: Development of methodology and normal values. Journal of Allergy and Clinical Immunology 67: 305-311, 1981.

ELECTRON PROBE MICROANALYSIS OF CALCIUM IN RAT PERITONEAL MAST CELL GRANULES

Principal Investigators: E. S. Chock, M. A. Donlon, and G. N. Catravas, *AFRRI*
C. E. Fiori, *National Institutes of Health, Bethesda, Maryland*
Technical Assistance: W. W. Wolfe, *AFRRI*

Mast cells contain preformed mediators that are stored within intracellular membrane-bound granules. These substances are released after stimulation of cell surface receptors by calcium-mediated exocytosis. With the objective of localizing calcium within these cells, we used electron probe microanalysis on purified rat peritoneal mast cells. In addition, isolated granules were examined for calcium, and comparisons were made between granules with perigranular membranes (M-granules) and membrane-free granules (MF-granules).

Calcium was precipitated in situ with 20 millimolar oxalic acid before routine embedding. Electron probe analysis (Figure 1) of granules in intact rat peritoneal mast cells revealed approximately tenfold higher calcium levels in granules compared to cytoplasmic levels. Calcium concentration within individual granules showed no marked concentration changes throughout the granule matrix. The isolated MF- and M-granules did not differ significantly in their calcium content.

Thus, the granule in the intact rat peritoneal mast cell contains calcium that is tightly associated with the granule matrix. The granule may function as an intracellular binding site for calcium as part of the mechanism in the maintenance of low cytoplasmic free-calcium levels.

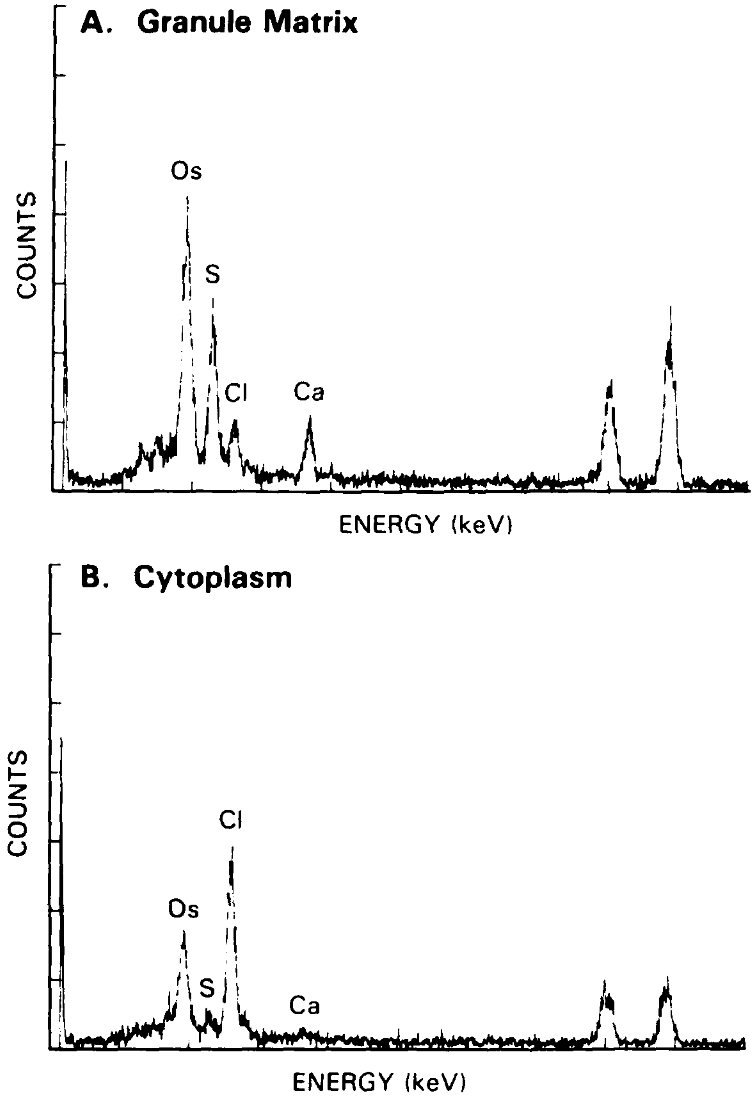

Figure 1. Comparison of calcium level in granule matrix and cytoplasm. (A) X-ray spectrum of granule matrix indicating presence of calcium. (B) X-ray spectrum of cytoplasm indicating low calcium content.

EARLY EFFECTS OF GAMMA RADIATION ON RAT KIDNEY FUNCTIONS

Principal Investigators: L. M. Amende, M. A. Donlon, and D. L. Kelleher
Technical Assistance: W. W. Wolfe

The effects of whole-body gamma radiation (9.0 Gy, cobalt-60) on water intake and renal function were examined in Sprague-Dawley rats. Water intake, specific gravity, osmolality, and urinary protein were monitored during the first 24 hr postirradiation. Rats were housed individually in metabolic cages. Urine was collected hourly for 3 hr and also at 6, 9, 12, and 24 hr following irradiation. All data were compared to sham-irradiated animals.

As shown in Figure 1, significant increases in water intake were observed at 2 hr postirradiation, with maximal increases occurring at 3 hr. Increased water intake continued for 24 hr. By 3 hr following irradiation, urine osmolality and specific gravity had decreased significantly, and maximal changes had occurred by 6 hr. Urine osmolality and specific gravity returned to sham-irradiated levels by 24 hr. Total urinary protein excretion was significantly greater by 2 hr in irradiated animals. The elevated urinary protein continued for 24 hr (4.05 ± 0.144 versus 2.04 ± 0.169 milligrams protein/24 hr).

These data indicate that radiation-induced alterations in kidney function occur within the first 3 hr following gamma irradiation.

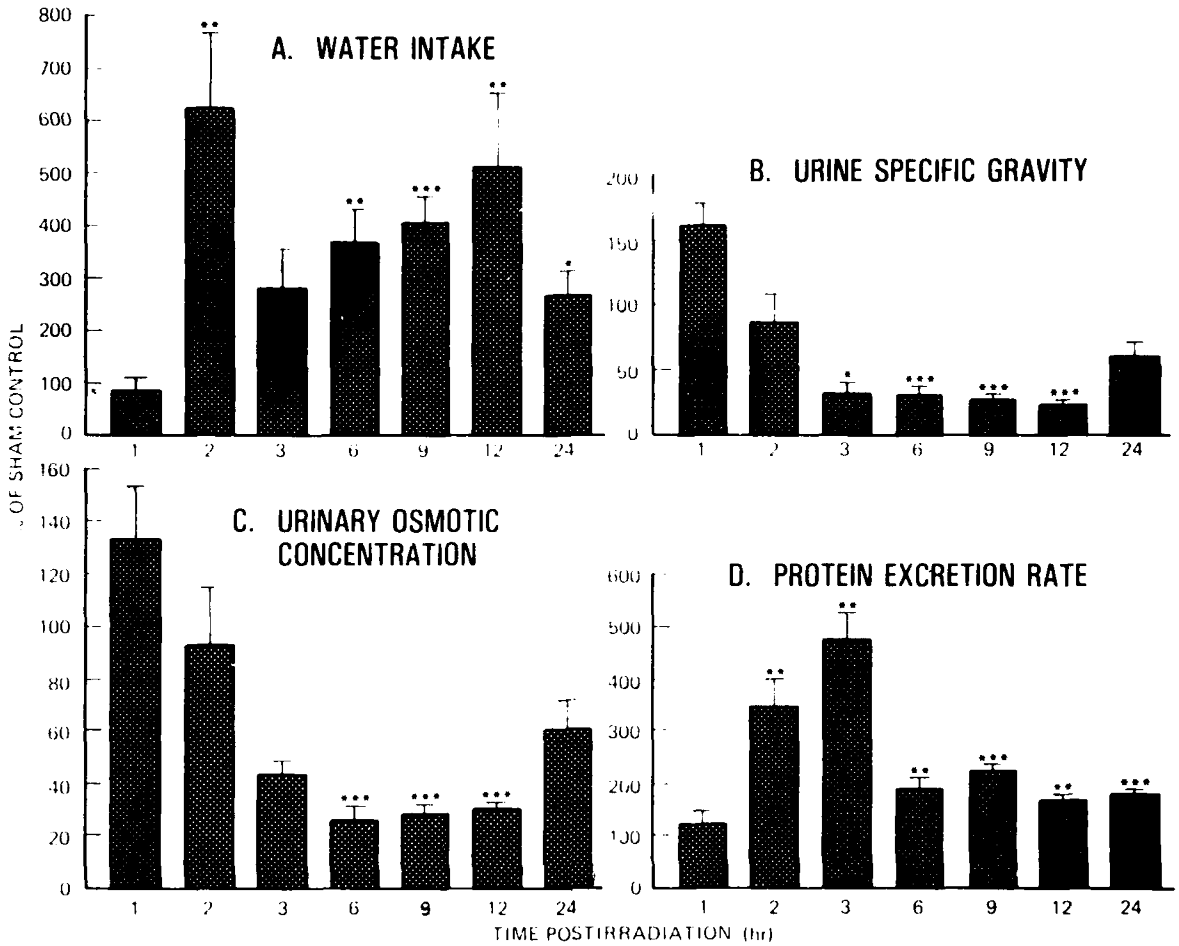

Figure 1. Variation in (A) water intake (ml/hr), (B) urine specific gravity (g/ml), (C) urine osmolality (mOsm/kg), and (D) urinary protein excretion (μg/hr) at various times after irradiation, expressed as percent of sham control values. Values plotted are means ± SEM of eight animals at each time point. Statistically significant differences compared with control: $*p < 0.05$, $**p < 0.01$, $***p < 0.001$.

RADIATION-INDUCED ALTERATIONS OF PROSTAGLANDIN AND THROMBOXANE EXCRETION IN THE RAT

Principal Investigators: M. A. Donlon, L. K. Steel, E. A. Helgeson, and G. N. Catravas
Technical Assistance: A. Shipp

Exposure to ionizing radiation induces subcellular biochemical and molecular alterations, which may result in cellular destruction. The biochemical changes that occur are often reflected as alterations in the composition of physiological fluids, which may be useful indicators not only of radiation injury but also of the extent of radiation exposure. The kidney is an important route for the elimination of endogenously derived biochemicals, and the analysis of substances in the urine of irradiated animals provides a noninvasive means for estimating radiation damage *in vivo*.

We have investigated the effects of whole-body gamma radiation on urinary prostaglandin excretion in rats. Animals were housed in individual metabolic cages, fed a bolus of food daily, and allowed water *ad libitum*. Animals in individual lucite cages were irradiated in groups of 10 using a cobalt-60 source. The urine was analyzed for prostaglandin E and thromboxane B_2 by radioimmunoassay. The results are shown in Figures 1A and B. Urinary prostaglandin E and thromboxane B_2 levels demonstrate dose-related increases in excretion rates following whole-body gamma irradiation. These changes suggest a potential use for these substances as biological indicators of radiation damage.

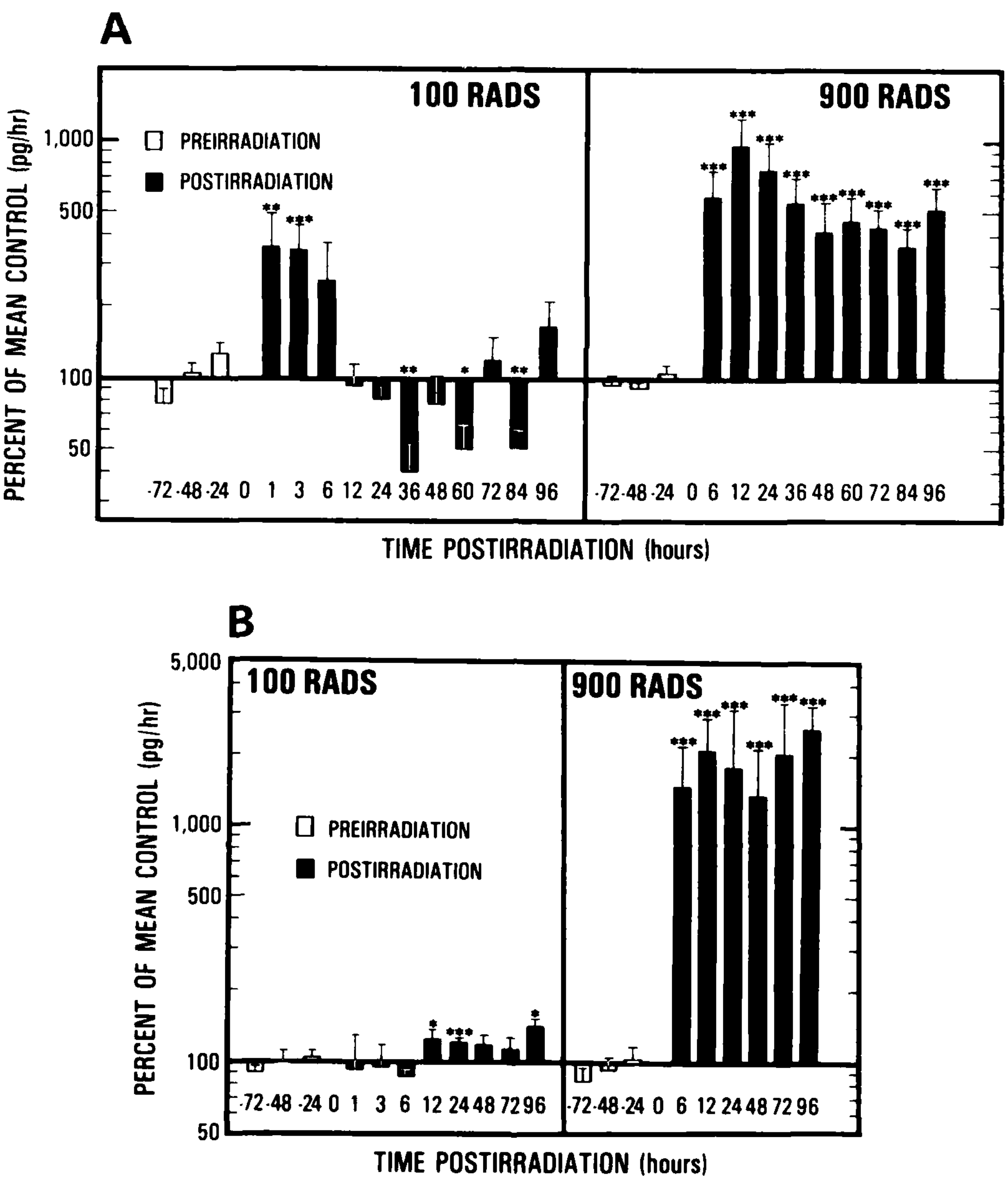

Figure 1. Urinary levels of thromboxane B_2 (A) and PGE (B) following gamma irradiation. Values represent geometric means (n = 10) in pre- and postirradiated urine samples. Error bars express antilogged mean plus 1 SEM. $*0.05 \geq p > 0.01$. $**0.01 \geq p > 0.001$. $***0.001 \geq p$.

EARLY KINETICS OF CALCIUM FLUXES AND HISTAMINE RELEASE IN RAT MAST CELLS STIMULATED WITH COMPOUND 48/80

Principal Investigators: D. E. McClain, M. A. Donlon, and G. N. Catravas
Technical Assistance: W. W. Wolfe

Radiation induces mast cell secretion, which is thought to play a role in early transient incapacitation. Mast cells contain the body's largest stores of peripheral histamine and more than 15 other chemicals that can exert pathophysiologic effects. As a part of our continuing study to understand the mechanism of radiation-induced histamine release, especially with regard to calcium (Ca^{2+}) metabolism, we measured the kinetics of Ca^{2+} uptake in rat peritoneal mast cells stimulated with a pharmacologic releasing agent, compound 48/80 (1).

Mast cells were purified to greater than 93% through an albumin gradient and preincubated for 30 min in 0.8 millimolar (mM) Ca^{2+} to re-equilibrate Ca^{2+} pools in the cells. Histamine release and Ca^{2+} fluxes were followed at 2-sec intervals beginning 3 sec after initial stimulation with compound 48/80 (1.0 microgram/milliliter) in 0.8 mM Ca^{2+}, using rapid mixing techniques and centrifugation through silicone oil to terminate the response. Ca^{2+} uptake during stimulation was determined by labeling the cell suspension buffer with $^{45}Ca^{2+}$. Histamine release was monitored fluorometrically.

The percent maximal response of histamine release and Ca^{2+} uptake versus the time after exposure to compound 48/80 is shown in Figure 1. Histamine release is completed by 12 to 14 sec, with half of the release completed by 5.7 sec ± 0.5 (mean ± SD, n = 10). Ca^{2+} uptake is completed by 18 sec, with half of the association occurring by 6.9 sec ± 0.7. The times of half-maximal response are significantly different (Mann-Whitney U test, $p < .002$). Ca^{2+} uptake from the external medium clearly occurs after initiation of the histamine release process, suggesting that at least the bulk of the Ca^{2+} that becomes associated with the cell after stimulation with compound 48/80 is not responsible for triggering the secretion process.

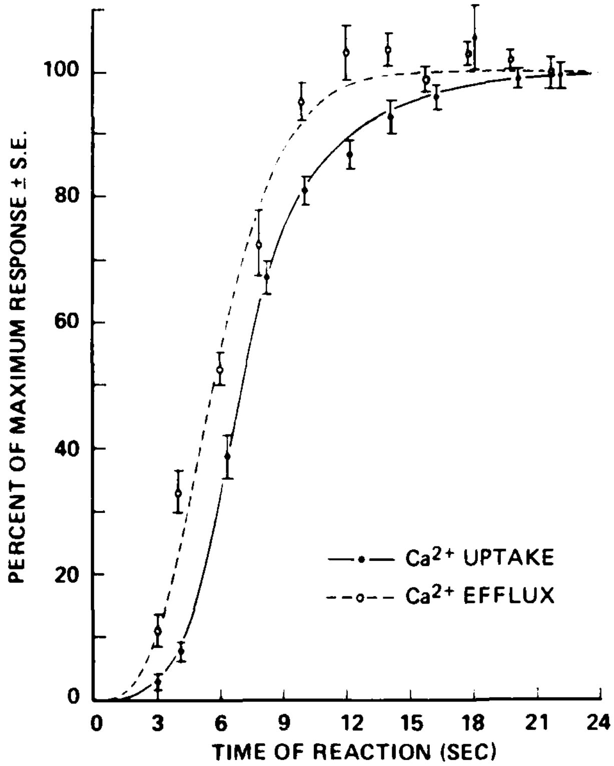

Figure 1. Simultaneous measurement of histamine release and Ca^{2+} uptake in mast cells incubated with 1.0 μg/ml compound 48/80. Cells incubated without secretagogue showed no net histamine release or Ca^{2+} uptake over time period shown. Each point represents mean ± SE of ten determinations.

REFERENCE

1. McClain, D. E., Donlon, M. A., and Catravas, G. N. Early kinetics of Ca^{2+} fluxes and histamine release in rat mast cells stimulated with compound 48/80. Federation Proceedings 42: 1821, 1983.

THE EFFECT OF GAMMA RADIATION ON MAST CELLS *IN VITRO*

Principal Investigators: D. E. McClain, M. A. Donlon, G. N. Catravas, and L. May
Technical Assistance: W. W. Wolfe

As an initial step in examining the effects of radiation on the secretory process, we studied the effects of gamma radiation on histamine release in the rat mast cell (1). Radiation damage was monitored by the measurement of spontaneous histamine release, trypan blue dye exclusion, membrane lipid fluidity, and the response of cells to a histamine-releasing agent, compound 48/80.

Purified cell suspensions were exposed to a range of gamma (cobalt-60) radiation up to 1000 grays (Gy) at 4°C. The effect of the radiation on the cells is shown in Figure 1. Spontaneous histamine release during irradiation was only slightly higher than that of controls. However, the histamine release response stimulated by compound 48/80 was inhibited in irradiated cells. Above 50 Gy, cells exposed to 1.0 microgram/milliliter compound 48/80 for 5 min at 37°C showed dose-related *inhibition of histamine* release, which diminished to 5.0% ± 0.5 at 1000 Gy (controls released 49.0% ± 0.1 of their histamine).

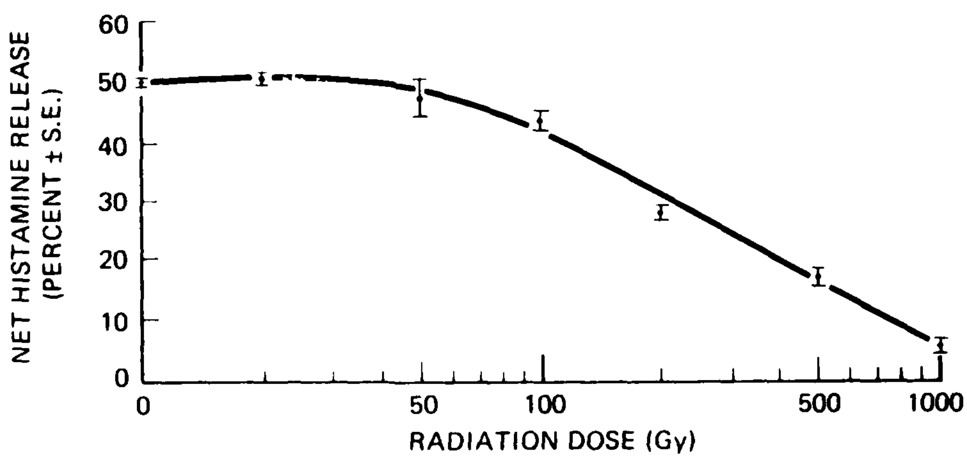

Figure 1. Irradiated cells were resuspended with normally aerated HBSS buffer (3×10^6 cells/ml). Aliquots (0.1 ml) of cell suspension were exposed to 1.0 µg/ml compound 48/80 for 3 min at 37°C. Reaction was terminated by addition of ice cold buffer. Net histamine release is defined as percent histamine released from 48/80-stimulated cells minus that released from controls.

The decreased response in irradiated cells does not appear to be related to a loss of cell viability since irradiated cells do not show either a significant increase in trypan blue uptake or a meaningful increase in spontaneous histamine release. Membrane fluidity was measured in irradiated cells using 16-doxyl stearic acid, a spin-label probe. No significant changes in electron paramagnetic resonance parameters were observed over the dose range, compared to controls.

The data demonstrate that gamma radiation (to 1000 Gy) does not induce spontaneous histamine release *in vitro*. Radiation above 50 Gy inhibits compound 48/80-stimulated histamine release. This phenomenon does not appear to be correlated with changes in cell viability or membrane fluidity.

REFERENCE

1. McClain, D. E., Donlon, M. A., Catravas, G. N., and May, L. The effect of gamma radiation on mast cells *in vitro*. *Federation Proceedings* 42: 1124, 1983.

CALMODULIN INHIBITION OF 48/80-STIMULATED HISTAMINE RELEASE IN THE RAT PERITONEAL MAST CELL

Principal Investigators: D. E. McClain, M. A. Donlon, S. Chock, and G. N. Catravas
Technical Assistance: W. W. Wolfe and K. T. Lambright

Histamine release by mast cells has been linked to postirradiation hypotensive effects and early transient incapacitation, but the mechanism is unknown. The mast cell in vitro is highly radioresistant. Therefore, it is thought that radiation leads to the abscopic production or release of agents that stimulate the mast cell to degranulate. Calcium is crucial to the histamine secretion process. Pharmacologic and immunologic agents that stimulate the noncytotoxic release of histamine from the mast cell produce an elevation of intracellular calcium, which triggers release. Much recent evidence suggests that the multiple functions of calcium (Ca^{2+}) in secretion involve calmodulin, an intracellular Ca^{2+}-binding protein thought to mediate many of the effects of Ca^{2+} in cellular processes.

In order to investigate the role of calmodulin in histamine secretion, purified mast cells were exposed to various concentrations of calmodulin in the presence of the histamine-releasing agents compound 48/80 and concanavalin A (1). Calmodulin alone does not lead to net histamine release by the mast cell. Calmodulin (10^{-9} to 10^{-5} molar) added to cells simultaneously exposed to compound 48/80 (0.3-2.0 micrograms/milliliter) induces a dose-related inhibition of histamine release with a 50% inhibition observed at $3\text{-}7 \times 10^{-7}$ M calmodulin. However, release stimulated by concanavalin A (50-100 μg/ml) was not affected by the same concentrations of calmodulin.

The mechanism by which calmodulin differentially affects histamine release by the two agents remains to be elucidated. Experiments show that calmodulin appears to interact specifically with the compound 48/80 receptor on the cell surface. It is not acting intracellularly, and it does not interact directly with compound 48/80. Calmodulin simultaneously inhibits histamine release and the Ca^{2+} uptake normally stimulated by compound 48/80. Calmodulin may serve as a useful tool to dissect the various steps in the release process.

REFERENCE

1. McClain, D. E., Donlon, M. A., Chock, S., and Catravas, G. N. The effect of calmodulin on histamine release in the rat peritoneal mast cell. Biochimica et Biophysica Acta 763: 419-425, 1983.

ESTABLISHMENT OF HEMATOPOIETIC MICROENVIRONMENT IN MATRIX-INDUCED ENDOCHONDRAL BONE

Principal Investigators: K. F. McCarthy and M. L. Hale, *AFRRI*
A. H. Reddi, *National Institute of Dental Research, National Institutes of Health, Bethesda, Maryland*
Technical Assistance: P. W. Jones III

The interrelationship between bone and bone marrow is not well understood. As indicated by the independent occurrence of hematopoiesis in yolk sac, fetal liver, and adult spleen, apparently no obligatory functional relationship exists between the two tissues. However, it is obvious that bone generates a special environment for hematopoiesis, for whenever true bone is formed, it generally leads to the development of new hematopoietic marrow.

The bone-associated factors generating this environment have not yet been identified. One experimental system that offers a unique opportunity for identifying and categorizing such factors is the matrix-induced endochondral bone-forming system (1, 2). In this system, the subcutaneous implantation of demineralized bone marrow results in the induction of endochondral bone and bone marrow reminiscent of embryonic long-bone development and morphogenesis.

Another experimental approach is the dissociative extraction of bone-associated proteins and the examination of these molecules for determining their support, differentiation, and mitogenic activity on rodent stem

cells in vitro. We have found that a 4-molar guanidine hydrochloride extract of bone matrix powder enhances hematopoietic stem cell survival in vitro. Specifically, one-half milligram of this protein extract increases the survival of hematopoietic stem cell culture in Medium 199 for 24 hr by a factor of 50 times over control values.

REFERENCES

1. Wientroub, S., Reddi, A. H., Hale, M. L., and McCarthy, K. F. Matrix-induced bone and marrow development: A model for postfetal hematopoiesis. Experimental Hematology 10 (Suppl. 19): 153-167, 1982.

2. McCarthy, K. F., Wientroub, S., Hale, M., and Reddi, A. H. Establishment of the hematopoietic microenvironment in the marrow of matrix-induced endochondral bone. Experimental Hematology, in press.

SECRETORY IGA, PEYER'S PATCHES, AND COMBINED INJURY: I. EFFECT OF SUBLETHAL IONIZING RADIATION ON RODENT PEYER'S PATCH LYMPHOCYTES

Principal Investigators: M. L. Hale and K. F. McCarthy
Technical Assistance: M. Tavens and P. W. Jones III

After exposure to sublethal doses of ionizing radiation, the regeneration of murine Peyer's patch lymphocytes was significantly slower than for lymphocytes from spleen, thymus, and peripheral lymph nodes. Long-Evans rats were exposed to 150 rads (40 rads/min) of whole-body irradiation from a cobalt-60, gamma-emitting source. On days 1-20 postirradiation, single cell suspensions of lymphocytes from thymus, spleen, peripheral lymph nodes, and Peyer's patches were

stained with monoclonal antibody reagents to detect Ia-positive cells, non-helper T-cells, and helper T-cells. Cells were then counterstained with Texas Red conjugated-F(ab')2 and were also stained with fluorescein diacetate to determine the viability of lymphocytes. The percentages of viable lymphocyte populations were analyzed using a dual-laser, fluorescence-activated cell sorter (Becton-Dickinson FACS-II).

We observed that viable lymphocyte populations in thymus, spleen, and peripheral lymph nodes from irradiated animals returned to normal levels (nonirradiated control animals) by 3-9 days postirradiation, whereas viable lymphocyte populations in Peyer's patches from irradiated animals remained suppressed for up to 20 days postirradiation. These results suggest that either the lymphocyte or, more likely, the microenvironment of Peyer's patches is more greatly damaged by ionizing radiation than that observed in other lymphoid tissue.

In addition, we have conducted studies on the effect of sublethal ionizing radiation on splenectomized rats (following the format described above). We found that the regeneration of Peyer's patch lymphocytes does not require a functioning spleen.

EXPERIMENTAL HEMATOLOGY DEPARTMENT

The Experimental Hematology Department investigates the effects of ionizing radiation and other militarily relevant stressors on the hematopoietic system. Emphasis is centered within three major categories of the Biomedical Effects Research Program: (a) the prevention and treatment of radiation effects, including radiation-induced hematopoietic dysfunction, medical and surgical therapy of combined effects, and radioprotectants; (b) the biomedical effects of fast neutrons; and (c) a technology base for experimental hematology and cellular radiobiology. Areas of research within these categories are organized within the framework of three Divisions in the Department: Hematology, Immunology, and Cellular Radiobiology.

The main objective of the Hematology Division is to delineate the mechanisms involved in regulation of the processes of proliferation and differentiation of the hematopoietic stem cell and its committed progeny in both granulocyte-macrophage and erythroid cell lines. Areas of research include

Enhancement of postirradiation recovery in stem and progenitor cell populations

Animal models for study of infectious disease and its effect on the hematopoietic system in normal hosts and irradiated hosts

Stem cell physiology, cellular regulation, and humoral regulation in the murine, canine, and monkey model systems

Early and late effects of gamma and neutron irradiation

Cellular and humoral hematologic and immunologic consequences of combined effects of ionizing radiation and traumatic injuries, and

Transplantation of bone marrow and peripheral blood cellular fractions that are capable of hematopoietic restoration in lethally irradiated large-animal species, such as the dog and monkey.

Experimental programs within the Immunology Division are aimed at the mitigation of gamma and neutron radiation-induced lymphomyelopoietic aplasia and its attendant cellular and humoral immune dysfunctions. Specific objectives include

- Novel applications of radioprotective agents

- Transplantation of bone marrow cells, and techniques to prevent graft-versus-host disease in the murine system

- Contributions of host intestinal microflora in irradiated animals

- Humoral control of the cellular immune and myelopoietic systems

- Lymphomyelopoietic alterations and mechanisms of action of wound trauma either alone or with radiation injury, and

- Cellular and humoral immune responses in the acute-phase reaction to inflammation and tissue injury in normal animals and irradiated animals.

The main objectives within the Cellular Radiobiology Division are to delineate the control of hemopoietic stem cell proliferation after exposure to ionizing radiation and to locate, identify, and quantitate radiation-induced or drug-induced DNA damage and to subsequently bring about its repair. Areas of research include

- Investigation of the relationship between cell proliferation and repair of molecular lesions produced by ionizing radiation

- Determination of the molecular basis of synergism between ionizing radiation and chemical agents

- Development of methodology for enhancing the proliferation of bone marrow stem cells post-irradiation, and

Investigation of, through biochemical and molecular approaches, the relationship between DNA damage and cell proliferation, including the chemical isolation of particular DNA lesions and the quantitation of its repair.

Attaining the research objectives or milestones within these projects will also add considerable information to fulfilling the military research requirements as recently published by the Army. They are the response of combat troops to nuclear radiation, the incidence of casualties from combined effects, and the biomedical effects of ionizing radiation. Specific requirements that have been identified include

Amount of biological repair (recovery) that occurs following exposure to nuclear radiation

Biological effects of cumulative exposure

Neutron relative biological effectiveness

Reliability of the extrapolation of large-animal models to man

Biological effects of combined injury, including the simultaneous insults and the sequential insults that the soldier may receive along with nuclear weapons effects, such as those associated with conventional and chemical munitions and the later development of sepsis, and

Mechanisms of biological damage to sensitive cells and the critical targets within them.

CANINE HEMATOPOIESIS IN A MODEL OF COMBINED INJURY

Principal Investigators: T. J. MacVittie, R. L. Monroy, D. F. Gruber, M. L. Patchen, and J. J. Conklin, *AFRRI*
M. P. Fink, *Naval Medical Research Institute, Bethesda, Maryland*

Collaborators: R. I. Walker and M. Smith, *NMRI*
G. Murano, *Bureau of Biologics, Food and Drug Administration*

Technical Assistance: J. L. Atkinson, B. Watkins, and T. A. Davis, *AFRRI*

Combined injuries are caused by two or more forms of energy. In the context of this paper, the primary form of energy is exposure to a sublethal dose of ionizing radiation. The combination of a subsequent sublethal exposure to mechanical or thermal trauma can change two individually sublethal events into a lethal response for the combined-injured host.

Combined injury, where one of the causes is ionizing radiation, presents another set of problems for the physician responding to a nuclear disaster or accident. A substantial sublethal exposure to gamma or mixed neutron-gamma radiation severely damages the hemopoietic system of mammals. Predisposition to bacterial sepsis by opportunistic pathogens and impaired wound healing are two of the major consequences of radiation-induced hemopoietic and immune suppression. Functional cells are decreased within days to critically low levels, and the precursor cells responsible for regeneration of mature cells may be depressed for weeks following sublethal doses of radiation.

The establishment of a canine model for radiation-induced aplasia and bacterial sepsis will allow us to investigate the mechanisms involved in mediating the cellular and humoral defense against sepsis in the irradiated and traumatized host. The large-animal model is also appropriate for assessing immunologic, pharmacologic, and surgical modes of intervention following combined injuries.

The canine model of combined injury at AFRRI has stressed three developmental aspects: (a) establishing the radiobiology of the canine hemopoietic system, (b) choosing a relevant peritoneal sepsis model, and (c) identifying several choices for trauma. This paper

stresses the relevance of the first aspect (that is, the radiation-induced suppression and recovery of the hematopoietic system) and also describes the fibrin clot sepsis model.

Purebred, male and female, young adult beagle dogs (9-12 kilograms) were used throughout this study. They were bilaterally exposed to cobalt-60 radiation at a dose rate of 0.6 grays (Gy) per min or neutron-gamma radiation from the AFRRI TRIGA reactor to a predetermined total midline absorbed dose. The neutron-gamma ratio free in air at the skin surface was approximately 6:1, which dissipates to approximately 1:1 at midline tissue with an average neutron energy of 0.8 mega electronvolts.

Experimental peritoneal sepsis was induced by placing an Escherichia coli-infected (2×10^8 organisms/kilogram) fibrin clot intraperitoneally (following initial laparotomy) in normal and irradiated dogs. A sterile clot was placed in control dogs.

Blood was withdrawn from the leg vein and bone marrow aspirated from the rib and iliac crest using heparinized syringes. Peripheral blood and bone marrow mononuclear cells were separated using Lymphocyte Separation Medium (LSM, Litton Bionetics, Kensington, Maryland). Granulocyte-macrophage (GM-CFC) and macrophage (M-CFC) colony-forming cells were assayed using the double-layer agar technique, and erythroid progenitors (CFU-e) were assayed using the plasma clot system.

The parameters measured were lethality, peripheral hematologic changes, D_0 (dose at which one third of subjects survive) values for GM-CFC and M-CFC, as well as recovery of the hemopoietic system following exposure to 1.5 Gy cobalt-60 or 0.75 Gy neutron-gamma radiation and its response to fibrin clot-induced peritoneal sepsis.

Lethality: Exposure to 1.5 Gy cobalt-60 radiation was sublethal for 100% of the dogs, while doses of 1.5 Gy and 1.25 Gy in the mixed neutron-gamma field resulted in approximately 85% and 67% lethality, respectively. Exposure to 0.75 Gy was 100% sublethal. D_0 values and relative biological effectiveness (RBE): Exposure of dogs over a dose range of 0.50 Gy to 3.50 Gy of either gamma or mixed neutron-gamma radiation resulted in significantly different D_0 values within GM-CFC and M-CFC populations. The results show D_0 values for gamma exposure of 0.73 Gy and 0.89 Gy for GM-CFC

and M-CFC, respectively. Exposure to mixed neutron-gamma radiation reduced these values to 0.30 Gy and 0.40 Gy, respectively. Calculated RBE value for GM-CFC was 2.4 and for M-CFC was 2.2. An approximate biologically equivalent dose for the 1.50-Gy cobalt-60 radiation was taken as 0.75 Gy for neutron-gamma exposure. Thus, hemopoietic recovery was determined in dogs exposed to 1.50 and 0.75 Gy gamma and neutron-gamma radiation, respectively. Equivalent recovery patterns were observed for each of these exposure doses.

E. coli sepsis in normal dogs produced a peak rise in peripheral blood leukocytes at 7 days postinfection, while platelet levels declined to levels less than 75% of normal through day 10, irrespective of surgical consequences and presence of a sterile clot. Bone marrow-derived GM-CFC increased significantly to values 270% of normal within 48 hr and then declined to values 200% of normal through day 10, followed by a slow decline to normal by 21 days postinfection and presence of a sterile clot. Peripheral blood-derived GM-CFC increased sharply to peak values nearly 9000% of normal 48 hr postinfection, then declined to levels 300% of normal by 96 hr, and remained elevated through day 14. A single dose of 1.50 Gy 4 hr before infection did not prevent the initial increase in peripheral blood leukocytes of peripheral blood leukocyte-derived GM-CFC (24-48 hr) but did eliminate the sustained increase seen with sepsis alone. Recovery of GM-derived GM-CFC and CFU-e were not significantly affected by E. coli infection postirradiation relative to irradiated-only values. A single 1.5-Gy dose and the selected E. coli dose are each nonlethal. The combined insult of irradiation plus sepsis (4-hr separation) is also nonlethal.

Additional studies are ongoing, using greater separation between the 1.5-Gy dose and time of infection. The E. coli fibrin clot technique is a good model for experimental peritoneal sepsis. The use of this technique in our canine radiation model will provide information on cellular and humoral mechanisms utilized in defense against bacterial sepsis in radiation-compromised hosts.

RELATIVE BIOLOGIC EFFECT: CANINE HEMOPOIETIC RESPONSE TO SUBLETHAL TOTAL-BODY IRRADIATION WITH COBALT-60 GAMMA OR MIXED NEUTRON-GAMMA RADIATION

Principal Investigators: T. J. MacVittie and R. L. Monroy
Collaborators: M. L. Patchen, J. H. Darden, and D. F. Gruber
Technical Assistance: J. L. Atkinson, B. Watkins, C. L. Feser, and L. D. Huff

Extensive studies have been performed on the radiobiology of the murine hemopoietic system. However, it is imperative that a reliable data base be collected on the effects of ionizing radiation on the hemopoietic system of larger mammals, such as the dog and nonhuman primate. Extrapolation of radiation effects across species lines is essential for determining a reliable human radiation response.

The advent of new culture techniques for assaying progenitor cells of the hemopoietic system has allowed us greater insight into the radiation-induced hemopoietic syndrome. The purpose of this long-range study is to determine the relative biological effectiveness (RBE) of cobalt-60 gamma or mixed neutron-gamma radiation on the proliferative ability of canine hemopoietic cells.

The parameters measured were lethality, peripheral hematologic changes, bone marrow cell differentials, D_0 (dose at which one third of subjects survive) values for granulocyte-macrophage (GM-CFC) and macrophage (M-CFC) colony-forming cells, as well as recovery of the hemopoietic system following sublethal exposures to 1.5 grays (Gy) cobalt-60 or 0.75 Gy neutron-gamma radiation.

Purebred, male and female, young adult beagle dogs (9-12 kilograms) were used throughout this study. They were bilaterally exposed to either cobalt-60 radiation at a dose rate of 0.1 Gy per minute or to mixed neutron-gamma radiation in the AFRRI TRIGA reactor at a dose rate of 0.6 Gy per min to a predetermined total midline absorbed dose. The neutron-gamma ratio free in air at the skin surface is approximately 6:1, which dissipates to approximately 1:1 at midline tissue with an average neutron energy at the surface of 0.8 mega electronvolts (MeV).

Blood was withdrawn from the leg vein and bone marrow was aspirated from the rib and iliac crest using heparinized syringes. Peripheral blood and bone marrow mononuclear cells were separated using Lymphocyte Separation Medium (LSM, Bionetics, Kensington, Maryland). GM-CFC and M-CFC were assayed using the double-layer agar technique, and erythroid progenitors (CFU-e) were assayed using the plasma clot system.

Lethality: Exposure to 1.5 Gy cobalt-60 radiation was sublethal for 100% of the dogs, while doses of 1.5 Gy and 1.25 Gy in the mixed neutron-gamma field resulted in approximately 85% and 67% lethality, respectively. Exposure to 0.75 Gy was 100% sublethal. D_0 values and RBE: Exposure of dogs over a dose range of 0.5 Gy to 3.5 Gy of either gamma or mixed neutron-gamma radiation resulted in significantly different D_0 values within GM-CFC and M-CFC populations (Table 1). The results show D_0 values for gamma exposure of 0.73 Gy and 0.89 Gy for GM-CFC and M-CFC, respectively. Exposure to mixed neutron-gamma radiation reduced these values to 0.3 Gy and 0.4 Gy, respectively. Calculated RBE values for GM-CFC was 2.4 and for M-CFC was 2.2. An approximate biologically equivalent dose for the 1.50-Gy cobalt-60 radiation was taken as 0.75 Gy for neutron-gamma exposure. Thus, hemopoietic recovery was determined in dogs exposed to 1.5 and 0.75 Gy gamma and neutron-gamma radiation, respectively. Equivalent recovery patterns were observed for each of these exposure doses.

Table 1. Radiosensitivity of Bone Marrow-Derived GM-CFC and M-CFC to Cobalt-60 or Mixed 0.8-MeV Neutron-Gamma Radiation: Relative Biological Effectiveness (RBE)

	GM-CFC		M-CFC	
	Cobalt-60	Neutron-Gamma	Cobalt-60	Neutron-Gamma
D_0 (rad)	73	30	89	40
RBE	2.4		2.2	

Peripheral Blood Leukocytes and Platelets: Nadirs were reached within 7 and 10 days, respectively. Peripheral blood leukocytes and platelets decreased to values 20%-30% of control, and required 6-7 weeks to return to within normal values irrespective of the exposure group. GM-CFC and M-CFC: Peripheral blood leukocyte-derived progenitors could not be detected within 24 hr after exposure. Ability to detect GM-CFC and M-CFC in the peripheral blood returned by day 14, and required 42 days to reach normal levels. GM-derived GM-CFC and M-CFC were reduced to levels approximately 10% of normal within 1 day, and returned gradually to normal levels over the next 29-35 days.

These data indicate a significant RBE for mixed 0.8-MeV neutron-gamma radiation in the canine hemopoietic system. Recovery of the hemopoietic system following biologically equivalent doses of radiation that reduce GM-CFC progenitors to levels less than 10% of normal required 4-6 weeks to reach preirradiation levels. The large-animal models described by R. L. Monroy et al. and G. N. Catravas et al. will provide a base from which further questions may be asked regarding the influence of quality and dose on combined injuries of radiation plus trauma and sepsis.

CANINE HEMOPOIESIS: RESPONSE TO EXPERIMENTAL *E. COLI* INFECTION IN NORMAL DOGS AND IN COBALT-60-IRRADIATED DOGS

Principal Investigators: T. J. MacVittie, M. L. Patchen, J. J. Conklin, and D. F. Gruber, *AFRRI*
M. P. Fink and R. I. Walker, *Naval Medical Research Institute, Bethesda, Maryland*

Collaborators: H. M. Gelston, *AFRRI*
G. Murano, *Bureau of Biologics, FDA*

Technical Assistance: J. Atkinson, B. Watkins, and T. Davis, *AFRRI*

Predisposition to bacterial sepsis by opportunistic pathogens is one of the major consequences of radiation-induced hemopoietic and immune suppression. The establishment of a canine model for radiation-induced aplasia and bacterial sepsis will allow us to investigate the mechanisms involved in mediating the cellular and humoral defense against sepsis in the irradiated and traumatized host.

Young adult male beagles (10-12 kilograms) were exposed to various doses of whole-body cobalt-60 radiation (bilateral at 10 rads/min) to determine the D_0 (dose at which one third of subjects survive) value for marrow granulocyte-macrophage colony-forming cells (GM-CFC). The chosen dose of 1.50 grays (Gy) reduced bone marrow-derived GM-CFC to values less than 10% of normal 24 hours after exposure. The calculated D_0 value for GM-CFC was 0.73 Gy. Experimental peritoneal sepsis was induced by placing an E. coli-infected (2×10^8 organisms/kg) fibrin clot intraperitoneally (following initial laparotomy) in normal and irradiated dogs. A sterile fibrin clot was placed in control dogs. The groups included (a) 1.50-Gy-irradiated only, (b) sepsis only, (c) sterile clot only, (d) 1.50 Gy + sepsis, and (e) 1.50 Gy + sterile clot. The parameters measured were peripheral blood leukocytes, platelets, plasma colony-stimulating activity, granulocyte-macrophage-derived GM-CFC, erythroid progenitors (CFU-e), and PBL-derived GM-CFC.

A single dose of 1.50 Gy whole-body irradiation significantly reduced all cellular parameters. Peripheral blood leukocytes and platelets were reduced to values 40% of normal within 5-10 days postexposure. Recovery of hemopoietic cells, GM-CFC, and CFU-e to normal values required approximately 28-35 days. E. coli sepsis in normal dogs produced a peak rise in peripheral blood leukocytes at 7 days postinfection,

while platelet levels declined to levels less than 75% of normal through 10 days, irrespective of surgical consequences and presence of a sterile clot. Bone marrow-derived GM-CFC increased significantly to values 270% of normal within 48 hr and then declined to values 200% of normal through 10 days, followed by a slow decline to normal by 21 days postinfection and presence of sterile clot. Peripheral blood leukocyte-derived GM-CFC increased sharply to peak values nearly 9000% of normal 48 hr postinfection, declined to levels 300% of normal by 96 hr, and remained elevated through 14 days.

A single dose of 1.50 Gy at 4 hr before infection did not prevent the initial increase in peripheral blood leukocytes or peripheral blood leukocyte-derived GM-CFC (24-48 hr), but did eliminate the sustained increase seen with sepsis alone. Recovery of GM-derived GM-CFC and CFU-e was not significantly affected by E. coli infection postirradiation relative to irradiated-only values. A single 1.5-Gy dose and the selected E. coli dose are each nonlethal. The combined insult of irradiation plus sepsis (4-hr separation) is also nonlethal.

Additional studies are ongoing, using greater separation between the 1.5-Gy dose and time of infection. The E. coli *fibrin clot technique* is a good model for experimental peritoneal sepsis. The use of this technique in our canine radiation model will provide information on cellular and humoral mechanisms utilized in defense against bacterial sepsis in radiation-compromised hosts.

CANINE HEMOPOIESIS: RESPONSE TO INFECTION WITH *E. COLI*

Principal Investigators:	T. J. MacVittie, M. L. Patchen, D. F. Gruber, and J. J. Conklin, *AFRRI*
	M. P. Fink, *Naval Medical Research Institute, Bethesda, Maryland*
Collaborators:	L. Casey, M. Smith, and R. Walker, *NMRI*
	G. Murano, *Bureau of Biologics, FDA*
	H. Gelson, *AFRRI*
Technical Assistance:	B. Watkins, J. Atkinson, and T. Davis, *AFRRI*

A model of peritoneal sepsis was needed in order to determine the mechanisms of the radiation- and trauma-induced predisposition to sepsis in the canine. Two models were selected, both involving an initial laparotomy followed by the injection of Escherichia coli (10 milliliters at 2 x 10^8 organisms/ml) into the wall of the large intestine, or the placement of freshly prepared fibrin clot containing the bacteria into an intraperitoneal space near the liver. The following results were obtained using the first model.

Control animals received an injection of saline or the placement of a sterile fibrin clot. The parameters measured were peripheral blood values (white cells and platelets), plasma content of colony-stimulating activity, acute-phase reactant (fibrinogen and C-reactive protein), bone marrow-derived granulocyte-macrophage colony-forming cells (GM-CFC), erythroid progenitors (CFU-e), and peripheral blood-derived GM-CFC.

Peripheral blood elements: A rise in peripheral blood leukocytes was observed to peak at 7 days postinfection and then decline to below normal levels by day 14. Platelet levels declined to less than 75% of normal through day 10, irrespective of surgical consequences.

Bone marrow: GM-CFC concentration declined during the initial 24 hr, rose sharply to values 270% of normal by 48 hr, and then declined to values 200% of normal through day 10 followed by a slow decline to normal by day 21 postinfection. CFU-e concentration declined significantly within 24 hr and then increased to values 150% of normal by 7 days.

Peripheral blood: GM-CFC increased sharply to peak values nearly 5000% of normal by 72 hr postinfection. These results, as well as those obtained from clinical measurements, will be compared with the fibrin clot approach in order to determine a valid model for canine peritoneal sepsis.

HEMOSTATIC CHANGES IN A CANINE MODEL OF COMBINED INJURY

Principal Investigators: G. Murano, *Bureau of Biologics, FDA*
T. J. MacVittie and J. J. Conklin, *AFRRI*
R. I. Walker, *Naval Medical Research Institute, Bethesda, Maryland*

Collaborators: L. Casey and M. Smith, *NMRI*

Based on the observation that hemorrhage is a frequent consequence of combined injury (i.e., blunt or penetrating trauma in association with burns, infection, and/or sublethal whole-body irradiation), an attempt was made to partially characterize the fluid phase status of the blood coagulation system in a canine model of combined injury.

In this report, we summarize data obtained in 16 dogs. Of these, two served as controls, three underwent laparotomy, two bowel resection, two splenectomy, one was exposed to 150 rads midline total-body (cobalt-60 gamma) radiation, two were irradiated (same as above) and splenectomized within 2 hr, and four were infected with a 10-milliliter bolus of E. coli at a concentration of 2 x 10^8/ml injected in the wall of the colon.

The observation (sampling) period ranged up to 28 days postintervention. All tests were calibrated and standardized using a three-dog plasma pool. The following determinations were made: Prothrombin time, partial thromboplastin time, thrombin time, reptilase time, fibrinogen, Factor VIII, antithrombin III (heparin cofactor), and FDP (fibrinogen/fibrin degradation products).

Although a substantial animal-to-animal variation was documented, results indicated that radiation alone (150 rads) did not significantly affect either the intrinsic or the extrinsic coagulation system. Infection with *E. coli* together with controlled surgical intervention [in the form of laparotomy, splenectomy (with or without radiation), or bowel resection] resulted in an increase (2-3 times) in the concentration of fibrinogen and Factor VIII, with the former peaking at about 3 days and the latter peaking erratically up to 7 days postintervention. The thrombin and reptilase times became concomitantly shortened. The concentration of antithrombin III was reduced only slightly at about 2 days. FDP were never elevated. Within approximately 10 days, all changes were normal.

These results reflect the lack of substantial activation of the coagulation-fibrinolytic system under the conditions described. They should serve as a basis for further development in establishing an appropriate model of combined injury.

NONSTEROIDAL ANTI-INFLAMMATORY DRUGS DECREASE RENAL BLOOD FLOW IN SEPTIC DOGS

Principal Investigators: M. P. Fink and L. C. Casey, *Naval Medical Research Institute, Bethesda, Maryland*
T. J. MacVittie, *AFRRI*

It is well established that nonsteroidal anti-inflammatory drugs (NSAID) protect experimental animals from endotoxic or septic shock, but there are several reports of these agents causing acute tubular necrosis in patients. Therefore, we studied the effect of NSAID on renal function in a canine peritonitis model.

Chronic arterial and Swan Ganz catheters were placed in eight beagles. After recovering for 3-4 days, baseline clearances of insulin (C_{in}) and paraaminohippurate (C_{PAH}) were measured. Hematocrit was measured to allow the calculation of renal blood flow. Peritonitis was induced by implanting an E. coli-infected fibrin clot in the peritoneum. Clearance studies were repeated 24 hr later (septic period). An intravenous injection of either indomethacin (2 milligrams/kilogram, n = 3) or ibuprofen (25 mg/kg, n = 5) was given; 1 hour later, clearance studies were repeated (post-drug period). All studies were performed in conscious animals after resuscitation to a wedge pressure of 6 torr.

Table 1 shows clearance data (mean ± SE). Since the effects of indomethacin and ibuprofen were similar, data from the two groups were combined.

Table 1. Baseline Clearance of Insulin and Paraaminohippurate in Normal and Septic Dogs Treated with Nonsteroidal Anti-Inflammatory Agents

Period	Indomethacin	Paraaminohippurate	Renal Blood Flow
Baseline	81.3 ± 09.5	209.9 ± 12.5	323.3 ± 21.5
Septic	99.5 ± 11.9	219.1 ± 33.2	338.4 ± 53.6
Post-drug	73.4 ± 09.1	113.0 ± 18.4	154.4 ± 25.0*

*p < .005 versus septic period

Treatment with NSAID significantly decreased renal blood flow in septic dogs. These data suggest that further information may be necessary before NSAID are used to treat septic patients.

SEPARATION OF PLURIPOTENT STEM CELLS FROM MONKEY BONE MARROW BY COUNTERFLOW CENTRIFUGATION-ELUTRIATION

Principal Investigator: R. L. Monroy
Collaborators: T. J. MacVittie, M. L. Patchen, and J. H. Darden
Technical Assistance: C. L. Feser, L. D. Huff, and C. Hattenburg

We have previously reported the use of counterflow centrifugation-elutriation to isolate an enriched pluripotent stem cell population from the canine bone marrow (1). This cell population was characterized by 50% of total nucleated cells, 25%-40% of the total granulocyte-macrophage colony-forming unit (CFU-GM), and the ability to reconstitute the bone marrow after lethal irradiation. However, the transplanted cell population contained 100% of the original contaminating lymphocytes.

In this report, the pluripotent stem cell population is shown to be separated from 55%-80% of the contaminating lymphocytes by counterflow centrifugation-elutriation. Heparinized bone marrow (multiple rib aspirates) was obtained from male rhesus monkeys (*Macaca mulatta*) weighing 7-9 kilograms (kg). The bone marrow was pretreated with Dextran to remove the contaminating red blood cells. The resulting nucleated cells were washed and entered into the elutriator (Beckman JE-6) at a flow rate of 7.5 milliliters/minute with a rotor speed of 2020 rpm. The flow rate was increased stepwise at 14.0 ml/min over a collection of 14 40-ml fractions. The centrifuge was stopped at fraction (Fr) 15, and the chamber contents were collected for the next 80 ml.

The resulting fractions were characterized for cellular composition; total number of nucleated cells; and the *in vitro* culture assays CFU-GM, CFU-erythroid (CFU-E), and CFU-megakaryocyte (CFU-MK). The elutriation procedure separates cells based on their size and density, with the smaller, less dense cells exiting first. This was consistently demonstrated as most lymphocytes were elutriated by Fr 7 into two peaks. Erythroid elements were elutriated from Fr 5 to Fr 10 with a peak at Fr 7 or 8, and myeloid elements were elutriated at Fr 10 to the chamber contents with a peak there.

Culture results (Figure 1) show that 90%-95% of the total CFU-E activity elutriates with the chamber contents, whereas CFU-GM activity was distributed into at least two peaks: one at Fr 7 or 8 with 20%-25% of the total activity and the other in the chamber contents. The CFU-MK activity was elutriated from Fr 7 to 13 with a peak at Fr 9 or 10.

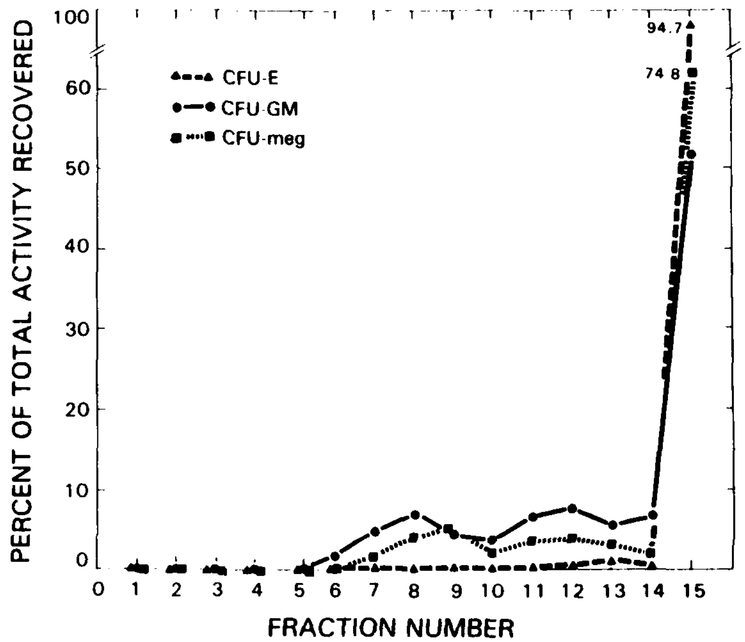

Figure 1. Elutriation profile of *in vitro* culture activities (CFU-E, CFU-GM, and CFU-meg)

A population of cells (Fr 5-11) characterized by a 50%-80% reduction in the contaminating lymphocytes, with 25% of the CFU-GM activity and 90%-100% of the CFU-MK activity, was evaluated for pluripotent stem cell activity by autologous transplantation into a lethally irradiated (9.0 grays) monkey. The monkeys (n = 2) received 1.88 x 10^7 nucleated cells/kg and 0.38 x 10^7 nc/kg, respectively. Each monkey showed a peripheral blood recovery profile similar to control animals that had been transplanted with autologous unfractionated bone marrow. Thus, we have demonstrated an elutriation procedure for both the enrichment of the pluripotent stem cell population and a reduction of contaminating lymphocytes.

REFERENCE

1. Jemionek, J. F., Monroy, R. L., MacVittie, T. J., Contreras, T. J., and Espy, S. B. Bone marrow reconstitution of lethally irradiated canines using autologous bone marrow fractions obtained by counterflow centrifugation-elutriation. British Journal of Haematology 51: 585, 1982.

CHARACTERIZATION OF HEMATOPOIETIC SYNDROME IN CANINE AFTER EXPOSURE TO NEUTRON IRRADIATION

Principal Investigator: R. L. Monroy
Collaborators: T. J. MacVittie and J. H. Darden
Technical Assistance: C. L. Feser, L. D. Huff, and C. Hattenburg

The objective was to define the dose range for the hematopoietic syndrome in a large-animal model exposed to a specific field and energy of neutrons.

Purebred beagle dogs, 1-3 years old, weighing 9-13 kilograms, male or female, were used in this study. The animals were divided into three groups to meet the objectives of the study. Group 1 had no therapeutic support administered. Group 2 had therapeutic support administered (fluids, antibiotics, and blood components). Group 3 had therapeutic support as in Group 2 and autologous bone marrow transplantation. The dogs received bilateral exposure in the AFRRI TRIGA reactor. The free-in-air field at the surface of the animal had a neutron-to-gamma ratio of 6:1, which was reduced to 1:1 at the midline of the animal. The doses reported are midline tissue doses.

Survival and the $LD_{50/30}$ (lethal dose for 50% of animals after 30 days) values are the ultimate parameters of these studies. Survival for each group is graphically summarized in Figure 1. The $LD_{50/30}$ value was determined to be 1.10 grays (Gy) for Group 1 and

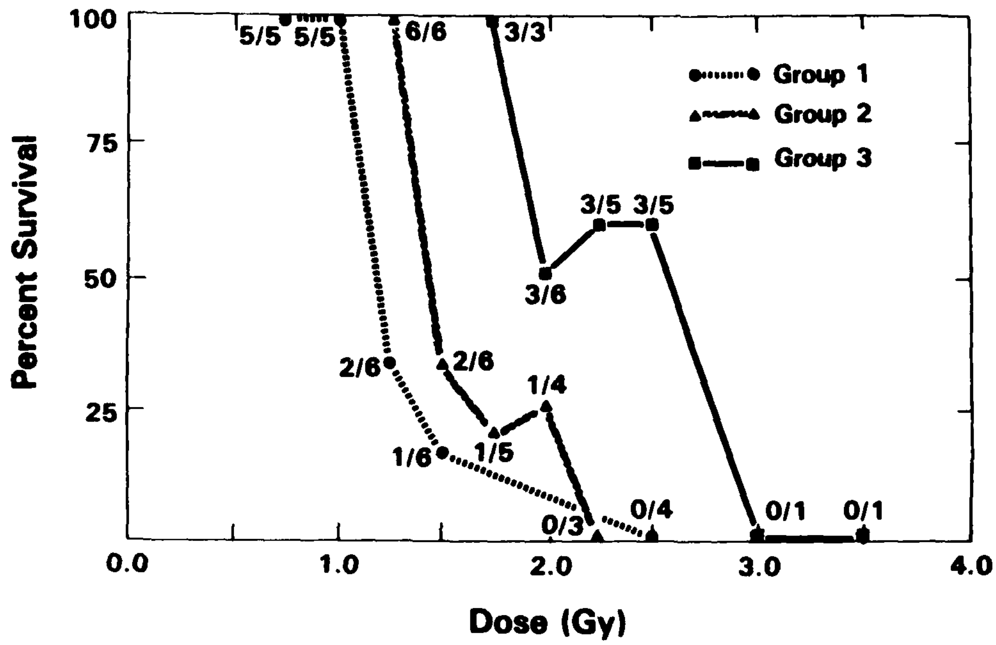

Figure 1. Evaluation of therapy on canine survival after neutron irradiation. Group 1, no therapeutic support; Group 2, therapeutic support; Group 3, therapeutic support and autologous bone marrow transplantation.

1.40 Gy for Group 2. The increase in the $LD_{50/30}$ is *attributed to an increase in the survival times associ-*ated with therapeutic support. This is critical for the recovery of the surviving hematopoietic elements. Autologous bone marrow transplantation has the potential to recover an animal from hemopoietic failure but not necessarily combined injury. In Group 3, transplantation was 100% effective at 1.75 Gy irradiation. However, between 2.00 and 2.50 Gy, the effectiveness of bone marrow transplantation was only 50%. All decedents of this group died between 5 and 10 days, with clinical symptoms characteristic of gastrointestinal damage.

On the basis of these data, the dose range for only the hematopoietic syndrome in the dog after neutron irradiation was found to be between 1.00 and 2.00 Gy. Apparent overlap of GI damage was observed at doses of 2.00 Gy and higher.

EFFECTS OF ENDOTOXIN ON SURVIVAL OF HYPER-TRANSFUSED MICE

Principal Investigator: R. M. Vigneulle
Collaborator: S. J. Baum
Technical Assistance: R. T. Brandenburg

Animal survival following exposure to a midlethal radiation dose usually depends on the recovery of hemopoiesis. It is generally agreed that bone marrow failure following irradiation results in the loss of the capability to produce granulocytes. The animal is at great risk for the development of infections and thus diminished capacity for survival, because of the reduced numbers of functional granulocytes during the first few weeks after irradiation. Ways to stimulate the production of granulocytes in the irradiated animal were investigated as an objective concerned with radiation and hemopoietic and immune dysfunction.

The technical objective of this study was to investigate stimulatory agents for increased granulocyte production following whole-body irradiation. The effects of endotoxin (a stimulatory agent) on the production of granulocytes can be divided into an immediate but transient effect and a more pronounced effect on the numbers of granulocytes available to the animal. The administration of endotoxin results in the transient mobilization of granulocytes into the blood from marginal pools, within hours. Also, endotoxin administration stimulates the production of granulocytes in the bone marrow through the stimulation of stem cell progenitors, an event occurring later. Endotoxin improves the survival of midlethally irradiated animals when administered immediately following or within 24 hr after exposure.

A hypertransfused mouse was selected as the model to test the hypothesis that endotoxin stimulates the production of granulocytes through increased progenitor cell proliferation, which may improve survival when the demand for erythropoiesis is suppressed. If a reduced erythropoiesis exists during and after lethal irradiation and is followed by a stimulation for granulopoiesis, then the production of granulocytes could be increased at a time when the postirradiated mouse is at great risk for infection for lack of functional granulocytes. The present investigation was concerned with the possibility that progenitors of the granulocytic series are further enhanced under these circumstances, by competing for the early multipotent progenitor cells.

The survival of hypertransfused B6CBF1 female mice exposed to 8.5 and 9.0 grays of cobalt-60 gamma rays and immediately given 10 micrograms of endotoxin intraperitoneally (i.p.) was significantly increased, compared to either irradiated mice given endotoxin or hypertransfused/normal mice comparably irradiated and given saline i.p. (1). Animals that had received the combined treatment (hypertransfusion, irradiation plus endotoxin) had increased survival compared to the other treatment groups at day 30 or at day 40 under controlled environmental conditions, but not when the recovery occurred under less controlled environmental conditions. Hypertransfused mice have greatly expanded pools of uncommitted progenitor and myeloid precursor cells, which apparently are unstimulated. After irradiation, when these pools were stimulated by endotoxin, granulocytopoiesis was enhanced, resulting in increased animal survival.

REFERENCE

1. Vigneulle, R. M., and Baum, S. J. Effects of endotoxin on survival of hypertransfused mice. Experimental Hematology 10 (12): 249-262, 1982.

EFFECTS OF PREIRRADIATION GLUCAN TREATMENT ON HEMOPOIETIC RECOVERY AND SURVIVAL

Principal Investigator: M. L. Patchen
Associate Investigators: T. J. MacVittie and L. K. Wathen
Technical Assistance: B. Watkins and J. Atkinson

Glucan, a B-1,3 polyglucose isolated from the inner cell wall of the yeast Saccharomyces cerevisiae, has been shown to profoundly stimulate hemopoiesis at the level of the pluripotent stem cell and the granulocyte, macrophage, and erythroid progenitor cells in normal mice (1-4) and to enhance endogenous spleen colony formation in sublethally irradiated mice (5).

In more recent studies, we have shown that mice intravenously administered 1.5 milligrams of glucan 24 hr before 650 rads of cobalt-60 radiation showed enhanced repopulation of both bone marrow and splenic pluripotent stem cells (CFU-s), granulocyte-macrophage and pure macrophage colony-forming cells (GM-CFC, M-CFC), erythroid burst- and colony-forming cells (BFU-e, CFU-e), and hemopoietic stromal cells (Table 1).

Table 1. Bone Marrow and Splenic Hemopoietic Recovery in B6D2F1 Mice Given 1.5 Mg of Glucan at 24 Hours Before 650 Rads of Total-Body Cobalt-60 Radiation

Days after irradiation	TNC		HSC		CFU-s		GM-CFC		M-CFC		BFU-e		CFU-e	
	RC	GLU	RC	GLU	RC	GLU	RC	GLU	RC	GLU	RC	GLU	RC	GLU
Bone marrow														
1	0.10	0.20	0.30	0.30	0.00	0.00	0.01	0.03	0.00	0.00	0.00	0.00	0.00	0.00
3	0.07	0.06	0.20	0.20	0.00	0.00	0.02	0.09	0.00	0.02	0.00	0.00	0.02	0.01
6	0.10	0.20	0.30	0.30	0.00	0.10*	0.03	0.10	0.01	0.02	0.00	0.20*	0.06	0.50*
8	0.30	0.50*	0.40	0.40	0.00	0.20*	0.10	0.50*	0.02	0.08*	0.02	0.40*	1.90	3.80*
10	0.40	0.70*	0.40	1.10*	0.10	0.30*	0.20	0.60*	0.04	0.20*	0.10	0.60*	2.30	5.20*
14	0.80	0.80	0.50	0.70	0.30	1.00*	1.00	1.40*	0.20	0.50*	0.30	1.70*	5.20	7.10*
21	1.30	1.50	1.30	0.70	1.00	2.70*	1.30	2.30*	0.30	0.70*	1.30	3.50*	6.00	7.20*
Spleen														
1	0.10	0.20	0.00	0.00	0.00	0.00	0.00	0.00	0.01	0.02	0.00	0.00	0.00	0.00
3	0.10	0.10	0.00	0.00	0.00	0.00	0.00	0.00	0.03	0.20*	0.00	0.00	0.00	0.00
6	0.10	0.20	0.01	0.10*	0.00	0.04*	0.00	1.30*	0.04	0.60*	0.00	0.00	0.00	0.07*
8	0.10	0.70*	0.30	1.40*	0.00	0.08*	0.00	5.40*	0.04	1.10*	0.00	2.40*	0.01	4.10*
10	0.20	0.90*	0.30	2.60*	0.00	1.70*	0.00	8.80*	0.06	6.30*	0.00	6.40*	0.03	4.70*
14	1.00	1.20	1.00	1.80*	1.30	4.10*	2.90	28.20*	0.70	11.20*	1.70	9.00*	5.20	5.40
21	1.20	1.30	1.40	1.10	8.00	5.70*	22.50	37.60*	5.20	11.90*	5.40	13.90*	11.70	7.70*

[a] TNC = Total nucleated cellularity per femur × $10^{[illegible]}$ or per spleen × 10^8; HSC = hemopoietic stromal cells per femur × 10^2 or per spleen × 10^2; CFU-s = pluripotent hemopoietic stem cells per femur × 10^3 or per spleen × 10^3; GM-CFC = granulocyte-macrophage colony-forming cells per femur × 10^4 or per spleen × 10^3; M-CFC = pure macrophage colony-forming cells per femur × 10^3 or per spleen × 10^4; BFU-e = erythroid burst-forming cells per femur × 10^3 or per spleen × 10^3; CFU-E = erythroid colony-forming cells per femur × 10^4 or per spleen × 10^5; RC = radiation control mice; GLU = glucan-treated and irradiated mice.

* $p < 0.01$

In general, hemopoietic recovery in glucan-treated mice preceded that in radiation control mice by approximately 6-8 days. In addition, when a similar dose of glucan was administered 24 hr before an otherwise lethal 900-rad dose of cobalt-60 radiation, approximately 40% of the glucan-treated mice exhibited long-term survival whereas 100% of the radiation control mice died by day 14 postirradiation (Figure 1).

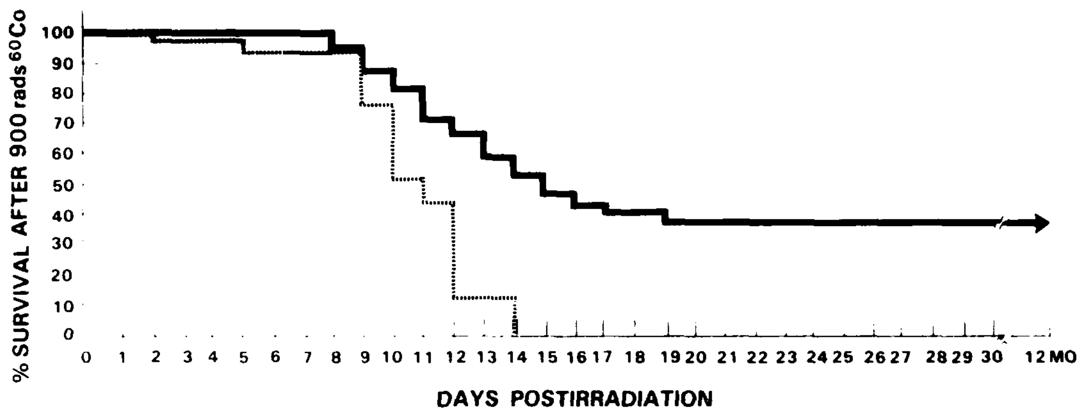

Figure 1. Effect of intravenous glucan-P administration on postirradiation survival in B6D2F1 mice. Broken line = radiation control (n = 25); solid line = glucan-P (75 mg/kg i.v.) administered 24 hr before 900 rads cobalt-60 radiation (n = 34).

These results indicate that glucan strongly enhances hemopoietic recovery following radiation injury, and also suggest that enhanced hemopoietic recovery can significantly alter the lethality attributed to the hemopoietic syndrome.

REFERENCES

1. Burgaleta, C., and Golde, D. W. Effect of glucan on granulopoiesis and macrophage genesis in mice. Cancer Research 37: 1739-1742, 1979.

2. Patchen, M. L., and Lotzova, I. Modulation of murine hemopoiesis by glucan. Experimental Hematology 8: 409-422, 1980.

3. Patchen, M. L., and MacVittie, T. J. Dose-dependent responses of murine pluripotent stem cells and myeloid and erythroid progenitor cells following administration of the immunomodulating agent glucan. Immunopharmacology 5: 303-313, 1983.

4. Patchen, M. L., and MacVittie, T. J. Temporal response of murine pluripotent stem cells and myeloid and erythroid progenitor cells to low-dose glucan treatment. Acta Haematologica 70: 281-288, 1983.

5. Patchen, M. L., and MacVittie, T. J. Use of glucan to enhance hemopoietic recovery after exposure to cobalt-60 irradiation. In: Macrophages and Natural Killer Cells. Norman, S. J., and Sorkin, E., eds. Plenum Press, New York, 1982, pp. 267-272.

HEMOPOIESIS IN BEAGLE FETUS AFTER *IN UTERO* IRRADIATION

Principal Investigator: S. R. Weinberg, *AFRRI*
Associate Investigators: T. J. MacVittie and A. C. Bakarich, *AFRRI*
Collaborators: M. P. McGarry, *Roswell Park Memorial Institute, New York State Department of Health, Buffalo, New York*

On day 33 of gestation, beagle fetuses were irradiated in utero (0.9 grays of cobalt-60 gamma irradiation, 0.4 Gy/min). Fetal hematocytopoiesis was studied during the third trimester of gestation (days 42-55). Peripheral blood nucleated cell counts were 33% lower than normal on day 44 and continued to be lower until day 49, when values became higher than normal. Splenic cellularities of irradiated pups on day 44 were more than three times those of the nonirradiated, but thereafter were similar to normal. Differences in hemopoietic progenitor cell activity between irradiated and normal fetuses were observed.

In comparison with the other fetal tissues, the fetal liver appeared to experience greater radiation injury. For example, on day 44, the irradiated liver BFU-E (erythroid burst-forming cells), CFU-E (erythroid colony-forming cells), and GM-CFC (granulocyte-macrophage colony-forming cells) per 10^5 cells were almost fivefold lower than normal values.

The spleens of irradiated beagle fetuses contained a marked increase in all hemopoietic progenitor cells (BFU-E, CFU-E, and GM-CFC) and recognizable proliferative granulocytic cells and nucleated erythroid cells.

The hemopoietic activity of irradiated bone marrow during days 42-44 was similar to that of the irradiated spleen, and compensated for the damaged liver. However, unlike the irradiated spleen, the irradiated bone marrow had decreased BFU-E activity compared with the values for the nonirradiated bone marrow during days 48-55. Until day 50, the irradiated marrow contained fewer recognizable proliferative granulocytic cells but more nucleated erythroid cells.

EFFECTS OF PRENATAL IRRADIATION ON FETAL, NEONATE, AND YOUNG ADULT MURINE HEMOPOIESIS

Principal Investigator:	S. R. Weinberg, *AFRRI*
Associate Investigators:	T. J. MacVittie and A. C. Bakarich, *AFRRI*
Collaborator:	M. P. McGarry, *Roswell Park Memorial Institute, New York State Department of Health, Buffalo, New York*

B6D2F1 mice received cobalt-60 radiation on day 10.5 of gestation at doses of 50 to 300 rads at a dose rate of 40 rads per minute. The animals were studied at four selected age periods: day 14.5 of gestation, neonate, juvenile, and 13-week-old adult.

Fetal liver cellularity, morphology, and hemopoietic progenitor cell concentration reflected injury after 200 rads. The 15-day-old (juvenile) mouse spleen cellularity was affected more than was bone marrow cellularity, but greater radiation injury was reflected by bone marrow hemopoietic progenitor cells. Fluctuations from normal hematopoietic values were greater in the 15-day-old juvenile than in the 9-day-old neonate, commencing with 50 rads. These included peripheral

blood parameters and marrow- and spleen-derived erythroid-, granulocytic-, and megakaryocytic-progenitor cells.

The consequences of prenatal irradiation (150 rads) were evident in the 13-week-old adult. This was manifested by reduced spleen cellularity and by perturbations in the concentrations of hemopoietic progenitor cells in the bone marrow.

MURINE NEONATE HEMOPOIESIS FOLLOWING *IN UTERO* TOTAL-BODY IRRADIATION

Principal Investigator:	S. R. Weinberg, *AFRRI*
Associate Investigators:	T. J. MacVittie and A. C. Bakarich, *AFRRI*
Collaborator:	M. P. McGarry, *Roswell Park Memorial Institute, New York State Department of Health, Buffalo, New York*

Irradiation (50-200 rads of cobalt-60 gamma rays) on day 10.5 of gestation in the mouse had the following residual effects on neonate and juvenile hemopoiesis: (a) greater damage observed in the 15-day-old juvenile than in the 9-day-old neonate, (b) greater fluctuation of peripheral blood hemogram indices from normal values in the 15-day-old animal than in the 9-day-old animal, (c) spleen cellularity affected more than bone marrow cellularity, (d) greater radiation injury reflected by bone marrow hemopoietic progenitor cells, and (e) a more pronounced decrease in medulla-erythropoietic and spleen-erythropoietic activity with each increase in dose of irradiation.

CELL GROWTH, MORPHOLOGY, AND SCANNING ELECTRON MICROSCOPY CHARACTERISTICS OF MURINE LONG-TERM CULTURES DERIVED FROM C57BL/Ks AND C3H/HeJ BONE MARROW CELLS IRRADIATED *IN VIVO*

Principal Investigator: S. R. Weinberg, *AFRRI*
Associate Investigators: T. J. MacVittie and A. C. Bakarich, *AFRRI*
Collaborator: M. P. McGarry, *Roswell Park Memorial Institute, New York State Department of Health, Buffalo, New York*

The relationship between bone marrow stroma and hemopoietic cells from irradiated C57BL/Ks and C3H/HeJ mice was studied. Mice were exposed to whole-body cobalt-60 radiation (60, 120, and 180 rads at 40 rads/minute). Long-term liquid cultures (LTC) were established with either intact bone marrow or dispersed bone marrow in cell suspension.

During the first 6 weeks, the nonadherent cell growth of irradiated and nonirradiated groups was better in LTC established from cell suspensions, compared to LTC from intact bone marrow. The difference was probably due to a delay in the initial put-down of the stromal layer of intact bone marrow LTC to support the hemopoietic cells.

Cell growth was maintained for a longer period of time in LTC from intact bone marrow. Differences in cell growth and morphology of nonadherent and adherent cellular elements were observed between LTC from C57BL/Ks and C3H/HeJ. Throughout the 14 weeks of study, cell growth was better with prolonged granulocytopoiesis in C57BL/Ks LTC compared to those of C3H/HeJ. In contrast, C3H/HeJ intact LTC showed more pronounced difference between the various radiation doses throughout the study (decrease in cell growth, fewer proliferating granulocytes, and more macrophages in the nonadherent cells), and C57BL/Ks cell suspension LTC reflected radiation injury in each parameter monitored only between weeks 2 and 6. Standard errors of the mean of LTC on coverslip cultures showed a more defined stromal layer (fat cells, fibroblasts, and macrophages) in C57BL/Ks cell-suspension LTC and C3H/HeJ intact LTC.

Data from C57BL/Ks mice suggest that postirradiation recovery in LTC is dependent on the presence of an intact stromal population. This was indicated between weeks 2 and 6 by the inverse relationship between cell growth and radiation dose in cell suspension LTC, and

no postirradiation injury in intact LTC. Residual radiation injury appears to be resolved after week 6 in the C57BL/Ks cell suspension LTC and intact LTC. C3H/heJ mice appear to be more radiosensitive and show significant radiation damage within 1 week of culture.

PHYSIOLOGIC RESPONSE OF GUINEA PIG ADRENAL CORTEX FOLLOWING EXPOSURE TO IONIZING RADIATION

Principal Investigator: G. M. Buchanan
Collaborator: L. K. Steel
Technical Assistance: J. L. Parker

Exposure to lower levels of ionizing radiation is defined as a nonspecific stressor, falling within the definition of the General Adaptation Syndrome (GAS). The corticotropin-glucocorticoid axis is a scientifically sound model of the radiation-induced stress response. Since the physiologic response of the adrenal cortex is central to the GAS concept, it was evaluated in terms of ultrastructural changes and alterations in circulating concentrations of corticotropin and cortisol following exposure to 2.00 grays of gamma radiation (cobalt-60).

Adrenal cortices of guinea pigs were prepared for electron microscopy, and data were collected by morphometric analysis. Serum concentrations of corticotropin and cortisol were measured by radioimmunoassay. Pilot studies of the liver and adrenal cortex revealed that significant ultrastructural changes took place on the third and fourth days postirradiation.

The mitochondrial/vacuolar ratio in the cells of the zona fasciculata proved to be a significant indicator ($p < .05$) of ultrastructural response on the third day postirradiation. Corticotropin concentrations were neither significantly nor consistently different from those of the control animals at 1-5 or 24-48 hr. Serum cortisol concentrations of the irradiated animals were

significantly higher than controls ($p < .05$) at 1 and 3 hr following exposure and significantly less ($p < .05$) at 5 hr. A significant difference was not observed again at 24 and 26 hr, but it was seen again ($p < .05$) at 28 hr.

The major conclusions from this research are that (a) electron microscopy, using morphometric analysis, is effective in detecting ultrastructural responses to lower levels of ionizing radiation; (b) cortisol, which is significantly responsive and capable of producing many of the clinical symptoms postirradiation, is the agent presumed responsible for physiologic changes after exposure to radiation; and (c) the adrenal cortex of the guinea pig is a satisfactory model of ultrastructural response to ionizing radiation.

TIME DEPENDENCE OF TRAUMA-INDUCED SURVIVAL OF MICE FROM COBALT-60 IRRADIATION

Principal Investigator: G. D. Ledney
Technical Assistance: E. D. Exum

In previous publications (1, 2) we established that wound trauma 24 hr before graded doses of cobalt-60 radiation resulted in the survival of mice that ordinarily would die from hematopoietic failure. In this study we investigated the timing of the wound relative to radiation exposure and its effects on (a) total number of survivors and (b) endogenous colony-forming units-spleen (E-CFU-s).

Wounding and irradiation were performed on 12- to 16-week-old B6CBF1 female mice. Methyoxyflurane-anesthetized mice were wounded in the anterior dorsal skin fold and the underlying panniculus carnosus muscle with a steel punch (repeatedly cleaned by immersing in 70% ethanol). The wound was 2.0-2.5 cm^2, which was 4% of the total skin surface. Wounding was done at various times either before or after exposure to cobalt-60, between 10:00 a.m. and 2:00 p.m. The wounds were

left untreated and open to the environment. Irradiated, nonwounded control mice were anesthetized before irradiation. All animals were exposed to whole-body radiation at a rate of 40 rads/min from bilateral cobalt-60 sources.

In the first series of experiments, 30-day survival studies were done with mice given either 9, 10, or 11 grays (Gy) (1 Gy = 100 rads). Groups of 16 mice each were wounded from 7 days before irradiation to 2 days after irradiation. Also, one group of mice was wounded 10 min before and another group was wounded 10 min after irradiation.

In the second series of experiments, groups of eight mice each were wounded before or after radiation at the intervals and radiation doses previously indicated. Ten days later these mice were euthanatized by cervical dislocation, the spleens were removed, and the number of E-CFU-s were determined by standard procedures.

The wound trauma-radiation survival (percent) studies are presented in Figure 1. Generally, survival depended on the radiation dose and the time of wounding relative to irradiation. Maximum numbers of survivors were obtained when wounding occurred within 1 day of exposure to either 9, 10, or 11 Gy. Noteworthy was the survival recorded in animals wounded up to 1 day after either 9 or 10 Gy. All radiation controls given either 9, 10, or 11 Gy died, and all wounded-only mice survived.

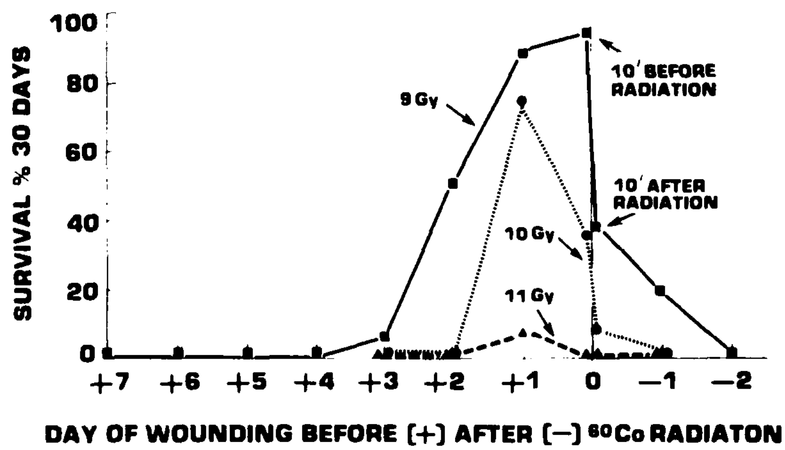

Figure 1. Thirty-day survival percentages of wounded irradiated B6CBF1 female mice. At each time point indicated, wounding was performed on 16 mice with exception that 47 mice were injured 1 day after irradiation. All control-irradiated mice died (data not shown) with exception that one mouse lived after 9.0 Gy. All control-wounded mice survived. ■——■, 9.0 Gy; ●·······●, 10.0 Gy; ▲----▲, 11.0 Gy.

Wounding shortly before irradiation (as seen in Figure 1) resulted in an increased amount of survival time in those animals that died after 9 or 10 Gy (data not presented). This effect was lost in animals wounded before 11 Gy. Wounding 1 day after irradiation significantly reduced the survival time when compared to (a) nonwounded, irradiated controls and (b) most animals wounded before or 10 min after irradiation.

The endogenous spleen colony studies are presented in Table 1. Generally, the quantities of E-CFU-s were the greatest when wounding was done in close proximity to radiation. The greatest E-CFU-s response appeared at the radiation dose (9 Gy) and time interval of wounding (1 day before) that resulted in the most survival (recorded in Figure 1). No E-CFU-s were detected in any of the radiation controls.

Table 1. Endogenous Spleen Colony-Forming Units in Mice After Wound Trauma and Radiation

Radiation Dose (Rad)	Time of Wounding Relative to Radiation: +4 D	+3 D	+2 D	+1 D	+10"	-10"	-1 D	Control-Treated
900	0.1 ± 0.1	0.4 ± 0.2	0.4 ± 0.2	3.4 ± 0.8	0.6 ± 0.3	1.1 ± 0.3	0	0
1000	1.6 ± 1.2	0	0.2 ± 0.2	0.6 ± 0.3	0	0	0	0
1100	0	0.1 ± 0.1	0	0.8 ± 0.8	0	0	0	0

\+ = Wounded before radiation

\- = Wounded after radiation

D = Days

" = Minutes

The data presented in this report concern the influence of wound timing and survival after exposure to radiation. Wound-induced survival from radiation may be ascribed to the proliferation of a cell population (E-CFU-s) associated with recovery from radiation injury.

AD-A147 778 AFRRI (ARMED FORCES RADIOBIOLOGY RESEARCH INSTITUTE) 2/2
ANNUAL RESEARCH REPO..(U) ARMED FORCES RADIOBIOLOGY
RESEARCH INST BETHESDA MD 30 SEP 83 AFRRI-ARR-17

UNCLASSIFIED F/G 6/18 NL

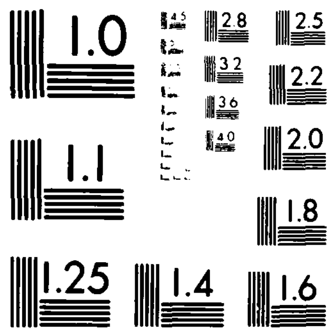

MICROCOPY RESOLUTION TEST CHART
NATIONAL BUREAU OF STANDARDS-1963-A

REFERENCES

1. Ledney, G. D., Stewart, D. A., Exum, E. D., and Sheehy, P. A. Skin wound-enhanced survival and myelocytopoiesis in mice after whole-body irradiation. Acta Radiologica: Oncology, Radiation Physics, Biology 20: 29, 1981.

2. Ledney, G. D., Exum, E. D., and Sheehy, P. A. Survival enhanced by skin-wound trauma in mice exposed to cobalt-60 radiation. Experientia 37: 193, 1981.

EFFECTS OF IMMUNOMODULATORY FACTORS ON IMMUNOCOMPROMISED HOSTS

Principal Investigator: D. F. Gruber
Technical Assistance: T. A. Davis

Although their mechanisms may be entirely different, both radiation and cancer, in general, are known to disrupt normal hemopoiesis. Lymphomyelopoietic dyscrasias, which are seen, may be due in part to the presence or absence of regulatory factors, or they may reflect a change in the femoral matrix micro-environment.

Medium conditioned by murine submandibular gland (SMG-CM) was selected to ascertain cellular responsiveness to growth factors. SMG-CM was selected for a number of reasons: (a) SMG-CM is known to stimulate epidermal growth, and has been referred to as epidermal growth factor. Epidermal growth factor might prove to be of considerable interest in wound repair and closure. (b) SMG-CM is a known source of nerve growth factor, which may be of some use in lacerative injuries. (c) SMG-CM is reported to be a potent source of colony-stimulating factor(s), and could prove of use in marrow transplantation or conditions of anergy.

Two tumor models available for immunosuppressive investigation were the Lewis lung carcinoma (3LL) and thymic lymphoma ascites tumor (EL-4). Soft-agar clonogenic assay techniques were used to assess response patterns of the granulocyte-macrophage (GM-CFUc) and monocyte-macrophage (M-CFUc) progenitor cell populations. Two sources of colony-stimulating activity were used.

It was determined that tumor-immunosuppressed hosts, in contrast to normals, responded in much different fashions to different sources of colony-stimulating activity. Progenitor cells in immunosuppressed animals responded to SMG-CM at levels that were 5-6 times higher than in normal animals. Preliminary experiments with irradiated animals (250, 500, and 750 rads of cobalt-60) have shown similar patterns (albeit lesser) of enhanced responsiveness (2.8-4 times) to SMG-CM.

The tumor- or radiation-immunosuppressed animal may be responding to a different or altered set of signals (growth factors, inhibitors, microenvironment, etc.). These experiments show the immunocompromised animal to be capable of responding. Certain immunomodulatory materials may therefore be capable of altering response patterns in compromised individuals.

HEMOPOIESIS IN PREGNANT BEAGLES FOLLOWING LOW-DOSE TOTAL-BODY IRRADIATION AND SURGERY

Principal Investigator: S. R. Weinberg, *AFRRI*
Associate Investigators: A. C. Bakarich, G. D. Ledney, and L. J. MacVittie, *AFRRI*
Collaborators: M. P. McGarry, *Roswell Park Memorial Institute, New York State Department of Health, Buffalo, New York*

Hemopoietic perturbations were observed in gravid beagles subjected to whole-body ionizing radiation during midpregnancy followed by the additional trauma of surgery. Alterations were seen in peripheral blood hemogram parameters, bone marrow morphology, and concentration of marrow-derived granulocytic- and erythrocytic-committed stem cells (Table 1).

However, the trauma of surgery combined with irradiation had no apparent effects on the contralateral uterine horn with the remaining pups. There were no indications of miscarriage, absorption of pups, or other complications of pregnancy.

Table 1. Comparison of Erythropoietic and Granulocytic Activities in Bone Marrow* and Peripheral Blood* of Pregnant Beagle

	Pregnant	Irradiated-Pregnant+	Post-Surgery‡ Pregnant	Irradiated-Pregnant
Percent values for bone marrow CFU-E/GM-CFC per 10^5 nucleated cells (normal beagle values = 145%-185%)				
Days 40-44	385	577	—	—
Days 47-50	100-325	—	517	—
Days 54-57	—	—	148-746	342
Percent values for peripheral blood RBC/WBC per mm^3 (normal beagle value = 59%)				
Days 30-33	32-58	—	—	—
Days 40-43	37-41	50	—	—
Days 47-50	30-31	54	31-46	32
Days 54-57	—	—	30-49	38

* Peripheral blood samples and bone marrow aspirates were taken at selected subsequent times during gestation.

+ Total-body irradiation on day 33 of gestation

‡ Surgery on day 41-49

MODULATION OF THE RADIOPROTECTIVE ENZYME SUPEROXIDE DISMUTASE BY SEROTONIN

Principal Investigator: B. Gray

Copper-zinc superoxide dismutase (SOD) is an endogenous radioprotective enzyme that catalyzes the reaction $2O_2^- + 2H^- \longrightarrow O_2 + H_2O_2$ and contributes to the control of O_2^- concentrations in cells (1). Regulation of O_2^- concentration is critical because high quantities are deleterious and certain enzymes require O_2^- as a substrate (2). Modulation of SOD enzyme activity is important metabolically, and assumes critical significance following absorption of ionizing radiation since a flux of free radicals ensues (3). The following work was done to determine if serotonin or other similar molecules modulate SOD.

Results of these studies show that serotonin and 5-hydroxy-L-tryptophan act as inhibitors of SOD when the ligands are in the semiquinoneimine free radical form. A number of other compounds (including histamine, tryptophan, and tryptamine) were not inhibitors of the enzyme. In addition, serotonin semiquinoneimine attached to SOD specifically with two molecules of ligand bound per molecule of enzyme. Moreover, serotonin semiquinoneimine was an irreversible inhibitor of SOD, acting as a poison for the enzyme. These results support similar observations of the reduction in SOD activity following exposure to other free radicals (4,5).

REFERENCES

1. McCord, J. M., and Fridovich, I. Superoxide dismutase: An enzymic function for erythrocuprein (Hemocuprein). Journal of Biological Chemistry 244: 6049-6055, 1969.

2. Hayaishi, O. Indoleamine 2,3-dioxygenase: A superoxide-utilizing enzyme. In: Frontiers in Physicochemical Biology. Pullman, B., ed. Academic Press, Inc., New York, 1978, pp. 283-297.

3. Bielski, B. H. J., and Gebicki, J. M. Application of radiation chemistry to biology. In: Free Radicals in Biology, Vol. III. Pryor, W. A., ed. Academic Press, Inc., New York, 1977, pp. 1-51.

4. Crouch, R. K., Gandy, S. E., Kimsey, G., Galbraith, R. A., Galbraith, G. M. P., and Buse, M. G. The inhibition of islet superoxide dismutase by diabetogenic drugs. Diabetes 30: 235-241, 1981.

5. Wandman, P. Specificity of superoxide dismutase in catalysing redox reactions: A pulse radiolysis study. In: Radiation Biology and Chemistry: Research Developments. Edwards, H. E., Navaratnam, S., Parsons, B. J., and Phillips, G. O., eds. Elsevier, Amsterdam, 1979, pp. 189-196.

CELL PROLIFERATION OF NORMAL AND OF STIMULATED GRANULOCYTE-MACROPHAGE COLONY-FORMING CELLS

Principal Investigator: M. P. Hagan
Collaborator: T. J. MacVittie
Technical Assistance: D. P. Dodgen

The 5-BrdUrd/313-nm light technique recently applied to the question of stem cell proliferation (1) has been used to study the proliferation of granulocyte-macrophage colony-forming cells (GM-CFC). The purpose of this work was to demonstrate that the capability of identifying cells in the first S-phase of BrdUrd labeling (which has been shown to be a property of the BrdUrd/313-nm light treatment) could identify the separate subpopulations that are dependent on generation-age.

For this purpose, BrdUrd infusion periods were chosen to be significantly longer than one GM-CFCc generation time (namely, infusion periods greater than 96 hr). At these times, the cell population in the initial S-phase after the start of the BrdUrd or BrdCyd infusion should be weighted toward slower cycling (and thus presumably precursor) cell populations.

The data in Figure 1 show that two cell populations with both qualitative and quantitative differences in their survival responses were observable after 4 days of

BrdUrd infusion. The survival curves for the more resistant component indicate a shoulder characteristic of cells in the first S-phase of BrdUrd labeling.

Since cells that have been labeled with a moderate level of BrdUrd (e.g., 1%-10% replacement of thymidine) and irradiated with 313 nanometers light during the initial S-phase of the labeling can survive at fluences approximately equal to those for unlabeled cells, it is important to confirm that both component curves in Figure 1 actually represent BrdUrd-labeled cell populations. This was accomplished by varying either the infusion period or the effective concentration of BrdUrd used for the labeling.

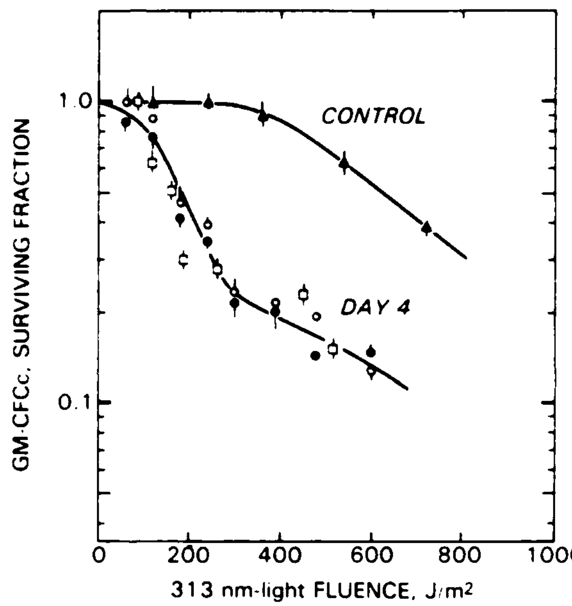

Figure 1. 313 nm-light survival of GM-CFCc after 4 days of BrdUrd infusion. B6D2F1 female mice were implanted either intraperitoneally (●) or subcutaneously (.) with model 1701 Alzet minipumps. After 4 days of infusion (1.3 mg/kg-hr), three mice per group were sacrificed, and cells from the femora were pooled and irradiated. Control GM-CFCc (▲) were infused with a subcutaneously implanted minipump containing saline. Open symbols represent replicate experiments. Error bars represent standard errors from triplicate samples.

REFERENCE

1. Hagan, M. P., and MacVittie, T. J. CFUs kinetics observed in vivo by bromodeoxyuridine and near-UV-light treatment. Experimental Hematology 9: 123-128, 1981.

REPAIR OF DEOXYRIBONUCLEIC ACID AFTER IONIZING RADIATION

Principal Investigators: M. P. Hagan and H. M. Jacocks III
Technical Assistance: D. P. Dodgen

Trimethylpsoralen treatment combined with 365-nanometer light irradiation recently has been used to block semiconservative deoxyribonucleic acid (DNA) synthesis, thus permitting the assay of repair synthesis. Using cesium chloride density gradient analysis, we have partially characterized the DNA synthesized during this synthesis blockade. In addition, we have used an insult with cobalt-60 gamma radiation to examine DNA repair synthesis after cross-linking.

"Background" radioactivity, representing DNA labeled after the trimethylpsoralen/365-nm light treatment, was shifted to hybrid-density through the incorporation of 5-bromodeoxyuridine (BrdUrd). After exposure to a high dose of cobalt-60 gamma irradiation, BrdUrd incorporation produced no hybrid-density DNA. At intermediate doses of cobalt-60 gamma radiation, both density types were found.

These results identify a possible source of error in the trimethylpsoralen/365-nm light technique for DNA repair studies, and underscore the importance for characterization of DNA when multiple damaging agents are used.

EFFECT OF PROSTAGLANDIN E_2 ON RADIATION KILLING IN SYNCHRONIZED AND ASYNCHRONOUS CHINESE HAMSTER CELLS

Principal Investigators: E. V. Holahan and M. P. Hagan
Technical Assistance: D. P. Dodgen and D. Wandres

Prostaglandins can apparently be synthesized by most tissues in the body, and recent evidence suggests that radiation can induce dramatic changes in these prostaglandin levels. Preliminary studies by Hanson and Thomas (Rush University, Chicago, Illinois) demonstrated that injection of a prostaglandin analog, 16-16 dimethyl prostaglandin E_2 (PGE_2), enhanced the radiation survival of murine intestinal stem cells. We have been investigating the effect of PGE_2 on tissue culture cells to determine if a cellular or molecular basis exists for this PGE_2-induced radiation protection.

When asynchronous V79 Chinese hamster cells were exposed to 14 millimolar (5 micrograms/milliliter) PGE_2 in alpha-MEM (Eagles' minimum essential medium) for 2 hr before X irradiation, no enhancement of radiation survival was apparent. However, if the cells were exposed to a similar PGE_2 treatment before a 30-min exposure to 1 micromolar N-ethyl maleimide (NEM), the PGE_2-plus-NEM radiation survival curve had a slightly larger shoulder (Dq = 2.7 Gy) than the NEM radiation survival curve (Dq = 2.0 Gy). Furthermore, PGE_2 can immediately enhance recovery from sublethal NEM damage when the PGE_2 exposure precedes irradiation by 30 min or more. We postulated that PGE_2 may stimulate an increase in intracellular nonprotein thiol content and that this increase may not be glutathione-mediated.

We are currently investigating whether PGE_2 confers a cell cycle-specific recovery from NEM-induced radiosensitization. Furthermore, we will be examining the effect of both NEM and PGE_2 on cellular nonprotein thiol content by measuring fluorometric changes of thiol-monobromotrimethylammoniobimane (qBBr) derivatives using techniques of high-performance liquid chromatography.

The ability to understand and effectively use the conditions under which radioprotectants like PGE_2 operate is necessary to the AFRRI task on radiation protection.

PHYSIOLOGY DEPARTMENT

The Physiology Department does research on the effect of radiation on the physiological function of biological systems. The Department uses an integrated approach that ranges from the use of single cells in tissue culture isolation to whole, awake performing animals.

The Department is divided into three major Divisions, whose research interests are as follows:

The research efforts of the Cellular Physiology Division are multifaceted, and are focused on understanding the effects of radiation at the cellular level. One of its goals is the study of radiation-induced hematopoietic dysfunction by elucidating the effects of radiation on the macrophage. These cells, although relatively radioresistant in terms of survival, are long-lived and play a pivotal role in both the immune response and host defenses. A second goal within the Division is the study of radiation-induced gastrointestinal dysfunction. Sublethal doses of ionizing radiation produce incapacitation through vomiting, diarrhea, and nausea, whereas supralethal doses result in the denudation of intestinal mucosal lining and bacterial toxemia. Both electrical and transport measurements are being used to study the cellular effects of radiation in intestinal epithelia. The third and last major area of research in this Division involves the study of ionic recovery mechanisms following radiation. This area of research is a part of the AFRRI task force directed toward understanding mechanisms of performance decrement and incapacitation.

Studies in the General Physiology Division concern investigation of the effects of mid-range and high-range doses of radiation (500-10,000 rads) on the cardiovascular and gastrointestinal systems. The acute effects of this range of supralethal radiation exposure is of particular interest to military commanders as they plan for operations in a nuclear warfare environment. Performance capabilities and limitations hold the key to mission success or failure and ultimately to survival. Radiation-induced hypotension has been implicated as the cause of early transient incapacitation, which is found with

such levels of radiation exposure. The study of radiation-induced hypotension includes measurements of blood volumes, cardiac output, arterial pressure, central venous pressure, and mean circulatory filling pressure as well as measurement of blood flow changes to specific end organs.

Research within the Neurophysiology Division is directed toward mechanisms of performance decrement and incapacitation. The breadth of research ranges from the single nervous system cell to the awake, performing monkey. Excitable cells are grown in tissue culture where they can be studied in great detail. Studies are being conducted to determine if radiation alters the ion channels responsible for the neurophysiological behavior of single cells. Cultured neurons with nicotinic and muscarinic acetylcholine receptors are being used to study the mechanisms of action of neurotoxic chemical warfare agents and how radiation may interact with these chemical effects. From single cells, another order of complexity can be achieved using isolated brain slices. Furthermore, various substances that may be released from nonneuronal cells following radiation are being examined for effects on neuronal excitability. Finally, the next level of organization used is the awake mammal. Nonhuman primates are taught specific tasks, and the effects of radiation on physiological and behavioral responses are studied.

COUPLING RATIO OF SODIUM POTASSIUM PUMP IN LOBSTER CARDIAC GANGLION

Principal Investigator: D. R. Livengood

The electrogenic sodium-potassium (Na-K) pump coupling ratio in the large neurons of the lobster cardiac ganglion was determined by two different electrophysiological techniques. A graphical analysis plotting $\exp(E_m F/RT)$ versus $[K]_o$ (potassium ion concentration outside the cell) after the pump was blocked by ouabain was used to determine values for $[K]_i$ (potassium ion concentration inside the cell), P_{Na}/P_K (permeability ratio of sodium to potassium), and the pump coupling ratio (1). These measurements were made 5 to 8 hr after the cells were penetrated with microelectrodes, and thus they represent nonsodium-loaded steady-state values. The value obtained for the pump coupling ratio under these conditions was 1.44 ± 0.06 ($n = 9$), or close to 3 sodiums for 2 potassiums (Table 1).

Table 1 Values Calculated for $[K]_i$, P_{Na}/P_K Ratio, and Pump Coupling Ratio in Normal Saline

EXPERIMENT NO.	RESTING POTENTIAL	OUABAIN DEPOLARIZATION	CORRELATION COEFFICIENT	$[K]_i$	P_{Na}/P_K	COUPLING RATIO
MN1206	−62	6.3	0.93	305	0.049	1.58
MN3166	−66	4.0	0.77	312	0.037	1.38
MN3116	−63	4.8	0.93	247	0.029	1.59
MN12096	−53	7.0	0.61	276	0.053	1.64
MN9015	57	8.0	0.94	156	0.015	1.20
MN9245	62	2.0	0.99	208	0.009	1.54
MN9305	−53	4.0	0.97	322	0.069	1.27
MN9115	−56	2.5	0.94	170	0.016	1.40
MN8155	61	3.8	0.98	286	0.024	1.32
	59.2 ±1.5	4.71 ±0.67		253.6 ±20.7	0.033 ±0.007	1.44 ±0.05

The second technique used to measure the coupling ratio was to iontophoretically inject Na ions into the neuron. Neurons were penetrated with three microelectrodes, two of which were filled with 2 molar (M) Na-citrate; the third electrode contained either 2 M K-citrate or 3 M potassium chloride. By passing current between the Na salt-containing electrodes, Na was injected into the cell soma. The injection system was calibrated by injecting ^{24}Na-citrate into counting vials from representative microelectrodes (calculated ^{24}Na transport number = 0.92). By knowing the Na load injected into the cells and by measuring the time-current area produced by the Na activation of the Na-K pump, the coupling ratio was calculated to be 1.54 ± 0.05 (n = 19) (Table 2), which is not significantly different from the value obtained by the first method (2). This value represents a sodium-loaded experimental situation. When Na was removed from the external bathing solution, the coupling ratio shifted to 2 Na to 1 K (2.0 ± 0.07, n = 4) (Table 3).

Table 2. Coupling Ratio Values Obtained From Injection Experiments

EXPERIMENT NUMBER	RESTING POTENTIAL (mV)	INPUT RESISTANCE (MΩ)	LOAD INJECTED (picoequiv.)	UNCOUPLED LOAD PUMPED OUT (picoequiv.)	COUPLING RATIO
I I67	-55	1.2	44.2	14.9	1.51
		1.2	24.3	11.2	1.85
		1.2	30.9	12.2	1.65
I I85	-53	2.8	35.0	10.5	1.43
I I86	-50	0.6	26.5	10.9	1.70
		0.6	37.5	19.1	2.04
		0.6	39.7	11.0	1.38
I W23	-60	1.3	23.9	7.3	1.44
		1.4	32.2	9.2	1.40
		1.4	36.8	9.0	1.32
I W16	-55	2.0	38.6	13.5	1.54
		2.0	35.0	11.2	1.47
		2.0	35.0	16.0	1.84
		2.0	58.9	22.5	1.62
I W24	-60	1.3	27.2	8.9	1.49
		0.8	47.3	15.7	1.50
I W76-1	-60	2.0	29.0	10.6	1.58
		2.4	31.3	6.1	1.24
		2.9	36.7	8.7	1.28
	AVG -56.1 ± 1.5				AVG 1.54 ±0.05

Table 3. Coupling Ratio Values Obtained From Injection Experiments in Sodium-Free Saline

EXPERIMENT NUMBER	RESTING POTENTIAL (mV)	INPUT RESISTANCE (MΩ)	LOAD INJECTED (picoequiv.)	UNCOUPLED LOAD PUMPED OUT (picoequiv.)	COUPLING RATIO
I W16	−52	1.4	66.6	35.1	2.12
		1.7	60.3	32.0	2.11
I W76-1	−58	2.37	28.15	12.7	1.82
		2.2	18.6	9.0	1.94

AVG 2.00 ±0.07

These results suggest that the pump normally operates with a 3:2 ratio both in steady state and under Na load, but in the absence of external Na, it can operate in a nonpotassium-saturated condition. These methods establish a method for studying the membrane permeability and recovery properties of a number of cell types in response to toxic insults such as radiation injury.

REFERENCES

1. Thomas, R. C. Electrogenic sodium pump in nerve and muscle cells. Physiological Reviews 52: 563-594, 1972.

2. Livengood, D. R. The coupling ratio of the Na-K pump in the lobster cardiac ganglion. Biophysical Journal 33: 45a, 1981.

PATCH CLAMP STUDIES IN CULTURED MACROPHAGES

Principal Investigator: E. K. Gallin
Technical Assistance: S. W. Green

Using gigaseal techniques, studies have demonstrated single-channel current activity in patches of membrane on intact macrophages. This work has also confirmed previous single-electrode voltage-clamp data demonstrating a negative-slope resistance region in macrophages.

Figure 1A depicts currents recorded using a patch electrode filled with 150 millimolar (mM) potassium chloride (KCl) and 5 mM ethylene glycol bistetracetic acid (EGTA). Discrete current fluctuations of 1.1 picoamperes were evident when the external surface of the patch membrane was clamped to the bath potential. The values (Figure 1A) of the potential across the patch membrane were obtained using the holding potential of the patch and the zero current value of the membrane potential, determined from the whole-cell clamp done later in the experiment. It is evident that the current fluctuations had several distinct levels of similar amplitude, suggesting that more than one channel (but only one type of channel) were present in this patch. As the membrane patch was hyperpolarized, both channel activity and size increased. Depolarizing the patch decreased the amplitude of the current fluctuations, until at potentials less negative than -33 millivolts (mV), channel activity disappeared. No channel activity was present at +46 mV. Channel amplitude increased ohmically over the voltage range examined, having a conductance of 16 picosiemens (Figure 1B). The extrapolated reversal potential of these currents fits reasonably well with the expected reversal potential for a potassium conductance, since under these conditions, potassium equilibrium potential (E_K) at the patch should be in the range of +5 to +12 mV.

The fact that the macrophage can be patch clamped opens up a myriad of experimental possibilities for characterizing the channels present in macrophages from a variety of sources, including small freshly isolated cells. In addition, the effects of specific ligands involved in secretory, chemotactic, or other cellular functions can be investigated.

ELECTROPHYSIOLOGICAL PROPERTIES OF THE MACROPHAGE-LIKE CELL LINE J774.1

Principal Investigators: E. K. Gallin and P. A. Sheehy

The J774 cell line, which exhibits both phagocytosis and chemotaxis, has been extensively studied as a model of macrophage function. Electrophysiological properties of J774.1 cells were determined using intracellular microelectrodes containing either 3 molar potassium chloride or potassium acetate (80-150 megaohms). The cells exhibited a wide range of resting membrane potentials (-8 to -91 millivolts), averaging -50.8 ± 3 SEM (n = 55). Their average input resistances and time constants were 117 Mohms ± 13 and 19 milliseconds (msec) ± 3, respectively. The specific membrane resistance was calculated from the time constant assuming a specific membrane capacitance of 1 microfarad/cm^2.

In some studies, cells were irradiated (2 kilorads, 500 rads/min, cobalt-60) to block cell division. Irradiated cells remained phagocytic but more than doubled their size within 4 days, thus becoming better subjects for intracellular recordings. These cells had resting membrane potentials, input resistances, and time constants of -60.1 mV ± 4 (range -18 to -92, n = 26), 94.5 Mohms ± 15, and 27 msec ± 6, respectively.

The majority of irradiated and control cells exhibited nonlinear current-voltage relationships characterized by prominent inward rectification and a high resistance or unstable region at -60 to -40 mV, similar to that

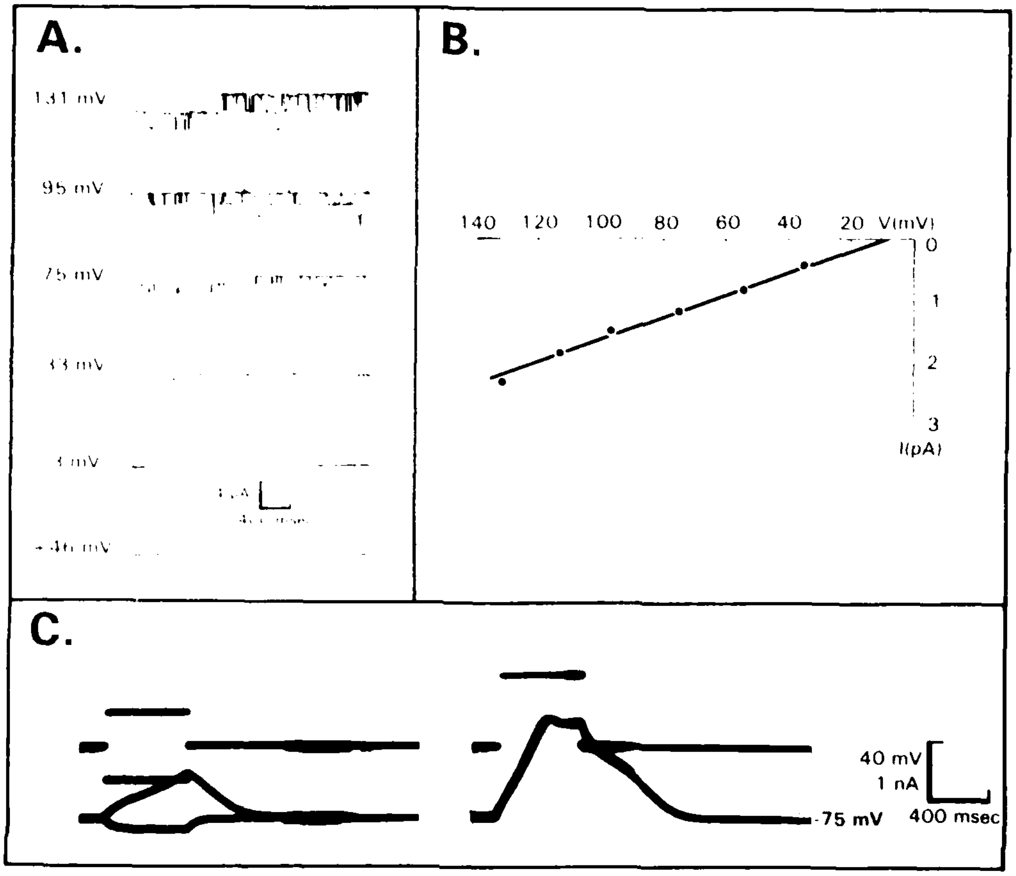

Figure 1. Patch clamp data from a mouse spleen macrophage. A. Single channel currents in a cell-attached patch with 150 mM KCl and 5 mM EGTA in electrode. Potential across patch membrane is indicated on left. Upward deflections represent inward currents. B. Current-voltage relationship of single channel currents shown in A. C. Whole-cell recording in current clamp mode of same cell shown in parts A and B.

In this study, the patch membrane was broken without destroying the gigaohm seal, and the cell was briefly clamped using the patch electrode. The cell had a zero current potential of -75 mV and showed pronounced inward rectification (Figure 1C). Similar channel activity and whole-cell clamp data were obtained in other experiments. The channel activity recorded under these conditions probably represents potassium currents through inward rectifying potassium channels, since the current fluctuations have the following characteristics: (a) they occur at voltages more negative than -33 mV, (b) they increase with membrane hyperpolarization, (c) they do not invert as the patch is depolarized beyond E_K, and (d) they are found in cells exhibiting inward rectification under whole-cell clamp.

previously reported in normal mouse macrophages (1). Addition of barium chloride ($BaCl_2$) eliminated both the inward rectification and the high-resistance region (Figure 1); rubidium and cesium also appeared to block, although less effectively. Spontaneous slow hyperpolarizations associated with an increase in conductance, similar to those previously noted in primary macrophage cultures, were seen in a few J774.1 cells. These data indicate that J774.1 cells exhibit electrophysiological properties similar to those of primary cultures of mouse macrophages, and may thus serve as a useful model for studies correlating macrophage effector functions with identified membrane ionic conductances.

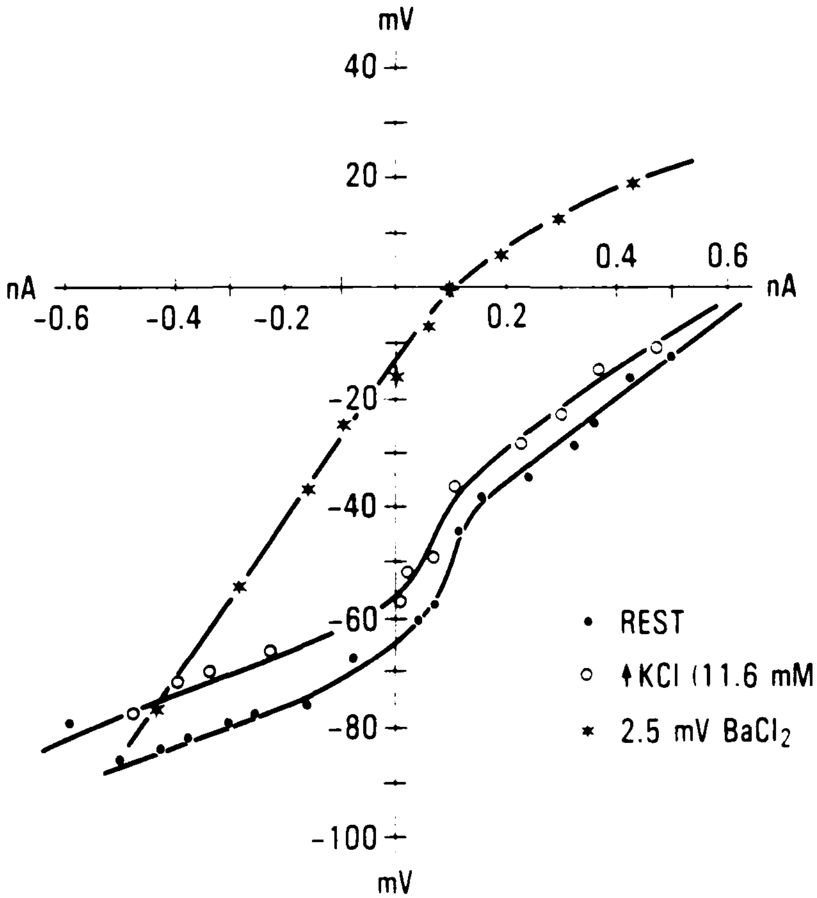

Figure 1. Current-voltage relationship of a J774.1 cell before and after the addition of 2.5 mM $BaCl_2$

RADIATION ENHANCES PMA-INDUCED H_2O_2 PRODUCTION AND LYSOSOMAL ENZYME CONTENT IN J774.1 CELLS

Principal Investigators: E. K. Gallin, S. W. Green, and P. A. Sheehy

J774 tumor cells exhibit a number of macrophage-like properties, some of which can be enhanced by lipopolysaccharides, 8-Br-cyclic adenosine monophosphate (AMP), and in vivo cultivation. We report that the exposure of J774.1 cells to a dose of radiation that inhibits cell division results in cell activation as assessed by lysosomal enzyme content, the reduction of nitroblue tetrazolium (NBT), and the release of H_2O_2 (hydrogen peroxide) in response to the activating agent phorbol myristate acetate (PMA). Cells were exposed to 20 grays (Gy) of cobalt-60 at 5 Gy/min (a dose that completely blocks tritiated thymidine incorporation). They were then cultured for up to 6 days, during which time they were assayed for total protein/cell, lysozyme and β-glucuronidase levels, Fc-mediated phagocytosis, and PMA-stimulation of both NBT reduction and H_2O_2 release.

Protein/cell doubled by day 2 postradiation and continued to increase through day 6. Intracellular levels of β-glucuronidase increased from 1681 ± 164 nanomoles/6 hr/milligram protein in nonradiated cells to 3029 ± 151 and 3273 ± 100 at 2 and 6 days postradiation, respectively. Lysozyme content also increased with time postradiation. Irradiated J774.1 cells incubated with PMA (1 microgram/milliliter) for 1 hr released 47 ± 5 and 126 ± 10 nmoles/mg protein of H_2O_2 at 2 and 6 days postradiation, respectively, compared to 25 nmoles/mg protein released by nonradiated cells. The percent of NBT-positive cells also increased from 5%-10% (control) to 70% at 4 days postradiation. More than 95% of cells in both control and radiated cultures ingested IgG-coated red blood cells throughout the study. The data indicate that, in addition to increasing cell size, radiation produces functional changes in J774.1 cells, and it may be a useful tool for modulating their activation.

REGULATION OF SODIUM-COUPLED HEXOSE TRANSPORT IN CULTURED KIDNEY EPITHELIA: THE IMPORTANCE OF CELL PROLIFERATION

Principal Investigator: A. Moran, *AFRRI*
Collaborators: J. S. Handler, *National Heart, Lung, and Blood Institute, National Institutes of Health, Bethesda, Maryland*
M. J. Hagan, *AFRRI*

We have previously shown that transport of the nonmetabolizable sugar alpha methyl glucoside (AMG) in LLC-PK_1 epithelia is regulated by the concentration of glucose in the growth medium. Glucose induces a change in the number of glucose transporters. The rate of AMG transport can be altered at any stage of development of the epithelium; cells that acquired a high transport rate in low-glucose medium lose transporters (down regulate) when transferred to a medium containing a high glucose concentration, and vice versa. Although it is not the result of cell selection, up and down regulation required 48 hr for expression. The rate of cell division assayed by incorporation of radiolabeled thymidine showed that LLC-PK_1 cells undergo significant cell division even after reaching confluency.

These findings raise the question of the role of cell division in this regulatory phenomenon. When cell division was inhibited by high doses of ionizing radiation (20 grays and above), thymidine incorporation essentially stopped. In contrast, AMG uptake was not as sensitive to radiation, and at 50 Gy, the uptake was still 70% of the uptake in the nonirradiated cells.

Down regulation was independent of radiation and cell division. However, radiation treatment strongly reduced the up regulatory expression (Figure 1). It is not clear whether the selective impairment of the up regulation of transporters is due to a process dependent on cell proliferation or to the expression of the gene specifically required for the up regulation process.

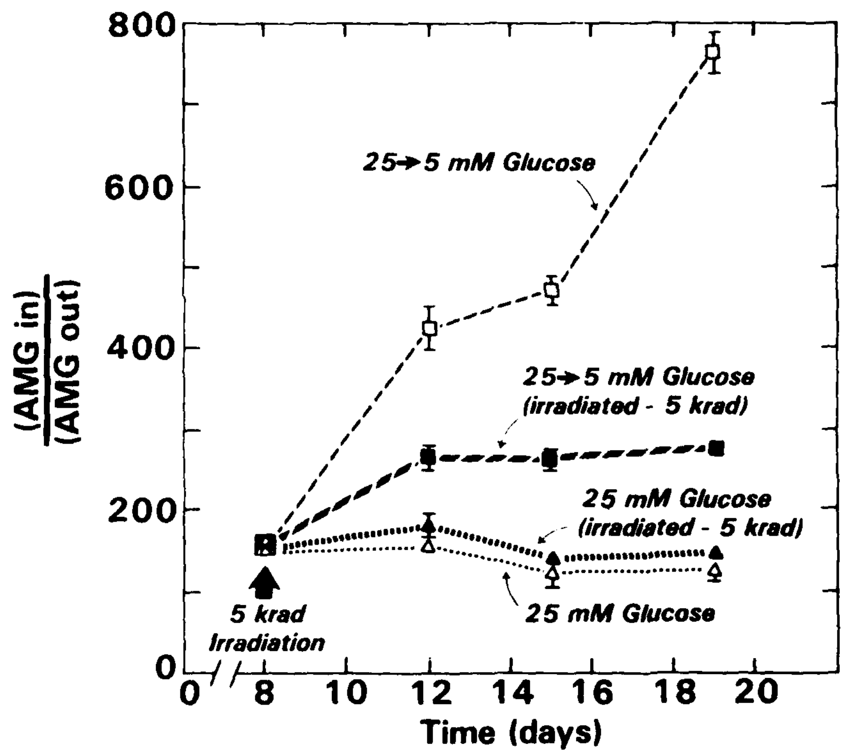

Figure 1. Effect of radiation on up regulatory process. Epithelia were grown in 25 mM glucose for 12 days before being switched to medium containing 5 mM glucose. Nonirradiated epithelia reached a plateau 1 week after switch. Irradiated epithelia reached only about one half of value reached by non-irradiated epithelia. Consistent with other findings, no change was observed in concentrating capacity of epithelium left in medium containing 25 mM glucose.

EFFECT OF RADIATION ON GASTROINTESTINAL TRANSPORT: MECHANISMS OF FLUID AND ELECTROLYTE LOSS

Principal Investigator: P. J. Gunter-Smith
Technical Assistance: T. Wilczynski and B. Case

Radiation produces profound effects on gastrointestinal physiology, which have collectively been called the gastrointestinal syndrome (1). Among these effects are fluid and electrolyte loss from the gastrointestinal tract, resulting in electrolyte imbalance of the organism (2, 3). In spite of these alterations in function, little is known concerning the mechanisms by which these changes occur.

The purpose of the present study is to elucidate the intestinal transport mechanisms associated with and responsible for radiation-induced fluid loss. In addition, the study seeks to determine the intracellular events leading to a radiation-induced change of the gastrointestinal tract from an absorptive organ to a secretory organ.

The electrolyte transport characteristics of the terminal ileum of New Zealand white rabbits were determined using the *in vitro* "short-circuit" technique. No difference was seen between the transepithelial short-circuit current (a measure of electrolyte transport) of control and irradiated animals determined 1 hr after 10, 50, or 100 grays (Gy) cobalt-60 irradiation. In addition, there were no apparent changes in the response of the tissue to an absorptive stimulus (alanine) or to a secretagogue (theophylline). In contrast, 24 hr following 10 Gy irradiation, the baseline short-circuit current was significantly greater than that of controls, and remained elevated for 96 hr. The response of the ileal segments to both alanine and theophylline decreased with time, becoming significantly decreased after 96 and 72 hr, respectively.

Since irradiated animals are also anorexic, the time course of short-circuit current changes of irradiated animals was compared to that of fasted controls. Although fasting produced changes in short-circuit current, irradiation produced changes in function that cannot be entirely accounted for by fasting.

These studies indicate that radiation induces changes in fluid and electrolyte transport properties, and are consistent with radiation-induced electrolyte secretion. Further studies are required to confirm this increased secretion and to determine the mechanisms associated with the change in the response of the tissue to both absorptive and secretory stimuli.

REFERENCES

1. Quastler, H. The nature of intestinal radiation death. Radiation Research 4: 303-320, 1956.

2. Curran, P. F., Webster, E. W., and Housepian, J. A. The effect of x-irradiation on sodium and water transport in rat ileum. Radiation Research 13: 369-380, 1960.

3. Jackson, K. L. and Entenman, C. The role of bile secretion in the gastrointestinal syndrome. Radiation Research 10: 67-79, 1959.

POSTRADIATION INCREASED INTESTINAL BLOOD FLOW BLOCKED BY ANTIHISTAMINES

Principal Investigators: L. G. Cockerham, T. F. Doyle, and M. A. Donlon
Technical Assistance: C. J. Gossett-Hagerman

Radiation-induced systemic hypotension is accompanied by increased intestinal blood flow and an increased hematocrit in dogs. Histamine infused into the small intestine causes an increase in intestinal blood flow and a copious secretion of fluid following edema. This study was performed to determine whether these effects could be diminished by prior administration of H_1 and H_2 histamine blockers.

Dogs were given an intravenous infusion of mepyramine (0.5 milligrams/minute) and metiamide (0.25 mg/min) for 1 hr before and 1 hr after radiation to block the effects of histamine. Mean systemic arterial blood pressure, intestinal blood flow, and hematocrit were monitored for the 2 hr. Systemic plasma histamine levels were determined simultaneously.

Data obtained indicated that the H_1 and H_2 blockers, given simultaneously, were successful in blocking the increased intestinal blood flow and the increased hematocrit seen after 10 kilorads of whole-body gamma radiation. However, the postradiation hypotension was unaffected, with the mean systemic arterial blood pressure falling to a level 28% below the preradiation level. Also, there was no significant difference between the preradiation and postradiation histamine levels.

These findings implicate histamine as a causative agent in the radiation-induced increase in intestinal blood flow and hematocrit but not for the gradual decrease in postradiation blood pressure.

POSTRADIATION HISTAMINE VARIATIONS IN THE BEAGLE

Principal Investigators: L. G. Cockerham, T. F. Doyle, and M. A. Donlon
Technical Assistance: E. A. Helgeson

Radiation-induced hypotension in the beagle is accompanied by increased intestinal blood flow and hematocrit. This study was performed in order to correlate these radiation-induced changes with plasma histamine levels following radiation. The histamine levels were monitored in the systemic arterial circulation and the hepatic portal vein before and after radiation. In order to examine the effect of radiation on the mobilization of total-body histamine stores, compound 48/80 was given intravenously and histamine responses were monitored in both control and radiated animals.

Data obtained indicated that 10 kilorads of whole-body gamma radiation produced a decrease in systemic mean blood pressure, an increase in intestinal blood flow, and an increase in hematocrit. Concurrently, the mean plasma histamine/systemic arterial circulation values increased and the plasma histamine/hepatic portal vein levels decreased. Compound 48/80 produced a marked increase in plasma histamine levels in both control and radiated animals; however, the levels found in the radiated animals were consistently lower than those in the controls. This implies that histamine may mediate these observed intestinal responses and that the mobility of histamine is decreased in radiated animals.

EFFECTS OF HIGH-ENERGY ELECTRON RADIATION ON VENOUS RETURN IN THE ANESTHETIZED RAT

Principal Investigator: R. N. Hawkins

In many animal species, whole-body radiation produces a shocklike sequela with an apparent decrease in venous return. To determine if a similar cardiovascular response occurs in rats, 14 chloralose-anesthetized animals were exposed to 10 kilorads of 18.5-megaelectronvolt electrons.

Preradiation cardiovascular values were mean arterial pressure, 109 ± 6 millimeters mercury (mm Hg); heart rate, 356 ± 18 beats per min; cardiac output, 113 ± 7 milliliters/min; total peripheral resistance, 1.0 ± 0.1 mm Hg · min/ml; mean circulatory filling pressure, 5.5 ± 0.3 mm Hg; and gradient for venous return, 5.5 ± 0.2 mm Hg. Radiation resulted in an immediate but transient decrease in mean arterial pressure to 68 ± 5 mm Hg. By 1 min after the end of the radiation pulse, the mean arterial pressure, heart rate, cardiac output, and total peripheral resistance were not significantly different from preradiation values, whereas mean circulatory filling pressure and gradient for venous return were significantly elevated ($p < 0.05$) to 7 ± 3 mm Hg and 6.5 ± 0.2 mm Hg, respectively. Throughout the remainder of the 60-min postradiation observation period, mean circulatory filling pressure and gradient for venous return remained greater than preradiation values.

These data show that the rat is able to make significant compensatory adjustments in venous return after exposure to ionizing radiation.

EFFECTS OF IONIZING RADIATION ON THE MONO-SYNAPTIC MUSCLE STRETCH REFLEX

Principal Investigator: D. J. Braitman
Technical Assistance: V. A. Kieffer

We have examined the effects of localized cervical spinal cord irradiation on the monosynaptic stretch reflex in bicep muscle. Monkeys have been trained on tasks that allow precise computer measurements of the monosynaptic component of the electromyogram activity recorded from bicep muscles during an abrupt stretch of the arm. Animals were trained and the baseline activity was established.

Six monkeys were exposed to 1200 to 1500 rads (13.5 mega electronvolts) in the AFRRI linear accelerator. After irradiation, two animals showed an increase in motoneuron activity during reflex movement, while others exhibited no significant change in electromyogram activity. We are conducting histological examinations of the spinal cord to determine if changes in morphology of the cord may account for the discrepancy in behavior.

DESENSITIZATION TO GLUTAMATE AND ASPARTATE IN PYRIFORM CORTEX BRAIN SLICES

Principal Investigator: D. J. Braitman
Technical Assistance: E. Solberg

The brain area known as pyriform cortex is very sensitive to ionizing radiation (1). In a continuing investigation of the mechanism of action of ionizing radiation on the central nervous system, examination has been made of the effects of excitotoxic amino acid neurotransmitters on isolated slices of rat pyriform cortex.

In a previous report (2), this laboratory presented electrophysiological and pharmacological evidence that neither L-glutamate nor L-aspartate appeared to be the excitatory neurotransmitter from the lateral olfactory tract to pyriform cortex pyramidal neurons. The present study has investigated the ability of repeated applications of these amino acid receptor agonists to desensitize the endogenous synaptic receptors in the in vitro pyriform cortex slice preparation.

Double-shock orthodromic stimulation to the lateral olfactory tract delivered every 4 sec throughout the experiment evoked field potentials that were recorded from the pial surface of the submerged, constantly perfused tangential slice of rat pyriform cortex [350 microns (μ) to 450 μ thick]. To quantify the action of amino acids added to the perfusate, the amplitude of the slow-wave component of the field, representing the population excitatory postsynaptic potential, was measured and compared to control values.

Initial application of 2 x 10^{-3} molar (M) glutamate for 5 min resulted in a significant decrease in the amplitude of the field potential due to the depolarizing action of glutamate. The amplitude of the field potential returned to control (pre-drug values) 10 to 15 min after termination of the drug application. A second perfusion of 2 x 10^{-3} M glutamate was less effective. That is, the amplitude of the field potential decreased less than it did after the first application of glutamate, suggesting desensitization of the receptor-mediated glutamate depolarization. Successive applications had even smaller effects (Figure 1). However, the amplitude of the field potential continued to return to control value after termination of the glutamate perfusion even though the glutamate receptors were still desensitized.

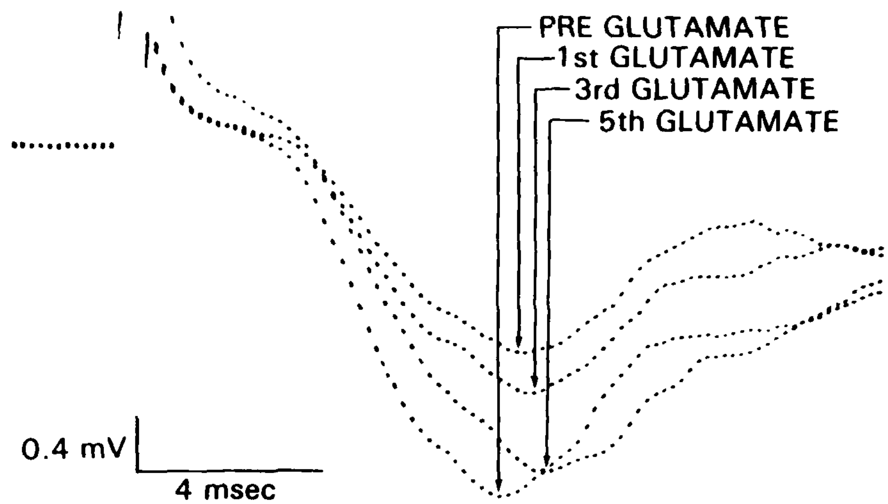

Figure 1. Tolerance produced by repeated applications of L-glutamate. Field potentials evoked by stimulation of lateral olfactory tract were progressively smaller in amplitude compared to control (pre-glutamate) after repeated 5-min applications of L-glutamate. Each trace represents average of five computer-averaged field potentials.

The response to repeated application of aspartate desensitized in a fashion similar to glutamate. The responses to D-glutamate, which is not taken up by the high-affinity uptake system, also desensitized after repeated applications. This indicates that the phenomena seen in these experiments did not involve the facilitation of an inactivation mechanism.

Thus, although exogenously applied L-glutamate and L-aspartate desensitize their postsynaptic receptor sites, they do so without affecting the receptors to the endogenous neurotransmitter. The failure to find cross-desensitization between L-glutamate and L-aspartate receptors and the receptors at the terminal synapses of the lateral olfactory tract is further evidence that neither glutamate nor aspartate is the excitatory transmitter on pyriform pyramidal neurons.

REFERENCES

1. Timiras, P. S., Wolley, D. E., Silva, A. J., and Williams, B. Changes in electrical activity of the olfactory cortex induced by radiation and drugs. Radiation Research 30: 391-403, 1967.

2. Hori, N., Auker, C. R., Braitman, D. J., and Carpenter, D. O. Pharmacologic sensitivity of amino acid responses and synaptic activation in *in vitro* prepyriform neurons. *Journal of Neurophysiology* 48: 1289-1301, 1982.

MEMBRANE CURRENTS OF CULTURED RAT SYMPATHETIC NEURONS UNDER VOLTAGE CLAMP

Principal Investigator: J. E. Freschi

The vertebrate superior cervical ganglion (SCG) is an attractive preparation for neurobiological studies because of its experimental accessibility and its diversity of synaptic interactions. Further experimental *simplification* can be achieved using tissue-culture techniques. Most of the physiological and pharmacological properties of SCG neurons *in vivo* can be reproduced in culture, yet cultured SCG neurons exhibit a high degree of plasticity, which allows the experimenter to select types of differentiated properties, such as neurotransmitter synthesis.

In order to exploit the advantages offered by tissue culture, I studied dissociated neonatal rat sympathetic neurons under two-electrode voltage clamp. This technique offers the opportunity to resolve more precisely the ionic mechanisms underlying neurotransmitter effects. Because of the small size or inaccessibility of mammalian neurons, few studies have used the two-electrode voltage clamp to study mammalian neuronal membrane currents.

The development of techniques for voltage clamping with single microelectrodes has facilitated the investigation of mammalian neurons, but inherent limitations of the technique have generally permitted examination of only small currents over a limited voltage range. Voltage clamp has been used with success by several groups of investigators to identify and characterize a

number of voltage- and time-dependent conductances in bullfrog sympathetic neurons. However, mammalian sympathetic neurons have not been studied as thoroughly.

There are several reasons for studying mammalian sympathetic neurons and comparing them with amphibian ganglion neurons. (a) Frog sympathetic ganglia comprise two types of principal neurons that differ in size, axonal conduction velocity, and synaptic inputs. No such subtypes of neurons have been described in mammalian sympathetic ganglia (although immunofluorescence studies suggest distinct peptidergic subpopulations). (b) Amphibian ganglion cells are unipolar and have a restricted pattern of synaptic innervation, whereas mammalian SCG neurons are multipolar and have a more diffuse pattern of innervation. (c) Luteinizing hormone-releasing factor has been identified as a possible neurotransmitter in frog ganglia but not in the mammalian SCG. On the other hand, angiotensin II has potent excitatory effects in mammalian but not frog sympathetic ganglia. (d) The rat SCG in culture has been a highly valuable preparation for developmental studies. Detailed knowledge of ionic conductances can form the background for studies into the developmental biology of ionic channels.

The purpose of this work is to describe the ionic conductances that can be identified on the basis of their voltage- and time-dependent characteristics. The results provide the basis for further detailed studies of individual ionic conductances identified in this report.

Sympathetic neurons, dissociated from neonatal rat superior cervical ganglia, were voltage-clamped with two microelectrodes. Depolarization from resting potential activated a rapid transient inward current carried by sodium and a slow inward current blocked by cobalt.

Depolarization from resting potential also activated up to three kinetically distinct outward currents, which were further studied by tail current analysis. Following long depolarizing steps, outward current decayed biphasically. The fast phase (delayed rectifier) decayed over 10-20 milliseconds (msec). The slow phase (calcium dependent) required as much as 1-2 sec to decay to baseline. A small component of the total outward current was a persistent current activated between -70 and -30 millivolts (mV) (M current), which decayed over 200-300 msec. This current was studied in isolation

following hyperpolarizing steps from potentials negative to the threshold for activation of the other delayed outward currents.

Tetraethylammonium blocked the fast tail current, partially inhibited the slow tail current, and reduced M currents. Cobalt selectively decreased the slow tail current. Muscarine blocked M current but not other outward currents.

A transient outward current was activated by depolarization from only holding potentials negative to -60 mV. This current peaked in 10-20 msec and decayed over about 50 msec. A persistent ("anomalous") inward current was evoked by hyperpolarizing steps from only holding potentials negative to -50 to -60 mV.

These seven membrane currents may be separately characterized on the basis of their voltage- and time-dependent properties. Further identification is aided by the use of channel-blocking chemicals, although the latter may lack specificity, especially when used to study potassium channels.

HISTAMINE AND HYDROGEN PEROXIDE MODULATE ELECTRICAL ACTIVITY OF HIPPOCAMPAL NEURONS

Principal Investigator: T. C. Pellmar

Factors that might mediate effects of ionizing radiation were tested on a hippocampal brain slice preparation. Ionizing radiation causes mast cells to release histamine as well as other factors. Histamine in concentrations as low as 1 micromolar has profound effects on CA1 pyramidal cells of the guinea pig hippocampus. The post-train afterhyperpolarization (AHP) (a calcium-mediated potassium current) is blocked by histamine. The reduction of the AHP can result either by a direct decrease in the potassium current or by a decrease in calcium influx. Voltage-clamp analysis has indicated that the latter is the actual mechanism. In the presence of pharmacological agents that block potassium currents, the slow inward calcium current can be directly observed. Addition of histamine under these conditions clearly reduces the net inward current. Potassium currents other than the calcium-mediated potassium current (i.e., A current, M current, and Q current) do not appear altered by histamine.

Lipid peroxidation is a likely consequence of the generation of free radicals during ionizing radiation. To generate free radicals in vitro, hydrogen peroxide (0.005%-0.01%) and ferrous sulfate were added to the bathing solution of hippocampal brain slices. Dramatic changes in the extracellular potentials elicited by orthodromic stimulation were observed in the CA1 pyrimidal cells. The orthodromically stimulated population spike recorded in the cell body layer was substantially reduced, as was the population excitatory postsynaptic potential (EPSP) recorded in the dendritic layer. Yet the presynaptic volley and the antidromic spike were unchanged. The decrease in the population EPSP was not sufficient to account for the decrease in the population spike. These data suggest that peroxide is altering both the efficacy of synaptic transmission and the efficacy of postsynaptic spike generation.

RADIATION SCIENCES DEPARTMENT

The Radiation Sciences Department manages both research and support functions in the fields of radiobiology and radiation physics. This includes the operation of radiation sources, dosimetry, medical imaging, and biophysics. The Department is made up of the Nuclear Sciences Division, Radiological Physics Division, Biological Spectroscopy Division, and Radiation Sources Division.

Nuclear Sciences Division

The Nuclear Sciences Division conducts research on the effects of ionizing radiation on the morphology and functional changes in the different organic systems by *in vitro* and *in vivo* radiotracer methods. *In vivo* studies deal mainly with the tissue distribution of various radiotracers and radiopharmaceuticals in various organs and tissues in both small- and large-animal models. *In vivo* studies use scintigraphic methods with scintillation cameras, tomographic imaging instruments, and computerized techniques of nuclear scintigraphic imaging.

The major areas of research in this Division include studies of

> Structural and functional changes of the respiratory system by use of radioactive gases and radiolabeled microspheres after exposure of experimental animals to various doses of photon and neutron irradiation
>
> Gastrointestinal and hepatobiliary kinetics
>
> Metabolic behavior of muscarinic receptors in tissues of irradiated experimental animals
>
> Radiation damage using biological detectors
>
> Structural and functional changes in the cardiovascular and central nervous systems in irradiated animals, using electronic and computer equipment of modern nuclear scintigraphic techniques.

Radiological Physics Division

The Radiological Physics Division serves both support and research functions in the field of physical radiation dosimetry. In support of radiobiology and other experiments conducted using AFRRI radiation facilities, the Division provides radiation field measurements and evaluations that are fundamental to the interpretation of experimental outcomes. Research programs include developmental efforts to expand and upgrade the radiation measurements program technology base, and investigative efforts on questions in operational dosimetry relevant to the military services.

Biological Spectroscopy Division

The primary function of the Biological Spectroscopy Division is to develop experimental techniques and models that use the methods of high-resolution nuclear magnetic resonance, electron spin resonance, and optical spectroscopy, to understand at a molecular level the damage and events incurred in a biological specimen following exposure to ionizing radiation. Future research at AFRRI and in collaboration with investigators at other research centers will concern (a) ionizing radiation damage in solid films of deoxyribonucleic acid (DNA), (b) muscular fatigue induced by ionizing radiation, (c) assessment of cardiovascular radiation injury using nuclear magnetic resonance spectroscopy, (d) nuclear magnetic resonance characterization of metabolism in culture single-cell systems, and (e) DNA interactions with drugs and proteins.

Radiation Sources Division

This Division operates, maintains, and upgrades AFRRI's major radiation source facilities, in direct support of the research mission, in accordance with applicable Federal Regulations and U.S. Nuclear Regulatory Commission license conditions. These facilities include a 1.0-megawatt (t) TRIGA Mark-F pulsing nuclear research reactor, a 54-MeV Varian electron linear accelerator, a 325-KCi cobalt-60 gamma photon irradiation facility, a 320-KeV Philips industrial X-ray unit, and a 4200-Ci Theratron-80 cobalt-60 gamma irradiator. The Division also provides consultation to management and staff on the use of radiation source facilities in support of the scientific research program.

EFFECT OF TWO TUMORS (METASTATIC AND NON-METASTATIC) ON TISSUE DISTRIBUTION OF GALLIUM-67 CITRATE IN THE RAT

Principal Investigator: A. Durakovic
Collaborators: R. R. Eng and J. J. Conklin
Technical Assistance: J. D. Stewart, M. E. Corral, M. E. Flynn, N. L. Fleming, and J. K. Warrenfeltz

We studied the effect of metastatic (13762) and non-metastatic (R3230 AC) mammary adenocarcinoma on the tissue distribution of gallium-67 citrate in Fischer 344 female rats. The homogenate (0.1 milliliter) of each tumor was injected subcutaneously in the right footpad of separate groups of rats and allowed to grow for 10 days. After the adequate tumor growth period, an arbitrary time of day 0 was established. The rats from the metastatic tumor group were studied from day 2 to 24, and the nonmetastatic tumor group from day 2 to 30.

All animals were injected with 30 microcuries of gallium-67 citrate, and were sacrificed by halothane anesthetic 48 hr after gallium-67 intravenous injection. The tissue samples of blood, lung, heart, liver, spleen, kidney, adrenal, stomach, small and large intestines, ovaries, and lymph nodes (popliteal, lumbar, and mediastinal) were obtained and counted in a gamma well counter. The control group consisted of four animals; the tumor-bearing groups consisted of seven to eight animals at each time point.

Statistical analysis was performed, and the results were expressed as percent dose per gram of the tissue. The liver uptake was not significantly altered by the presence of either malignant or nonmalignant tumor, except for increased uptake on day 24 in the metastatic tumor group ($p < 0.05$). The splenic uptake of gallium-67 was not different between either of the tumor groups and the controls. Adrenal uptake of gallium-67 was higher on days 10 and 14 ($p < 0.01$), and also in the popliteal lymph nodes on days 7, 10, and 18 in the metastatic tumor group ($p < 0.05$). The lumbar and mediastinal lymph nodes were not different from the control. No difference in the lymph nodes was observed in the nonmetastatic tumor group. This group demonstrated inconsistent elevation of gallium-67 in the lung on days 15 and 30 ($p < 0.05$) and in the thymus on day 30 ($p < 0.05$).

All results demonstrate that the distribution of gallium-67 in normal tissues appears to be largely unaffected by the presence or the type of metastatic or nonmetastatic mammary adenocarcinoma in rats. The results of this work are consistent with (a) reports indicating that gallium-67 concentration in the target tissues of tumor-bearing animals remains unchanged (1, 2), and (b) data of gallium-67 distribution in human tissue in which diversion of gallium-67 to tumor tissue did not affect its concentration in normal tissues (3). Our data indicate that host reaction to the tumor does not modify uptake characteristics in the normal tissues of tumor-bearing animals.

REFERENCES

1. Sephton, R. and Harris A. Gallium-67 citrate uptake by cultured tumor cells, stimulated by serum transferrin. Journal of the National Cancer Institute 54: 1263-1266, 1975.

2. Sephton, R., Hodgson, G., DeAbrew, S., and Harris A. Ga-67 and Fe-59 distributions in mice. Journal of Nuclear Medicine 19: 930-935, 1978.

3. Nelson, B., Hayes, R. L., Edwards, C. L., Kniseley, R. M., and Andrews, G. A. Distribution of gallium in human tissues after intravenous administration. Journal of Nuclear Medicine 13: 92-100, 1971.

TISSUE DISTRIBUTION OF GALLIUM-67 IN RATS BEARING METASTATIC ADENOCARCINOMA IN THE FOOTPAD AND FLANK REGION

Principal Investigator:	A. Durakovic
Collaborators:	R. R. Eng and J. J. Conklin
Technical Assistance:	J. D. Stewart, M. E. Corral, M. E. Flynn, N. L. Fleming, and J. K. Warrenfeltz

The effect of metastatic mammary adenocarcinoma (13762) on the tissue distribution of gallium-67 citrate was studied in female Sprague-Dawley rats (250 grams). The tumor homogenate (0.1 milliliter) was introduced subcutaneously in the right footpad or the right flank region of the experimental animals. Two weeks after tumor homogenate administration, all animals were injected intravenously with 60 microcuries gallium-67 citrate. Twenty-four hr postinjection, the whole-body scintigram was obtained for each animal by measuring 93-, 184-, and 300-kilo-electronvolt gallium-67 energy peaks by the use of a gamma camera with a high-energy collimator (Elscint LFC-9). After whole-body scans were obtained, all animals were sacrificed using halothane anesthesia.

The tissue samples of blood, liver, spleen, lung, femur, stomach, small and large intestines, kidney, adrenal, ovary, uterus, lymph node, heart, as well as nonnecrotic and necrotic tumors were obtained and counted in an LKB Ultrogamma well counter. The control group consisted of 6 animals, footpad tumor group 8, and flank tumor group 12. Statistical analysis of the tissue samples was performed, and results were expressed as a mean percent dose per gram of tissue weight.

The scintigraphic images demonstrate normal distribution in the control animals with prominent liver, abdominal, and hip joint concentration. Footpad tumor-bearing animals demonstrated increased gallium-67 accumulation in the region of the tumor and the ipsilateral popliteal lymph node. The flank tumor group demonstrated a distinct difference of gallium-67 concentration in the viable and necrotic tumors. The solid tumor showed high gallium-67 concentration in both scintigraphic and *in vitro* studies, with markedly diminished uptake in the necrotic central area of the tumor.

Organ distribution of gallium-67 in the control animals demonstrated the highest concentration in the liver, femur, spleen, and kidney, followed by the stomach and the large and small intestines. The lowest concentration of gallium-67 was found in the brain, lymph nodes, and heart. Footpad tumor-bearing animals had the highest gallium-67 concentration in the tumor tissue and ipsilateral popliteal lymph nodes. Distribution was similar to the control group in most of the tissues, with the exception of higher gallium uptake in the lung and spleen ($p < 0.05$). Flank tumor-bearing animals had the highest gallium concentration in the solid tumor, followed by the spleen, liver, lung, stomach, large intestine, and small intestine. Gallium-67 uptake was significantly higher in the lung and the spleen ($p < 0.05$); other organs showed no difference from the control values.

Our data demonstrate that metastatic mammary adenocarcinoma results in high gallium-67 concentration in the viable tumor without affecting gallium-67 distribution in the other organs. The lack of gallium-67 incorporation in necrotic regions of the tumor, which are evident by scintigraphic and tissue distribution data, support the theories of reduced flow and of depleted receptor sites and carrier mechanisms in the nonviable tumor (1-4).

REFERENCES

1. Swartzendruber, D. C., Nelson, B., and Hayes, R. L. Gallium-67 localization in lysosomal-like granules of leukemic and nonleukemic murine tissues. Journal of National Cancer Institute 46: 941-952, 1971.

2. Gunasekera, S. W., King, L. J., and Lavender, J. P. The behaviour of tracer gallium-67 towards serum proteins. Clinica Chimica Acta 39: 401-406, 1972.

3. Hoffer, P. B., Huberty J., and Khayam-Bashi, K. J. The association of Ga-67 and lactoferrin. Journal of Nuclear Medicine 18: 713-717, 1977.

4. Larson, S. M., Rasey, J. S., Allen, D. R., Nelson, N. J., Grunbaum, Z., Harp, G. D., and Williams, D. L. Common pathway for tumor cell uptake of gallium-67 and iron-59 via a transferrin receptor. Journal of National Cancer Institute 64: 41-53, 1980.

EFFECT OF WHOLE-BODY IRRADIATION WITH PHOTONS AND FISSION NEUTRONS ON ORGAN DISTRIBUTION OF GALLIUM-67 IN THE RAT

Principal Investigator: A. Durakovic
Collaborators: R. R. Eng and J. J. Conklin
Technical Assistance: J. D. Stewart, M. E. Corral, M. E. Flynn, N. L. Fleming, J. K. Warrenfeltz, J. L. Munno, and S. Miller

The retention of gallium-67 has been reported to significantly decrease after acute whole-body irradiation. Swartzendruber and Hubner (1) have observed this finding in mice, and have associated it with radiation damage to the synthetic sites of a carrier molecule for gallium-67, in the cellular organelles such as lysosomes. Subsequent reports confirmed the finding of reduced whole-body retention of gallium-67 after irradiation in the rat, explaining it by an alteration in serum binding of gallium-67 after a single-dose whole-body photon irradiation of 720 roentgens. Bradley et al. (2) studied radiation effects on the distribution of gallium-67 in the rat, and reported decreased tissue uptake of gallium-67 after irradiation. They postulated an association of the radiation-induced gallium decrease in the rat with increased serum iron levels and reduced unsaturated iron-binding capacity, resulting in decreased tissue uptake and increased urinary excretion of gallium-67.

In the present work we have studied the effect of a single-dose whole-body irradiation with cobalt-60 and fission neutrons on the gallium-67 distribution in different organs of the rat at various intervals after irradiation. All experiments were performed on female Sprague-Dawley rats (250 grams) maintained on a normal rat feed and water ad libitum.

Each of three groups of animals was irradiated with a specific dose of cobalt-60 photons (2, 4, and 6 grays) at 0.4 Gy/minute. Three other groups received whole-body fission neutron irradiation at 2, 4, and 6 Gy (by a Mark-F TRIGA reactor). Irradiated animals were injected with 1.11 mega becquerel gallium-67 citrate on the day of irradiation and also 6, 14, 22, and 30 days after irradiation. Animals were sacrificed at 48 hr after gallium-67 administration, and the concentration of gallium-67 was determined in the blood, lung, heart, liver, spleen, kidney, adrenal, stomach, small and large intestines, ovaries, uterus, lymph nodes (right and left popliteal, lumbar, and mediastinal), thymus, muscle,

femur, and brain. The tissue samples were counted in an LKB Ultrogamma well counter. The results are expressed as percent dose gallium-67 per gram of tissue with a standard error of the mean. Each time point of the experimental groups consisted of five animals. A group of five nonirradiated control animals was sacrificed by halothane anesthetic along with irradiated animals at each time interval, and the distribution of gallium-67 was obtained in the same organs.

Our data demonstrate that whole-body photon radiation had little effect on the gallium-67 concentration in the examined organs for most of the experimental time intervals. Gallium concentration in the control animals was highest in the bone, followed by the liver, spleen, kidney, lymph nodes, and stomach. The lowest concentration of gallium-67 was observed in the brain, heart, and skeletal muscle. Most of the tissues were not affected in their gallium-67 uptake by either photon or neutron irradiation. The exceptions of significant decrease of gallium-67 were observed in the liver (2 and 4 Gy) on day 2 and (6 Gy) on days 8, 16, and 24 after cobalt-60 irradiation ($p < 0.05$); lung (6 Gy) 24 days; spleen (6 Gy) 32 days; stomach (4 Gy) 2 and 16 days; and the small and large intestines (6 Gy) on 16 and 24 days postirradiation ($p < 0.05$). An increase in gallium-67 uptake was observed in the mediastinal (6 Gy) at 16 and 24 days; popliteal lymph nodes (6 Gy) at 24 days; and lumbar lymph nodes (4 and 6 Gy) at 2, 6, and 24 days post-irradiation ($p < 0.05$).

Neutron-irradiated animals demonstrated no consistent differences in gallium-67 uptake when compared to the controls. The exceptions of lower gallium-67 uptake were noted in the lung (2 and 4 Gy) at 16 and 24 days; stomach (4 Gy) at 8 days; small and large intestines (2, 4, and 6 Gy) at 2, 16, and 24 days; thymus (2, 4, and 6 Gy) at 2 and 32 days; and spleen (4 Gy) at 8 days postirradiation ($p < 0.05$). Increased gallium-67 uptake was observed in popliteal lymph nodes (2, 4, and 6 Gy) at 2, 16, and 32 days postirradiation ($p < 0.05$); lumbar (2 Gy) at 16 days; and mediastinal lymph nodes (4 Gy) at 2 and 16 days postirradiation ($p < 0.05$).

These results demonstrate that gallium-67 distribution and quantitative tissue uptake are not consistently altered after photon or neutron irradiation at the doses of 2, 4, and 6 Gy in the five time intervals after irradiation. Our data indicate that the pronounced decrease of gallium-67 in the tissue, which has been described within 24 hr after irradiation (3), is not present at the radiation levels and the time intervals of our experiments.

Different authors have observed a significant decrease of gallium-67 tissue uptake after acute whole-body irradiation. Discussion of the mechanisms of gallium decrease postulated the radiation effect on specific cellular organelles and synthetic sites of gallium carrier molecules (1). In our studies, neither cobalt-60 nor neutron irradiation produced a consistent alteration in gallium tissue uptake. This could be due to our longer experimental intervals after irradiation, compared to other studies in which a radiation effect on decrease of gallium uptake was observed. Our observations, based on 48 hr uptake of gallium-67 at different time intervals after cobalt-60 or fission neutron irradiation, suggest a possibility of the restitution of gallium uptake and transport mechanisms, known to be altered by acute whole-body irradiation.

REFERENCES

1. Swartzendruber, D. C., and Hubner, K. F. Effect of external whole body X-irradiation on gallium-67 retention in mouse tissues. Radiation Research 55: 457-468, 1973.

2. Bradley, W. P., Alderson, P. O., and Weiss, J. F. Effect of iron deficiency on the biodistribution and tumor uptake of gallium-67 citrate in animals. Journal of Nuclear Medicine 20: 243-247, 1979.

3. Fletcher, J. W., Herbig, F. K., and Donati, R. M. Gallium-57 citrate distribution following whole-body irradiation or chemotherapy. Radiology 117: 709-712, 1975.

MYOCARDIAL SCINTIGRAPHY WITH TECHNETIUM-99m PYROPHOSPHATE AND GATED BLOOD POOL HEART FUNCTION STUDIES IN DOGS AFTER ACUTE IRRADIATION OF THE HEART

Principal Investigator: A. Durakovic
Collaborators: R. R. Eng and J. J. Conklin
Technical Assistance: J. D. Stewart, J. C. Munno, M. E. Corral, N. L. Fleming, J. K. Warrenfeltz, S. Miller, and M. E. Flynn

Cardiac radiation damage has been described in various animal models and in human studies. Radiation-induced heart injury in the experimental model was first suggested by Hartman in 1927 (1), followed by numerous reports describing wide tolerances to irradiation (2-4). More recent reports suggest that the acute cardiac morbidity dose is in a lower range (3000-7000 roentgens in the dog) than previously considered (5, 6).

In this work, we have studied the effect of a single dose of cobalt-60 irradiation (3000 and 6000 rads) on heart function and tissue damage by cardiac function (MUGA) studies and technetium-99m pyrophosphate scintigraphic studies in male beagle dogs. Two groups of three beagle dogs were irradiated bilaterally with a single dose of cobalt-60 irradiation confined to the heart. The midline-tissue dose rate was 57 rads/min. Three dogs with isoproterenol-induced myocardial infarct served as a model for the infarct-avid study.

Baseline technetium-99m pyrophosphate and MUGA studies were obtained before the administration of isoproterenol or radiation. MUGA studies were performed on irradiated animals on days 3, 9, and 22 after irradiation, and pyrophosphate studies on days 1, 6, and 8 after irradiation. The animals with isoproterenol-induced heart damage received MUGA studies on days 2 and 7 and pyrophosphate studies on days 4 and 9 after drug administration. Control animals were sacrificed at parallel time intervals.

All animals were sacrificed by an intravenous euthanatizing agent (T-61). The heart was dissected out of the thoracic cavity. Tissue samples were obtained of the left and right ventricles, apex, septum, left and right atria, left and right auricles, papillary muscle, aorta, pulmonary artery, and left and right lungs. The samples were counted in an LKB Ultrogamma well counter. Statistical analysis was

performed, and technetium-99m activity was expressed as a percent dose per gram of the tissue with a standard error of the mean. Electrocardiographic recordings were obtained on each animal during heart function studies. All tissue samples were analyzed by histopathological examination.

The results demonstrate scintigraphic evidence of diffuse myocardial damage in isoproterenol-injected dogs, as observed by the intensity of technetium-99m pyrophosphate uptake of 4/4+ on day 4 after isoproterenol administration. The study was negative on day 1 and day 8. Ejection fraction did not change significantly from the baseline values during three post-isoproterenol intervals.

Electrocardiographic studies of isoproterenol-treated dogs demonstrated acute myocardial damage on day 4, corresponding to positive technetium-99m pyrophosphate scans. Electrocardiographic data demonstrated chronic postnecrotic changes on day 8 after isoproterenol injection. Histopathological examination of the heart in the isoproterenol group demonstrated disseminated foci of myocardial necrosis with fibroplasia and inflammatory infiltrates. The tissue samples of different segments of the hearts of irradiated dogs showed no evidence of elevated technetium-99m pyrophosphate uptake in either the 3000- or 6000-rad group. Scintigraphic studies demonstrated no difference in the myocardial images between baseline and postirradiation studies. MUGA studies demonstrated no difference between the baseline left ventricular ejection fraction (LVEF = 43.0 $\pm$ 4.2) and the 3000-rad group on either day 3 (LVEF = 49.7 $\pm$ 0.3) or day 22 (LVEF = 52.5 $\pm$ 13.5) postirradiation. In the 6000-rad group no difference in LVEF was seen between the baseline (51.3 $\pm$ 1.7) and the irradiated group (46.3 $\pm$ 1.8) at 9 days postirradiation.

Our results indicate that radiation-induced changes in the heart of a dog irradiated with 3000 and 6000 rads include minimal to mild multifocal cardiac and pulmonary perivasculitis, without necrotic changes by histological examination. No evidence was seen of radiation-induced heart damage by either gated acquisition heart studies or technetium-99m pyrophosphate scintigraphic studies in dogs in the early time periods after irradiation.

REFERENCES

1. Hartman, F. W., Bolliger, A., Doub, H. P., and Smith, F. J. X-ray: An experimental and clinical study. Bulletin of Johns Hopkins Hospital 41: 36-61, 1927.

2. Phillips, S. J., Reid, J. A., and Rugh, R. Electrocardiographic and pathologic changes after cardiac X-irradiation in dogs. American Heart Journal 68: 524-533, 1964.

3. Stone, H. L., Bishop, V. S., and Guyton, A. C. Progressive changes in cardiovascular function after unilateral heart irradiation. American Journal of Physiology 206: 289-293, 1964.

4. Fajardo, L. F., and Stewart, J. R. Experimental radiation-induced heart disease. American Journal of Pathology 59: 299-316, 1970.

5. Senderoff, E., Kaneko, M., Beck, A. R., and Baronofsky, I. D. The effects of cardiac irradiation upon the normal canine heart. American Journal of Roentgenology 86: 740, 1961.

6. Kundel, H. L. The effect of gamma irradiation on the cardiovascular system of the rhesus monkey. Radiation Research 27: 406-418, 1966.

ALTERED GASTRIC EMPTYING DURING RADIATION-INDUCED VOMITING

Principal Investigator: A. Dubois
Collaborators: J. P. Jacobus, M. P. Grisson, R. R. Eng, and J. J. Conklin

The relation between radiation-induced vomiting and gastric emptying is unclear, and the treatment of this condition is not established. Therefore, we explored (a) the effect of cobalt-60 irradiation on gastric emptying of solids and liquids and (b) the possibility of preventing radiation-induced vomiting with the dopamine antagonist domperidone.

Twenty dogs were studied on 2 separate days, blindly and in random order, following intravenous injection of either a placebo or 0.06 milligram/kilogram domperidone. On a third day, they received 800 rads whole-body irradiation after either placebo ($n = 10$) or domperidone ($n = 10$). Before each study, each dog was fed chicken liver tagged in vivo with 1 microcurie (mCi) technetium-99m sulfur colloid (solid marker), and 1 mCi indium-111 diethylenetriamine pentacetic acid in water (liquid marker). Dogs were placed in a Pavlov sling for the subsequent 3 hr, and radionuclide imaging was performed at 10-min intervals.

The slope of the exponential decline of intragastric contents (%/hour) of technetium-99m (K solids) and indium-111 (K liquids) was determined for each study. Irradiation produced vomiting in 9 of 10 dogs given placebo but only in 1 of 10 dogs pretreated with domperidone ($p < 0.01$). As shown in Table 1, gastric emptying of both liquids and solids was significantly suppressed by irradiation ($p < 0.01$) after placebo and after domperidone.

These results demonstrate that radiation-induced vomiting is accompanied by suppression of gastric emptying. Furthermore, prevention of vomiting with domperidone does not alter the delay of gastric emptying produced by ionizing radiations.

Table 1. Time of Gastric Emptying (Hr) in Irradiated and Nonirradiated Canines After Administration of Either Placebo or Domperidone

	Placebo		Domperidone	
	Basal*	Irradiation*	Basal	Irradiation
K liquids (In)	22.2 ± 5.4	4.5 ± 2.0	18.6 ± 3.0	4.2 ± 1.2†
K solids (Tc)	9.0 ± 3.0	1.0 ± 0.8	7.2 ± 1.2	1.8 ± 0.6†

* Gastric emptying: basal and after irradiation

† $p < 0.05$, compared to basal.

EFFECTS OF IONIZING RADIATIONS ON GASTRIC SECRETION IN RHESUS MONKEYS

Principal Investigator: A. Durakovic, *AFRRI*
E. D. Dorval, *Uniformed Services University of the Health Sciences, Bethesda, Maryland*

Collaborators: R. R. Eng and J. J. Conklin, *AFRRI*
P. Colombaro and A. Dubois, *USUHS*

The effects of ionizing radiation on gastric secretion are largely unknown. The aims of this study were to determine the acute and late effects of a single 800-rad total-body cobalt-60 irradiation on gastric secretion in rhesus monkeys.

A technetium-99m diethylenetriamine pentacetic acid dilution technique was used on 3 separate days to measure acid output in six conscious chair-adapted rhesus monkeys. This method does not require complete aspiration of the gastric contents, it corrects for gastric emptying, and it permits the study of both basal and meal-stimulated acid output without disturbing normal gastric function.

On the day of irradiation, five out of six monkeys retched and/or vomited, and acid secretion was completely abolished in all animals (see Table 1). Both effects appeared within 40 min after exposure and persisted after meal stimulation, although no vomiting was observed later than 80 min after irradiation. Acid secretion was abolished even up to 60 min after disappearance of retching and vomiting. Two days later, acid secretion had returned to preirradiation levels.

Table 1. Mean Acid Output (μEq/min. $\pm$ SE)

	Basal	After Meal
Control Day	9.0 ± 4.7	32.7 ± 5.7
Day of Irradiation	0.1 ± 0.1*	1.7 ± 1.7*
2 Days After Irradiation	11.3 ± 4.7	28.7 ± 5.1

*$p < 0.05$, compared to control day

Thus, cobalt-60 irradiation immediately and transiently produced vomiting and abolished gastric acid secretion. Both effects could be caused by the release of hormones or neurotransmitters, although they could result from receptor inactivation (1).

REFERENCE

1. Garvey, T. Q., Kempner, E. S., Steer, C. J., et al. Molecular sizes of receptors for vasoactive intestinal peptide and secretin determined by radiation inactivation. Gastroenterology 82: 1064, 1982.

DIFFERENTIAL EFFECTS OF COBALT-60 AND FISSION NEUTRON IRRADIATION ON LYMPH NODE UPTAKE OF TECHNETIUM-99m SULFIDE COLLOID

Principal Investigator:	R. R. Eng, *AFRRI*
Collaborators:	G. N. Ege, *Princess Margaret Hospital, Toronto, Canada*
	A. Durakovic, V. James, and J. J. Conklin, *AFRRI*
Technical Assistance:	M. E. Flynn, J. D. Stewart, M. E. Corral, N. L. Fleming, and J. K. Warrenfeltz, *AFRRI*

In this study, we evaluated the effects of cobalt-60 and fission neutron irradiation (whole-body) on male Sprague-Dawley rats for the ability of popliteal lymph nodes to retain radiocolloid.

In 1966, Dettman (1) found that, by using local irradiation (250 kilovolts X rays) to the right popliteal node, the nodal distribution of gold-198 colloid in dogs was not significantly different from that of control values at doses of 2000, 4000, and 10,000 roentgens (R). Barrow noted that 800 R of whole-body X irradiation of rabbits did not interfere with the gold-198 colloid uptake in reticuloendothelial cells (2).

In our study, we injected a different radiocolloid (0.55 mega becquerel technetium-99m antimony sulfide colloid) (Tc-99m ASC) via the footpad, and then whole-body irradiated the rats. Uptake values of Tc-99m ASC by the left and right popliteal nodes increased significantly by 2 to 14 days after the rats were irradiated with cobalt-60 (6 grays, 0.4 Gy/min), compared to the mean control values ($p < 0.05$, Figure 1). For the 10-Gy cobalt-60-irradiated group of rats, the left nodal uptake values for Tc-99m ASC were significantly higher than the mean control value for only day 8 ($p < 0.05$) and not before. Nodal uptake values for the 6-Gy fission neutron group were not significantly different from the mean control values.

The differences in nodal uptake of Tc-99m ASC as a function of radiation dose and type of radiation in our study may be a result of changes in macrophage phagocytic activity and/or structural alteration of the popliteal lymph nodes.

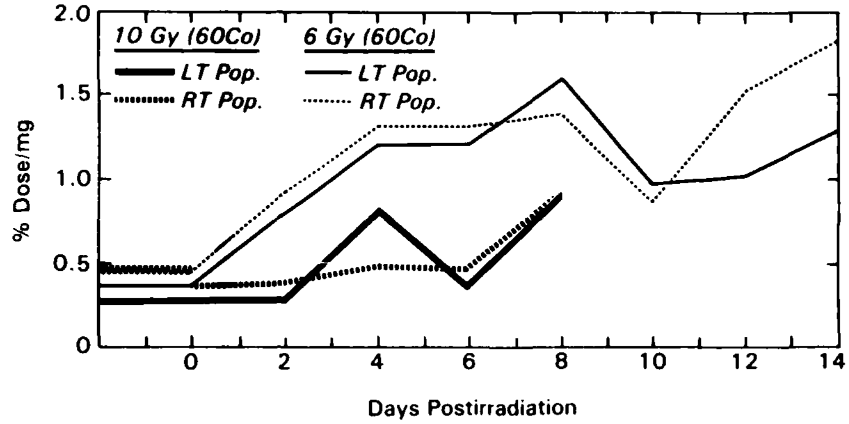

Figure 1. Uptake of technetium-99m antimony sulfide colloid after cobalt-60 irradiation

REFERENCES

1. Dettman, P. M., King, E. R., and Zimberg, Y. H. Evaluation of lymph node function following irradiation or surgery. American Journal of Roentgenology Radiation Therapy and Nuclear Medicine 96: 711-718, 1966.

2. Barrow, J., Tullis, J., and Chambers, F. W., Jr. Effect of X-radiation and antihistamine drugs on the reticuloendothelial system measured with colloidal radiogold. American Journal of Physiology 164: 822-831, 1951.

EFFECTS OF A METASTATIC (13762) AND A NON-METASTATIC (R3230AC) MAMMARY ADENOCARCINOMA ON RADIOCOLLOID LOCALIZATION IN REGIONAL LYMPH NODES IN FISCHER 344 RATS

Principal Investigator:	G. N. Ege, *Princess Margaret Hospital, Toronto, Canada*
Collaborators:	J. Nold, R. R. Eng, A. Durakovic, and J. J. Conklin, *AFRRI*
Technical Assistance:	M. E. Flynn, N. L. Fleming, and J. K. Warrenfeltz, *AFRRI*

Effects of a metastatic and a nonmetastatic tumor on radiocolloid localization in regional lymph nodes in the rat were studied, in order to examine further the hypothesis that the suppression of radiocolloid uptake results from inhibition of macrophage phagocytic function by tumor products.

In the present model, homogenates of autologous spleen and two weakly immunogenic tumors were introduced unilaterally into the footpad of rats. The primary drainage popliteal lymph nodes of both the experimental foot and control foot were removed 2.5 hr after the bilateral dorsal pedal injection of technetium-99m antimony sulfide colloid. The nodes were weighed and counted, and the results were expressed as percent radiocolloid uptake/milligram of lymph node tissue. All nodes were examined histologically.

The data show a statistically significant increase in lymph node weight with a concomitant decrease in radiocolloid uptake, not consistently associated with histologically demonstrated lymphatic metastases. On the basis of these data, the proposed "jelly-bean hypothesis" suggests that decreased radiocolloid uptake induced by a regional neoplasm may result from proliferation of nonphagocytic cellular elements within the regional lymph nodes and alterations in the cellular and humoral environment at the site of radiocolloid injection, all of which impede the transport of interstitially administered radiocolloid and its access to the phagocytic macrophages within primary regional lymph nodes.

COMPUTER MONITORING OF MOLYBDENUM-99m TECHNETIUM-99m GENERATOR PERFORMANCE

Principal Investigator: R. R. Eng
Collaborators: C. J. Munno, S. Miller, M. P. Grissom, and J. J. Conklin

A computer program has been formulated to calculate generator elution efficiencies and the number of technetium-99m plus technetium-99 atoms in a particular elution. Other data of interest are also generated, such as activity of technetium-99m available for elution and current molybdenum-99 activity in the generator.

A DEC (Digital Equipment Corporation) PDP 1170 computer system was used to calculate data. Julian dates (365 days/year) and 24-hour time were entered into the computer, and time (hours) from elution to elution was automatically calculated and stored. Data for each elution were stored in memory so that technetium-99m generator performance could be monitored during its use.

Equation 1 calculates the microcuries (mCi) of molybdenum-99 (A) on the generator's column at time T (hours), starting with mCi of molybdenum-99 (B) at the calibration date and time of the generator. *Lambda 1* (λ_1) is the molybdenum-99 decay constant (λ_1 = 0.693/66.02 hr).

$$A = B\, e^{-\lambda_1 T} \qquad (1)$$

Equation 2 calculates the mCi of technetium-99m for elution at time T based on the molybdenum-99 activity (A_{-1} mCi) at the time of the previous elution (T_{-1}). Any technetium-99m activity remaining on the generator from the previous elution is represented by C_0. The decay constant for technetium-99m is 0.693/6.02 hr. The constant is 0.867856. The decay efficiency of molybdenum-99 to technetium-99m is represented by

$$C = 0.867856\,(A_{-1})(\lambda_1/\lambda_2-\lambda_1)(\lambda_2/\lambda_1)$$
$$(e^{-\lambda_1 T} - e^{-\lambda_2 T}) + C_0 e^{-\lambda_2 T} \qquad (2)$$

Molybdenum-99 decays directly to technetium-99m with an efficiency of 86.7856%, and decays to technetium-99 with an efficiency of 13.2144%.

Equation 3 calculates elution efficiency of technetium-99m (E) at time T.

$$E = (\text{mCi Tc-99m Eluted}/C)(100) \qquad (3)$$

The next part of the computer program calculates the number of technetium-99m plus technetium-99 atoms in a particular elution. The calculations are based on the fact that one atom of molybdenum-99 will decay to an atom of technetium, whether it be the technetium-99m or technetium-99 radionuclide. The equations are expressed in microcuries (mCi) of molybdenum-99 (M) that have decayed to technetium-99m and technetium-99 since the previous elution with an elution efficiency correction. The final equation converts mCi of molybdenum-99 to atoms of technetium-99m plus technetium-99. The mCi of molybdenum-99 are denoted M for the contribution of mCi molybdenum-99 converted to technetium-99m plus technetium-99 for the present elution, M_{-1} for the contribution from the previous elution, M_{-2} for the contribution from two elutions previous, M_{-3} for the contribution from three elutions previous, and so on. The subscripts for elution efficiencies have similar meanings: E represents the present elution efficiency, E_{-1} the elution efficiency from the previous elution, and E_{-2} the elution efficiency from two elutions previous. The subscripts for molybdenum-99 activity have the same meaning as those for E. A means the molybdenum-99 activity on the generator for the present elution, A_{-1} the molybdenum-99 generator activity at the previous elution, and A_{-2} the molybdenum-99 generator activity two elutions previous.

Equations 4 through 9 represent mCi of molybdenum-99 (that have decayed to technetium-99m and technetium-99) contributed from each of the previous elutions, back to five elutions previous. Residual contributions from six elutions previous and beyond are insignificant contributions. If one were eluting a molybdenum-99/technetium-99m generator for the first time, the M_{-1} through M_{-5} would be zero.

$$M = (A_{-1} - A)(E/100) \qquad (4)$$

$$M_{-1} = (A_{-2} - A_{-1})(1 - E_{-1}/100)(E/100) \qquad (5)$$

$$M_{-2} = (A_{-3} - A_{-2})(1 - E_{-2}/100)(1 - E_{-1}/100)(E/100) \qquad (6)$$

$$M_{-3} = (A_{-4} - A_{-3})(1 - E_{-3}/100)(1 - E_{-2}/100)(1 - E_{-1}/100)(E/100) \qquad (7)$$

$$M_{-4} = (A_{-5} - A_{-4})(1 - E_{-4}/100)(1 - E_{-3}/100)(1 - E_{-2}/100)(1 - E_{-1}/100)(E/100) \qquad (8)$$

$$M_{-5} = (A_{-6} - A_{-5})(1 - E_{-5}/100)(1 - E_{-4}/100)(1 - E_{-3}/100)(1 - E_{-2}/100)(1 - E_{-1}/100)(E/100) \qquad (9)$$

Equation 10 sums the molybdenum-99 contribution, and Equation 11 calculates the number of technetium-99m plus technetium-99 atoms (TC) in a specific elution.

$$M_{sum} = M + M_{-1} + M_{-2} + M_{-3} + M_{-4} + M_{-5} \tag{10}$$

$$TC = (M_{sum})\,(1.26896 \times 10^{13}\ \text{Tc-99m \& Tc-99 atoms/mCi Mo-99}) \tag{11}$$

DESIGN AND FABRICATION OF PHYSICAL RADIO-PROTECTANTS

Principal Investigators: R. T. Devine and G. H. Zeman
Collaborator: F. M. Sharpnack

Protection of personnel on the nuclear battlefield is an important part of the mission of AFRRI. In September 1981, a visit to the U.S. Army Research Institute of Environmental Medicine (USARIEM) was made by members of the AFRRI staff. During this visit were displayed vests that use water as a coolant for personnel in armored vehicles. It was suggested that this layer of water over the trunk might provide some degree of protection from neutron radiation in a battlefield environment.

In March 1982, in the process of answering an inquiry on a "neutron cloth," it was determined that Toray Industries of Japan has developed a B_4C-impregnated polyester fiber and woven it into a cloth. It was then decided to determine the properties of the cloth and cooling jackets in combination, since the cloth might act as an absorber for neutrons thermalized by the water jackets. This raised the fundamental problem of how to determine experimentally the value of protection by these pieces of equipment. This led to the development of a humanoid phantom, with some immediate possibilities of verification of the results through existing calculations.

In fiscal year 1983, copies of two of the coolant vests were obtained from USARIEM, and some of the "neutron cloth" was received from the Japanese manufacturer. A phantom was constructed from a Lucite cylinder 30 centimeters (cm) in diameter and 60 cm in height. Three holes of 3.80 cm were placed parallel to each other through a diametrical plane at 3 cm above the center, 3 cm below the center, and 6 cm from one of the ends. Blank plugs were made from Lucite stock to fill the holes when not in use. Plugs were also made from 3.8 cm Lucite stock, which had three holes 1.20 cm in diameter located symmetrically in a 1.57-cm circle. The length of the holes in this plug allowed the positioning of ion chamber tips 1.89 cm from the closed end of the plug and 16.1 cm and 4.1 cm from the open end. These corresponded to the entrance, midline, and exit doses, respectively. These correspond to points calculated in Report Number 38 of the National Commission on Radiation Protection.

Experiments will be performed during the next fiscal year with the protective vests and the neutron cloth in this phantom in the AFRRI reactor, to determine the protection factors.

PAIRED ION CHAMBER RESPONSE COEFFICIENTS

Principal Investigator: G. H. Zeman
Collaborators: D. W. Shosa, K. P. Ferlic, and W. S. Bice, Jr.

Evaluation of tissue dose from mixed neutron-gamma radiation by means of paired ion chamber measurements requires accurate knowledge of the chambers' response coefficients. These coefficients are defined as follows:

$$R_T = k_T D_N + h_T D_G$$

$$R_U = k_U D_N + h_U D_G$$

In the above, D_N and D_G are the desired neutron and gamma doses in tissue, respectively; R_T and R_U are the respective readings of tissue-equivalent and non-hydrogenous ion chambers as normalized to the cobalt-60 sensitivity of each chamber; and k_T, h_T, k_U, and h_U are the paired chamber response coefficients.

Values of the response coefficients for AFRRI neutron-gamma fields have been calculated (1-4) for the spherical 50-cm^3 ion chambers, which have formed the backbone of the AFRRI reactor dosimetry program. The results (shown in Table 1) for the most part have confirmed earlier estimates of these factors.

Table 1. Summary of AFRRI 50-cm^3 Paired Chamber Constants*

k_T	h_T	k_U	h_U	Reference
1.000	1.040	0.120	1.040	Sayeg, J.A. (AFRRI CR 65-6)
0.980	1.040	0.080	1.000	Shosa, D.W. (AFRRI TN 71-7)
0.960	1.040	--	--	Trambraegel, G.E. et al (AFRRI TN 73-16)
0.940	1.040	0.084	1.040	Kearsley, E.E. (unpublished, 1977)
0.900	1.046	0.082	1.046	Ferlic, K.P. (unpublished, 1979)
				Present work for:
0.976 ± 0.3%⁺	1.045	0.105 ± 7%	1.041	H_2O-shielded fields
0.960 ± 1.3%	1.088	0.087 ± 15%	1.061	Pb-shielded or unshielded

* Constants are expressed in units muscle-rad per cobalt-60 roentgen, and include corrections for chamber wall effects.

⁺ Percentages give the range of k_T and k_U values calculated for different TRIGA reactor in-air neutron spectra.

However, note that the value of k_T in use between 1979 and 1983 differed by over 5% from that presently derived. The potential impact of this difference on free-in-air dosimetry results is presently being assessed. Note that depth-dosimetry measurements have routinely been performed using 0.5-cm^3 ionization chambers, and calculation of the response coefficients for these chambers is currently under way. Experimental verification of the calculated results is also proceeding through the neutron dosimetry intercomparison project described separately.

REFERENCES

1. Zeman, G. H., and Bice, Jr., W. S. Kerma factors for use in 37-group neutron spectrum calculations. Technical Report TR 83-3, Armed Forces Radiobiology Research Institute, Bethesda, Maryland, 1983.

2. Ferlic, K. P., and Zeman, G. H. Spectrum-averaged kerma factors for reactor dosimetry with paired ion chambers. Technical Report TR 83-2, Armed Forces Radiobiology Research Institute, Bethesda, Maryland, 1983.

3. Zeman, G. H. Paired ion chambers for fission gamma neutron fields. Technical Report, Armed Forces Radiobiology Research Institute, Bethesda, Maryland, in press.

4. Zeman, G. H., and Ferlic, K. P. Spectrum averaged kerma, W, and ion chamber constants for water moderated fission neutrons. Seventh International Congress on Radiation Research, Amsterdam, July 1983.

ELECTRON AND PHOTON DOSIMETRY INTERCOMPARISON

Principal Investigators: G. H. Zeman and M. A. Dooley
Collaborator: J. G. Campbell
Technical Assistance: R. A. Brewer

The Radiological Physics Division has participated in an electron and photon dosimetry intercomparison study sponsored by the Radiation Physics Division of the National Bureau of Standards (NBS), on a periodic basis since 1970. This study involves the irradiation by AFRRI (and other participating laboratories) of Fricke dosimeters that have been prepared and distributed by NBS and subsequently evaluated by NBS. The results of each study demonstrate the ability of the participants to accurately deliver prescribed doses of photon and electron radiation.

Table 1 summarizes the results of the last 10 years of AFRRI participation in this intercomparison. With few exceptions, AFRRI has achieved a ±5% accuracy level over the last 10 years for all three categories of radiation.

A significant milestone in the 1983 participation was the complete implementation at AFRRI of the recent dosimetry protocol of Task Group 21 of the American Association of Physicists in Medicine (1). Use of this protocol resulted in highly accurate results without the need for an anamolous 6% correction factor for linear accelerator irradiations, which had been used in the past. Thus the new dosimetry protocol was found to be more accurate than previous dosimetry procedures (2).

Table 1. Ten-Year Results of AFRRI Participation in Fricke Dosimetry Uniformity Studies of National Bureau of Standards (NBS)

Study Date	Percentage* Difference from NBS Cobalt-60	LINAC Electrons†	LINAC X rays
May 1983	+2.4 (2)‡	-1.8 (4)	-5.7
Nov 1981	-3.3	-2.6 (2)	-4.4
Jan 1981	+3.3 (2)	+1.1 (3)	--§
May 1980	--	-0.3	-3.5
Oct 1979	--	+4.3 (2)	--
May 1979	+3.7 (2)	+0.9 (2)	--
Oct 1978	+7.5 (2)	+1.2 (2)	--
Apr 1978	--	+2.8 (2)	--
Jun 1977	--	-4.5 (4)	--
Nov 1976	--	+2.8 (2)	--
Apr 1976	--	+1.5 (2)	--
Nov 1975	+2.9	--	-16.4 (2)
Apr 1975	--	+3.4 (2)	--
Oct 1974	--	-2.3 (2)	--
Apr 1974	--	+5.4 (2)	--
Oct 1973	--	+5.6 (2)	--
Apr 1973	--	-8.2	--

* Percentages are average of separate dosimeters' differences.

† Linear accelerator electron irradiations ranged in energy from 8.2 to 20.2 million electron volts (MeV), while X rays ranged from 3.5 to 13 MeV.

‡ Number of separate dosimeters in each category is shown in parentheses, if more than one.

§ Dash indicates no participation in that category.

REFERENCES

1. Protocol for the determination of absorbed dose from high energy photon and electron beams (draft). Task Group 21 of the American Association of Physicists in Medicine. Radiation Therapy Committee, July 1982.

2. Radiation Dosimetry: Electrons with initial energies between 1 and 50 MeV. Report Number 21. International Commission on Radiation Units and Measurements, Washington, DC, 1972.

NEUTRON DOSIMETRY INTERCOMPARISONS

Principal Investigators: M. A. Dooley, G. H. Zeman, and P. K. Blake, *AFRRI*

Collaborators: L. G. Goodman, R. B. Schwartz, and C. M. Eisenhauer, *National Bureau of Standards, Washington, DC*

Not since the 1973 International Neutron Dosimetry Intercomparison (INDI) sponsored by the International Commission on Radiation Units and Measurements (1) has AFRRI formally intercompared its neutron ionization chamber measurements with those of other laboratories. Beginning in summer 1983, the Radiological Physics Division began a neutron dosimetry intercomparison study with the Nuclear Radiation Division of the National Bureau of Standards (NBS).

The purpose of the study was to validate paired ionization chamber measurements and techniques in use at AFRRI, and to provide a basis for future dosimetry programs between the two institutions. While the intercomparison study is to continue into fiscal year 1984, preliminary data are available (2) for results obtained by the two groups at the NBS californium-252 facility and at the AFRRI TRIGA (Training Research Isotope General Atomic) reactor.

These data (Table 1) compare kerma rates measured by NBS and AFRRI relative to calculated kerma rates for each source. (Neutron-gamma spectra of reference 3 were used to calculate values for the TRIGA reactor.) The californium-252 data show excellent agreement between measurements made by the two groups, while the reactor data reveal AFRRI measurements to be higher than those of NBS. Further measurements by both groups are in progress to resolve previous differences, to include additional fields, and to clarify certain technical problems identified in the preliminary study.

Table 1. National Bureau of Standards (NBS) and AFRRI Kerma Comparisons: Ratio of Measured to Calculated Kermas

Source	Dosimeter Pair	NBS			AFRRI		
		K_n	K_g	K_T	K_n	K_g	K_T
Cf Unmoderated	TE-GM*	1.07	0.96	1.03			
	TE-C†				0.91	1.04	0.96
	TE-Mg‡	1.11	0.89	1.03	1.08	0.94	1.03
Cf Moderated	TE-GM	0.93	1.05	1.01			
	TE-C				0.83	1.05	0.98
	TE-Mg			0.99			1.02
AFRRI Bare	TE-Mg	0.88	0.84	0.85	1.00	0.90	0.93
AFRRI 6" Lead	TE-GM	0.81	4.1	0.87			
	TE-Mg	0.78	5.4	0.87	0.82	6.8	0.94

* Refers to use of an Exradin 0.5-cm^3 tissue-equivalent (TE) ion chamber in conjunction with a Geiger Muller counter

† Refers to use of AFRRI spherical 50-cm^3 TE and graphite ion chambers

‡ Refers to use of Exradin 0.5-cm^3 TE and graphite ion chambers

REFERENCES

1. An international neutron dosimetry intercomparison. Report Number 27 of International Commission on Radiation Units and Measurements, Washington, DC, Feb 1978.

2. Progress Report on Program in Support of Neutron Dosimetry. Work Unit Code 00052, DNA IACRO 83-847, Nuclear Radiation Division, National Bureau of Standards, 31 Oct 1983.

3. Verbinski, V. V., Cassapakis, C. G., Hagan, W. K., Ferlic, K., and Daxon, E. Calculations of the neutron and gamma-ray environment in and around the AFRRI TRIGA reactor. Volume II. Report Number DNA 5793 F-2, Defense Nuclear Agency, Washington, DC, 1 Jun 1981.

EXPERIMENTAL INVESTIGATION OF RADIATION-INDUCED CABLE CURRENTS

Principal Investigators: G. H. Zeman and P. K. Blake, *AFRRI*
Collaborators: D. E. Cunningham, *Hershey Medical Center, Hershey, Pennsylvania*
G. P. Bender, *U.S. Naval Academy, Anapolis, Maryland*
Technical Assistance: R. A. Brewer, *AFRRI*

Radiation-induced currents in cables used for ionization chamber measurements are a source of noise that interferes with electrical signals from small-volume ion chambers. The mechanisms generating these currents are believed to be leakage current due to compton electrons ejected from conductors, dielectric polarization due to trapping of ejected electrons, and ionization currents in extracameral air volumes. Experimental investigation of these currents revealed the following:

Radiation-induced currents of 10^{-14} to 10^{-15} amps per meter per roentgen/min were measured in several cable types in close agreement with data for other cables (1).

Old and presumably radiation-damaged lengths of RG-62 cable gave currents up to 1000 times greater than those of new cable.

Irradiation of cable connectors increased radiation-induced currents up to 50%.

Radiation-induced leakage currents from cable patch panels far exceeded those induced in cables.

The above currents added as much as 30% to ionization currents measured with 0.5-cm^3 ion chambers in AFRRI reactor and cobalt-60 exposure rooms.

Based on these findings, a recabling of TRIGA Exposure Room 2 was undertaken to minimize radiation-induced cable currents. Key design features included elimination of the in-room cable patch box, use of heavy-duty Belden 8232 triaxial cable with earthed outer shield mated to ion chamber leads with coaxial BNC connectors, as well as shielding of cable connectors and slack length with lead within the exposure room. These measures reduced the radiation-induced cable currents to less than 1% of the currents collected from 0.5-cc

ionization chambers in Exposure Room 2. Similar measures are planned for the other exposure rooms.

REFERENCE

1. Spokas, J. J., and Meeker, R. D. Investigation of cables for ionization chambers. Medical Physics 7: 135-140, 1980.

EXTERNAL EFFORTS IN RADIATION DOSIMETRY

Principal Investigators: G. H. Zeman and R. T. Devine
Collaborators: R. L. Chaput, J. Campbell, S. G. Levin, R. W. Young, L. F. Myers, and J. J. Conklin

Continuing progress in radiation dosimetry is an essential component of an advancing radiobiologic research program. This progress is best achieved by drawing on the expertise of both in-house and external specialists in radiological physics. Consequently, a program of external efforts in radiation dosimetry has been developed to meet specific research needs of AFRRI, in addition to the more broad-scale needs of the Defense Nuclear Agency and military services. An overview of the purpose and status of these external efforts is given below.

Radiation Field Characterization for AFRRI TRIGA Reactor. This work by Science Applications Inc. (SAI) of La Jolla, California, included transport calculations and activation foil measurements of neutron-gamma energy spectra in AFRRI TRIGA exposure rooms. Status: Completed (1, 2).

Monkey Dosimetry Calculations in AFRRI TRIGA Reactor. This effort by Oak Ridge National Laboratory (ORNL) used radiation transport calculations to define the neutron-gamma energy spectra and dose deposited in head and thorax regions of reactor-irradiated monkeys, in the visual discrimination task chair array and the physical activity wheel. Status: Completed (3).

Phantom Dosimetry for Laboratory/Field Radiation Efforts. This contract to SAI involves the development of a computerized monkey model, including skeletal and lung anatomy for definitive midhead, midthorax, and bone marrow dosimetry calculations for the visual discrimination task chair array in two TRIGA radiation fields. Status: Preliminary review of draft monkey model (4) has been completed. A final review is scheduled before the completion of this contract during fiscal year 1984.

Neutron Spectrum in Monkey Phantom. This SAI contract will provide experimental verification via activation foils of computed neutron dosimetry results for a phantom irradiated in two AFRRI TRIGA reactor fields. Parallel evaluation of National Bureau of Standards (NBS) irradiated activation foils will document the accuracy of the measurement techniques. Status: Experimental work is scheduled for January 1984; contract completion, during fiscal year 1984.

Battlefield Radiation Environments. This SAI contract is to define potential neutron and gamma ray energy spectra and dose in battlefield situations. Status: A draft report (5) is under review; contract completion is scheduled for fiscal year 1984.

NBS Program to Support Neutron Dosimetry. This program establishes close technical ties between AFRRI and NBS dosimetry programs in four key areas (6): intercomparison of ionization chamber measurements, integral detector (activation foil) dosimetry, experimental microdosimetry, and theoretical microdosimetry. Status: Begun in fiscal year 1983, this program is projected to continue through fiscal year 1985.

Calorimetry Dosimetry. This project will bring the calorimetry dosimetry expertise of Battelle Pacific Northwest Laboratories, Richland, Washington (7), to bear on fundamental questions in AFRRI neutron dosimetry, and pulsed reactor and high-dose-rate linear accelerator dosimetry. Status: Experimental program to begin in fiscal 1984.

REFERENCES

1. Verbinski, V. V., Cassapakis, C. C., Hagan, W. K., Ferlic, K. P., and Daxon, E. E. Radiation field characterization for the AFRRI TRIGA reactor. Volume I. Baseline measurements and evaluation of calculated data. Report Number DNA 5793F-1, Defense Nuclear Agency, Washington, D.C., 1 June 1981.

2. Verbinski, V. V., Cassapakis, C. C., Hagan, W. K., Ferlic, K. P., and Daxon, E. E. Calculation of the neutron and gamma-ray environment in and around the AFRRI TRIGA reactor. Volume II. Report Number DNA 5793F-2, Defense Nuclear Agency, Washington, D.C., 1 June 1981.

3. Johnson, J. O., Emmett, M. B., and Pace, J. V., III. Calculations of radiation fields and monkey mid-head and mid-thorax responses in AFRRI TRIGA reactor facility experiments. Report Number ORNL/TM-8807, Oak Ridge National Laboratory, Oak Ridge, Tennessee, July 1983.

4. Kaul, D. C. Rhesus monkey phantom progress report. SAI Letter Report of 30 Sep 1983, Science Applications Inc., La Jolla, California.

5. Kaul, D. C., Dolatshahi, F., Egbert, S., and Wilson, W. Radiation environments for personnel casualty correlations (DRAFT). Report Number DNA 001-83-C-0252, Defense Nuclear Agency, Washington, D.C., 28 Oct 1983.

6. Grundl, J. A., and Eisenhauer, C. M. Progress report on program in support of neutron dosimetry. Work Unit Code 0052. Nuclear Radiation Division, National Bureau of Standards Letter Report of 31 Oct 1983. Report Number DNA IACRO 83-847, Defense Nuclear Agency, Washington, D.C.

7. Calorimetry Dosimetry Development -- PNL Proposal No. 300A02228. Letter Proposal of 15 Sep 1983.

TRIGA FISSION PRODUCT GAMMA RADIATION

Principal Investigators: G. H. Zeman, M. A. Dooley, and M. L. Moore
Technical Assistance: D. A. Schacter and R. A. Brewer

In preparation for using the AFRRI TRIGA reactor for certain low-dose-rate applications, the levels of residual fission product gamma radiation from the core have been measured. Spherical 50-cm^3 ion chambers for these measurements were positioned 100 centimeters (cm) from the centerline of the unshielded reactor in Exposure Room 1, 120 cm from the floor. Measurements were made over a 1-week period following a 30-min run at 1 megawatt (MW).

The results (Figure 1) show that fission product gamma levels as high as 190 roentgens (R)/min shortly after the run decayed to 0.17 R/min by 1 week later. The

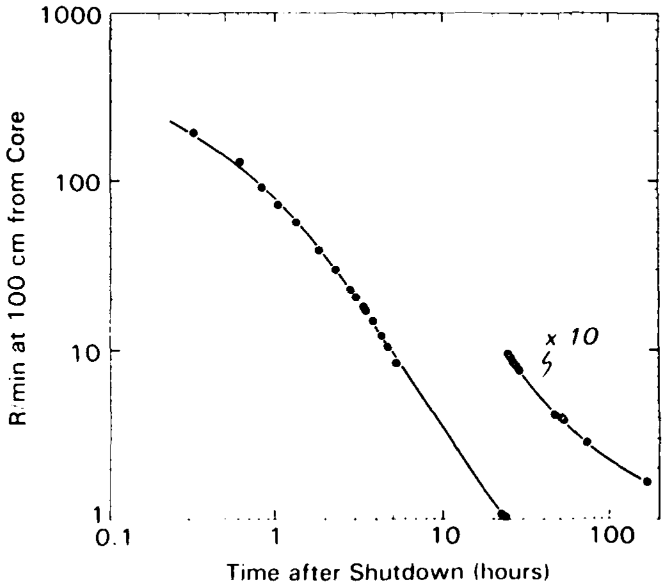

Figure 1. Fission product gamma radiation levels after a 30-MW-min run

following empirical relationships were derived between gamma exposure rate G at 100 cm distance and time T after the 30-MW-min run.

$$\ln(G) = 4.41 - 1.05\ln(T) - 0.227(\ln T)^2 + 0.039(\ln T)^3$$

$$\ln(T) = 3.14 - 0.809(\ln G) + 0.109(\ln G)^2 - 0.020(\ln G)^3$$

where G is expressed in units R/min and T is in hours. These relatively high levels of residual fission product gamma radiation may severely constrain the design of certain low-dose-rate reactor applications. Extension of the present results to various shielded configurations of the reactor is planned in the future.

DOSIMETRY OF RHESUS MONKEYS IRRADIATED WITH THE AFRRI TRIGA REACTOR

Principal Investigators: G. H. Zeman, K. P. Ferlic, and E. E. Dooley
Collaborators: R. W. Young and C. G. Franz

Behavioral effects of reactor radiation on rhesus monkeys (Macaca mulatta) studied at AFRRI over the last 2 decades form an essential data base (1) in development of combat casualty criteria for the armed forces of the United States and NATO. Through the course of the AFRRI studies, the irradiation techniques and the dose specification procedures differed, making difficult the complete intercomparability of results.

A series of phantom dosimetry measurements completed in 1979-1980 have now been compiled to allow the interconversion of midhead and midthorax doses as well as free-in-air kerma at the midhead and midthorax locations. Included in the compilation were data for different reactor shield configurations and for both the visual discrimination task chair array and the physical activity wheel array. In addition to total dose comparisons, the compilation included data on neutron-to-gamma dose ratios free in air and at depth.

The results (2) of this work facilitate the more accurate retrospective analysis of AFRRI data on the behavioral effects of reactor radiations.

REFERENCES

1. Franz, C. G., Young, R. W., and Mitchell, W. E. Behavioral studies following ionizing radiation exposures: A data base. Technical Report TR 81-4, Armed Forces Radiobiology Research Institute, Bethesda, Maryland, 1981.

2. Zeman, G. H. (compiler). Phantom dosimetry for TRIGA reactor irradiations in chair and wheel arrays. Technical Report, Armed Forces Radiobiology Research Institute, Bethesda, Maryland, in press.

USE OF A RADIOTHERAPY TREATMENT-PLANNING COMPUTER FOR DOSIMETRY OF THE AFRRI COBALT-60 FACILITY AND THERATRON-80

Principal Investigators: G. H. Zeman and M. A. Dooley, *AFRRI*
Collaborator: K. Working, *Naval Hospital Bethesda*
Technical Assistance: D. K. Lyell and W. A. Dinan, *AFRRI*

Cobalt-60 tissue-to-air ratios (TAR's) and isodose distributions have been generated by computer for experimental animal irradiations in the AFRRI cobalt-60 facility and the Theratron-80 teletherapy unit. The computer was the Atomic Energy of Canada, Ltd, Treatment Planning Computer (TPL) of the Naval Hospital Bethesda.

Experiments at AFRRI verified that the irregular field mode of the TPL gave accurate TAR's along the beam central axis for phantom irradiation in the cobalt-60 facility. Likewise, it was demonstrated that the fixed rectangular beam mode gave accurate isodose distributions along the central axis. However, both computer

modes proved inappropriate for dosimetry near the ends (head/tail) of total-body irradiated animal phantoms with this uncollimated cobalt-60 source.

Figure 1 exemplifies TPL isodose plots that demonstrate the utility of this technique for quantitating dose uniformity in irradiated animals.

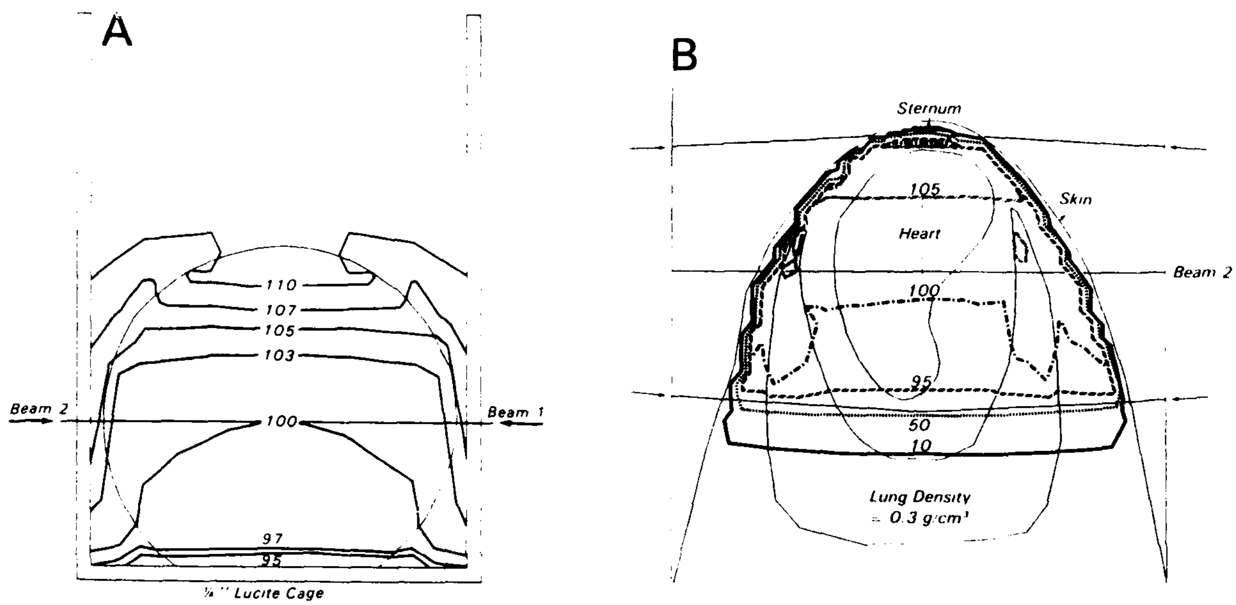

Figure 1. Computer-generated central axis isodose distributions. (A) Bilateral total-body irradiation of 15-kg (15 cm diameter) miniature swine within 0.25-inch lucite restraining box in AFRRI cobalt-60 facility. Note +10% hot spot near location of spine. (B) Bilateral partial-body irradiation of heart of 13-kg (10 cm thick) beagle using lead-blocked fields of Theratron-80 cobalt-60 teletherapy unit. Chest contour was obtained from experimental animal; internal anatomy was hand drawn for illustration only. Note +5% hot spots in parts of lung, while bulk of lungs was beyond edge of direct beams. Dose uniformity over heart was within ± 5%.

SEMI-AUTOMATED IONIZATION CHAMBER MEASUREMENT SYSTEM

Principal Investigators: G. H. Zeman and M. A. Dooley
Collaborator: R. T. Devine
Technical Assistance: R. A. Brewer and D. A. Schaeter

Accurate measurements of low-level direct currents from gas-filled ionization chambers are essential in radiobiology dosimetry. During fiscal year 1983, a major instrumentation upgrade was completed to enhance the accuracy, reliability, and scope of ionization current and charge measurements at AFRRI. Key elements of this program are as follows:

Replace the Keithley Model 301 Operational Amplifier current integrators with Keithley Model 616 Electrometers, which offer continuous readouts of current (10^{-16} to 10^{-1} amperes) or charge (10^{-15} to 10^{-5} coulombs).

Minimize electrical and microphonic cable noise, leakage, and radiation-induced cable currents through the installation of an improved cabling system for ionization chamber measurements.

Automate data collection through a Hewlett Packard Model 85 Computer and Hewlett Packard Model 3421A Data Acquisition and Control Unit, with locally developed software for ion chamber applications.

The new measurements system has been proven to be more rapid, reliable, and capable of an expanded scope of measurements than heretofore possible. Figure 1 exemplifies the system capabilities.

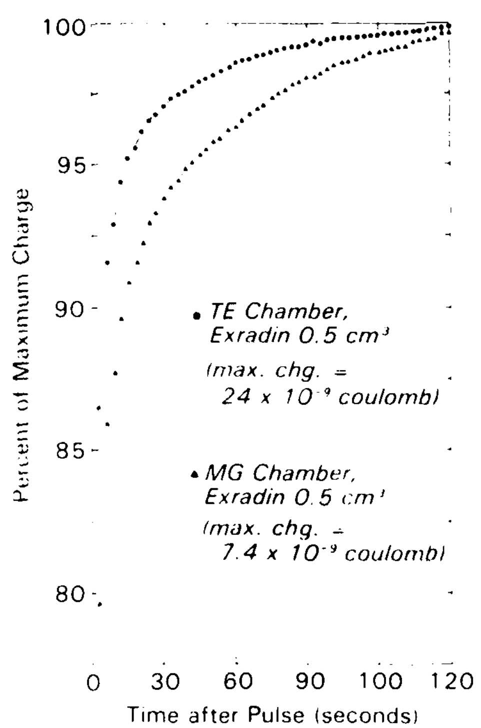

Figure 1. Ionization chamber charge measurements following a TRIGA pulse. Integrated current measurements are shown for Exradin 0.5 cm^3 tissue-equivalent (TE) ion chamber, with methane-based tissue-equivalent gas, and magnesium (MG) chamber, with argon. Measurements were at 3-sec intervals following a TRIGA reactor 1580-rad pulse with neutron-to-gamma kerma ratio of 10:1. Differing time courses of chambers' responses are apparent. This is presumably because of a dose component due to fission product and activation gamma rays.

SURFACE DOSES IN COBALT-60 IRRADIATION

Principal Investigator: G. H. Zeman
Technical Assistance: E. J. Golightly and J. Ritz

The classical picture of high-energy photon dose deposition is that of minimal dose at the surface of irradiated objects, with a gradual buildup of dose until the depth of maximum dose (D_{max}). Recent measurements (1, 2) at the AFRRI cobalt-60 facility and Theratron-80 cobalt-60 unit demonstrated that this classical dose deposition pattern applies only to well-collimated beams at large source-to-surface distances (SSD).

As shown in Figure 1, Theratron-80 irradiations at short SSD and cobalt-60 facility irradiations at any SSD failed to produce the classical "skin-sparing" effect. The excess dose delivered in the first 1-mm depth during short SSD irradiations was presumably due to secondary electrons ejected from the cobalt-60 source or collimator mechanisms (1-3). The data in Figure 1 emphasize the advantage of enclosing irradiated objects in containers with walls at least 0.35 grams/cm^2 thick (e.g., one-eighth-inch lucite) to prevent significant dose gradients in the buildup region.

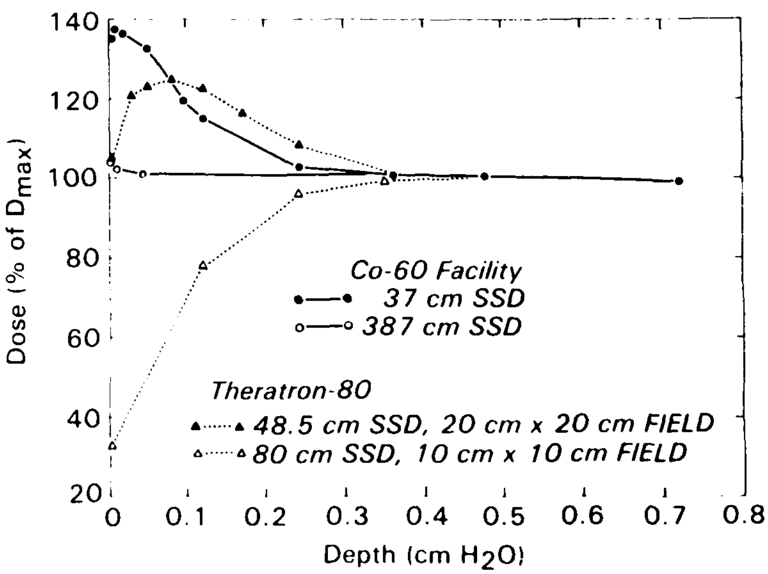

Figure 1. Surface dose measurements for AFRRI cobalt-60 sources

REFERENCES

1. Zeman, G. H. Surface doses in the AFRRI cobalt-60 facility. Technical Report, Armed Forces Radiobiology Research Institute, Bethesda, Maryland, in press.

2. Zeman, G. H. Performance and dosimetry of AFRRI theratron-80 cobalt-60 unit. Technical Report, Armed Forces Radiobiology Research Institute, Bethesda, Maryland, in press.

3. Leung, P. M. K., and Johns, H. E. Use of electron filters to improve the buildup characteristics of large fields from cobalt-60 beams. Medical Physics 4: 441-444, 1977.

OPERATIONAL RADIATION DOSIMETRY

Principal Investigators: E. E. Kearsley, G. H. Zeman, M. A. Dooley, and P. K. Blake
Collaborator: R. T. Devine
Technical Assistance: D. A. Schachter

The AFRRI TRIGA reactor has been used for three preliminary investigations in the area of personnel dosimetry for neutron radiation. In close collaboration with the Dosimetry Center of the Naval Medical Command, National Capital Region, the following experiments were conducted to meet specific needs in existing operational dosimetry programs:

> A technique using a liquid scintillation counter was developed to measure the phosphorus-32 content of neutron-irradiated sulfur foils used in the U.S. Navy DT-526/PD dosimeter. The new technique is more rapid and simpler for routine use than previous techniques, and offers comparable sensitivity to neutron radiation.

The lyoluminescence of sucrose exposed at AFRRI to fission spectrum neutrons and to cobalt-60 gamma rays was investigated. Measurements indicate that there is adequate sensitivity to consider using the lyoluminescence of sugars as potential mixed neutron-gamma criticality dosimeters.

To resolve questions regarding the energy dependence of U.S. Navy DT-583 neutron-gamma dosimeters when used underwater by divers, dosimeter irradiations were conducted within the TRIGA reactor pool. It was found that the neutron responses of the DT-583 (with cadmium shield removed) maintained constant proportion to those of sulfur and gold activation foils at distances from 5 to 40 centimeters from the core. While further work is needed, these results suggest that the DT-583 neutron energy dependence may be acceptable for underwater applications.

Further efforts in operational neutron dosimetry evaluations and research are scheduled for fiscal year 1984.

ERYTHROCYTE GHOST MEMBRANES

Principal Investigator: M. J. McCreery
Associate Investigators: N. B. Joshi and C. E. Swenberg

It is well recognized that cellular membranes, due to their inherent complexity, offer many possible target sites for radiation damage. Although radiation effects on erythrocyte ghost and red blood cell sulfhydryl groups have been extensively studied (1, 2), similar investigations of radiation-induced structural and functional alterations of sulfhydryl moieties in neuronal membranes are few (3). In addition, previous fluorescent studies on the effects of ionizing radiation on erythrocyte ghost membranes have yielded inconsistent results (4, 5). We have investigated the effects of gamma irradiation, with total accumulative doses of up to 1 megarad, on (a) synaptosomal plasma membranes isolated from rat cortex using spin label methods and (b) hemoglobin-free erythrocyte ghosts prepared from human blood using fluorescence probe methods.

We have measured the gamma-induced alterations in human erythrocyte ghost membranes using the fluorescent probes 1,6-diphenyl-1,3,5-hexatriene (DPH) and 1-anilinonaphthalene-8-sulphonate (ANS). The data suggest that ionizing radiation causes a decrease in membrane fluidity. Hemoglobin-free erythrocyte ghosts were prepared from human blood by the procedure of Dodge et al. (6). Test tubes were immersed in an ice bath containing the ghost suspension (in 137 millimolar sodium chloride, 20 mM Tris-chloride, pH 7.4) and then were cobalt-60-irradiated with accumulative doses from 500 rads to 50 kilorads (krad). Membrane samples were diluted with buffer to a final protein concentration of 0.45 milligram/milliliter and DPH, or ANS was added to the preparation after irradiation (final concentration 20 micromolar and 10 micromolar, respectively). Fluorescence intensity, polarization, and lifetime were measured using an SLM subnanosecond spectrofluorometer, and the emission spectrum was recorded with a Perkin-Elmer spectrofluorometer at 25°C.

Results indicate that both ANS and DPH fluorescence intensity (Figure 1) and the fluorescence polarization increased monotonically with increasing dose. At the highest doses investigated, the percentage increase in fluorescence intensity for ANS was 7% compared to 20% for DPH, whereas fluorescence polarization at 50 krad increased 4% and 7% compared to nonirradiated

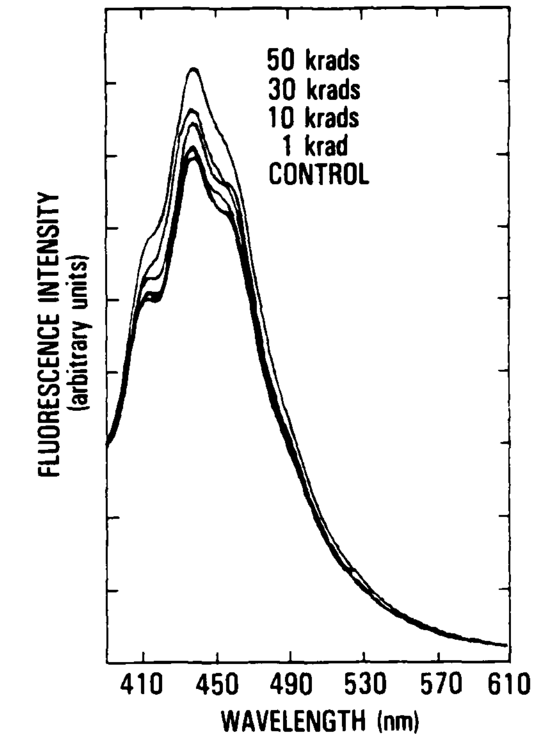

Figure 1. Fluorescence spectrum of DPH incorporated in cobalt-60-irradiated erythrocyte ghosts. Excitation wavelength, 365 nm. Fluorescence spectrum at lowest dose investigated (500 rads) was the same, within experimental resolution, as at a dose of 1 krad.

values for ANS and DPH, respectively. The single exponential lifetime of DPH-fluorescence increased with increasing radiation dose, whereas the apparent increase in fluorescence lifetime of ANS was complicated by multiple components. The fluorescence lifetime and differential phase lifetime increased in the same fashion except for a small decrease observed at 100 krad. The results of these experiments are summarized in Table 1.

Table 1. Dependence of DPH Fluorescence Parameters in Erythrocyte Ghosts on Total Dose Cobalt-60 Irradiation

	Control	1 krad	10 krads	50 krads	100 krads
Polarization	0.330	0.341	0.351	0.353	0.361
Lifetime (ns)	11.340	11.360	11.400	11.480	10.920
Differential Polarized Lifetime (Nanoseconds)	0.331	0.337	0.358	0.376	0.365
Steady State Anisotropy	0.247	0.256	0.265	0.268	0.274

Assuming hindered isotropic torsional motion for the fluorophore (7), the rotational rate (in radians/second) and the limiting fluorescence anisotropy (r_∞) were calculated. The calculated values are given in Table 2. For comparison we note that the rotational rate of 7.1 x 10^7 radians/second for nonirradiated erythrocyte ghosts is considerably smaller than the reported rate of 15.8 x 10^7 radians/second for DPH in saturated phosphatidylcholine vesicles (8). The increase in fluorescence intensity, polarization, and lifetime with increasing doses of gamma irradiation suggest that the membrane fluidity decreases on irradiation. This decrease in membrane fluidity could be due to cross-linkage of lipids.

Table 2. Rotational Rate, Limiting Anisotropy, and Cone Angle for DPH in Erythrocyte Ghosts for Several Cobalt-60 Irradiation Doses

	Control	1 krad	10 krads	50 krads	100 krads
Rotational Rate (x 10^{-5} Radians/Sec)	713.8	662.2	594.2	558.7	552.4
Limiting Anisotropy	0.217	0.226	0.234	0.236	0.241
Cone Angle (Deg)*	35.1	33.9	32.9	32.7	31.9

* Calculated using infinite conical well model of Kinosita, Kawato, and Ikegami, Biophysical Journal 20: 289, 1977

Previous fluorescent studies on the effects of ionizing radiation on erythrocyte ghost membranes have yielded inconsistent results. Yonei and Kato (9) and Purohit et al. (5) reported observations that led to very different conclusions by the respective authors as to the change in fluidity and hydrophobicity of these membranes. We report here that these differences can be reconciled by consideration of fluorescence quenching by hemoglobin and methemoglobin, which may contaminate erythrocyte ghost preparations to varying degrees.

Erythrocyte ghosts were prepared by the method of Dodge et al. (6) with some modifications, which resulted in nearly hemoglobin-free membranes. Control and hemoglobin-enriched (20 micrograms/milliliter and 125 μg/ml) suspensions were then cobalt-60-irradiated with total doses from 1 krad to 50 krad. DPH and ANS, respectively, were added to the exposed and unexposed membrane suspensions, and their fluorescence characteristics were measured. The addition of hemoglobin reduced the fluorescence intensity and lifetime with both DPH and ANS. Exposure to ionizing radiation further decreased these spectral parameters. The addition of 125 μg/ml hemoglobin produced a 79% reduction in fluorescence intensity of DPH compared with control. At 50 krad cobalt-60, the fluorescence intensity decreased by an additional 4%. The irradiated hemoglobin-doped ghosts exhibited a blue shift of the Soret bands in the absorption spectrum, suggesting the production of methemoglobin.

It is concluded that the conflicting reports on radiation damage in erythrocyte ghosts can be rationalized on the basis of hemoglobin contamination. In the absence of hemoglobin, exposure to ionizing radiation results in an increase in both fluorescence intensity and polarization, whereas added hemoglobin results in a quenching of fluorescence intensity with increasing radiation dose. The quenching of DPH and ANS fluorescence by hemoglobin can be explained in terms of radiative and nonradiative transfer of excitation energy.

REFERENCES

1. Sutherland, R. M., and Phil, A. Repair of radiation damage to erythrocyte membranes: The reduction of radiation-induced disulfide group. Radiation Research 34: 300-314, 1968.

2. Shapiro, B., and Kollman, G. The nature of the membrane injury in irradiated human erythrocytes. Radiation Research 34: 335-346, 1968.

3. Koteles, G. J. New aspects of cell membrane radiobiology and their impact on radiation protection. Atomic Energy Review 17: 3-30, 1979.

4. Yonei, S., and Kato, M. X-ray induced structural changes in erythrocyte membranes studied by the use of fluorescent probes. Radiation Research 75: 31-45, 1978.

5. Purohit, S. C., Bisby, R. H., and Cundall, R. B. Structural modification of human erythrocyte membranes following gamma irradiation. International Journal of Radiation Biology 38: 147-158, 1980.

6. Dodge, J. T., Mitchell, C., and Hanahan, D. J. The preparation and chemical characteristics of hemoglobin free ghosts of human erythrocytes. Archives of Biochemistry and Biophysics 100: 119, 1963.

7. Weber, G. Theory of differential phase fluorometry: Detection of anisotropic molecular rotation. Journal of Chemical Physics 66: 4081-4091, 1977.

8. Lakowicz, R., Prendergast, F. G., and Hogen, D. Differential polarized phase fluorometric investigations of diphenylhexatriene in lipid bilayers. Quantitation of hindered depolarizing rotations. Biochemistry 18: 17-28, 1979.

9. Yonei, S., and Kato, M. X-ray induced structural changes in erythrocyte membranes studied by the use of fluorescent probes. Radiation Research 75: 31-45, 1978.

SYNAPTOSOMES AND MEMBRANES

Principal Investigator: C. E. Swenberg
Associate Investigators: A. Lunsford and M. J. McCreery

Rat cortex synaptosomal plasma membranes were made according to the method of Jones and Matus (1). Test tubes with equal volumes of synaptosomal plasma membranes (in phosphate buffer, pH 7.0) were placed in an ice bath and cobalt-60-irradiated with accumulative doses of 500 rads to 1 megarad (Mrad). Following irradiation, samples were labeled with 4-mal by incubation for 3 hr at room temperature. Excess spin label and free protein were removed by repeated centrifugation. Electron paramagnetic resonance (EPR) spectra were recorded using a Varian E-109 spectrometer operating at X-band in the absorption mode. The spectrometer was interfaced with a Nicolet 1180 computer for analyses of data.

The in-phase electron paramagnetic resonance spectra exhibited both immobilized and very mobile components. A typical spectrum is shown in Figure 1. An analysis of the room temperature EPR spectrum required at least three classes of spin-labeled sites. In the more restrictive two-component model, the intensity of both the strongly (S) and weakly (W) immobilized components and the W/S (peak height ratio) was found to decrease with increasing gamma dose. The apparent

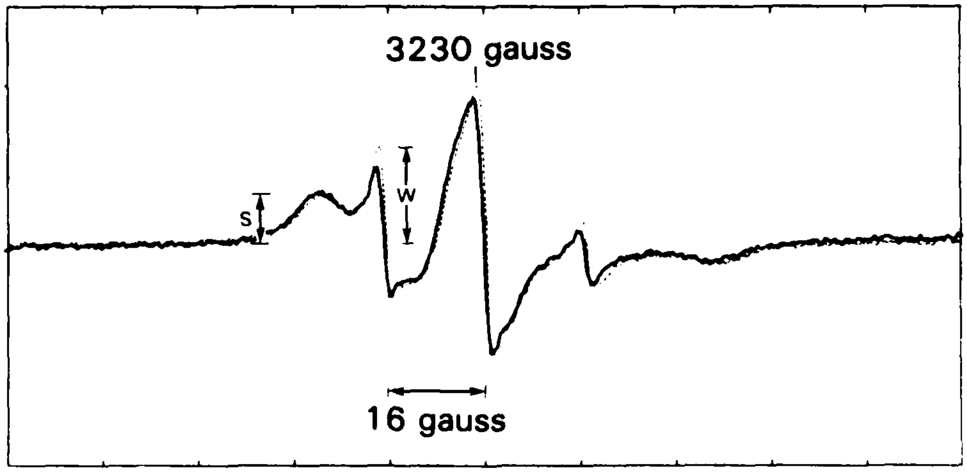

Figure 1. Effect of cobalt-60 irradiation on EPR spectrum of 4-mal spin labeled rat cortex synaptosomal plasma membranes (T = 25°C). Dotted line, control; solid line, 10 krads. Dotted curve shifted for visualization only. No g-shift detectable within experimental resolution. Spectrometer settings: 100 kHz; modulation amplitude = 1 gauss; time constant = 0.128 sec; scan time = 2 min, 10 scans; power = 10 mW; protein concentration 10 mg/ml.

conflict of these data with the reported increase in W/S for erythrocyte ghosts (2) (for doses greater than or equal to 1 Mrad) could be due to differences in the radiosensitivities of synaptosomal plasma membranes and erythrocyte ghosts. These differences between synaptosomal plasma membranes and erythrocyte ghosts deserve further study.

The labeled sulfhydryl moieties responsible for the W component presumably reside near the aqueous interface of the membrane, for this component is undetectable at -50°C due to pronounced line broadening. The more rapid decrease in intensity of W compared to S is consistent with theoretical assumptions that free radicals generated by ionizing radiation preferentially damage the more exposed sulfhydryl groups. At low microwave power (P), the integrated EPR signal (I) for equivalent protein concentrations is proportional to the total number of sulfhydryl sites labeled (N_{SH}) times the square root of the microwave power (P). Table 1 shows the reduction in N_{SH} with increasing cobalt-60 dose as inferred from the relationship $I = KN_{SH}\sqrt{P}$, where K is a constant of experimental design. Data for the nonirradiated sample were normalized to unity. Also reported is the decrease in the W/S ratio (non-integrated value, peaks heights only) with increasing total dose.

Table 1. Dependence of Labeled Sulfhydryl Sites (N_{SH}) and Disorder Parameter (W/S) on Cobalt-60 Irradiation Dose

Dose	Control	200 Rads	600 Rads	1 Krad	10 Krads	50 Krads	100 Krads
N_{SH}	1.0	0.87 ± 0.05*	0.87 ± 0.05	0.74 ± 0.05	0.87	-	-
W/S	1.0	0.92 ± 0.05	0.91 ± 0.05	0.93 ± 0.05	0.79 ± 0.05	0.67 ± 0.05	0.66

*Standard deviation (four separate experiments)

If corrections are imposed on the experimental EPR spectra to account for decreases arising from non-reactive sulfhydryl sites, then the resultant spectra still display different spectral parameters. This can be seen by measurements of the integrated intensity dependence of S and W on microwave power for a control and an irradiated sample after corrections for number of sites labeled (N_{SH}) have been imposed. The integrated intensity (I) dependence of the spectral components were fitted to the Bloch equation

$$I/N_{SH} = CT_2 \sqrt{P} /(1 + BPT_1T_2) \tag{1}$$

where C is a constant of experimental design, B is a known numerical constant, and T_1 and T_2 are the spin-lattice and spin-spin relaxation times. Figure 2 illustrates for both control and gamma-irradiated samples the saturated dependence of the integrated relative intensity of the deconvoluted EPR components on microwave power. All values of T_1 and T_2 reported in the figure are relative to the strongly immobilized component of the control sample since the constant C was not determined.

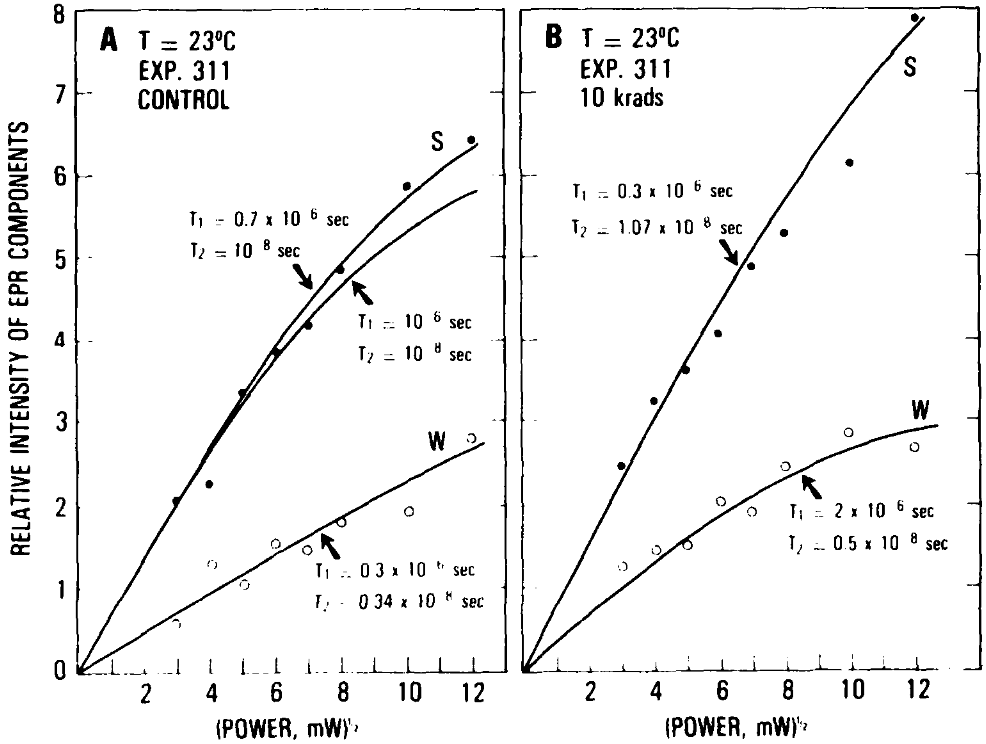

Figure 2. Integrated intensity dependence of spectral components S and W on microwave power. Solid lines are fits to equation 1.

REFERENCES

1. Jones, D. H., and Matus, A. I. Isolation of synaptic plasma membrane from brain by combined flotation-sedimentation density gradient centrifugation. Biochemical Biophysics Acta 356: 276, 1974.

2. Grezelinska, E., et al. A spin label study of the effect of gamma radiation on erythrocyte membrane. Influence of lipid peroxidation on membrane structure. International Journal of Radiation Biology 36: 325, 1979.

RADIATION-INDUCED MUSCULAR FATIGUE

Principal Investigator: M. J. McCreery
Associate Investigator: R. C. Lyon

Muscular fatigue is one of the most common symptoms experienced after therapeutic or accidental exposure to ionizing radiation. It is observed at almost all dose levels, has a short onset, and can be accompanied by other common symptoms of acute radiation sickness.

Laboratory animals subjected to exhaustive exercise showed increased fatigability and performance decrement following radiation exposure (1-2). However, the underlying mechanism of radiation-induced fatigue remains a mystery. Radiation may perturb the production and/or utilization of high-energy phosphates in contracting muscle. We have studied radiation-induced changes in muscle energetics by in vivo phosphorus-31 nuclear magnetic resonance (NMR) measurements of whole mice.

Following whole-body gamma irradiation, the presence of high-energy phosphates were monitored in resting and fatigued mice. Spectra were collected on a Nicolet NT 200 wide-bore pulse NMR spectrometer operating at 80.99 megahertz for phosphorus-31. A glass NMR tube

(inner diameter 23 millimeters) was modified by removing the closed end. Each mouse easily entered the tube and was restrained vertically from both ends by vortex plugs. The lower abdomen and hindquarters were positioned within the receiver coils of the probe. Phosphorus-31 spectra of whole mice are characterized by the six peaks shown in Figure 1.

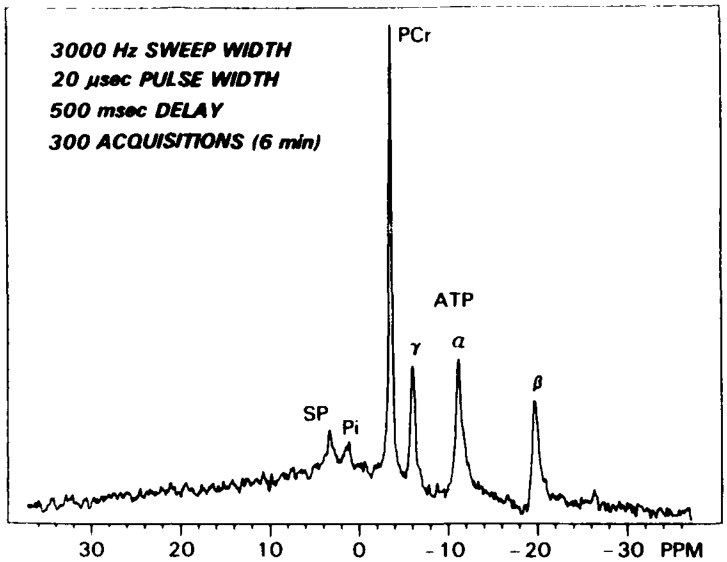

Figure 1. Phosphorus-31-NMR spectra of whole mouse. Parameters: 6000-Hz sweep width, 20-μsec pulse width, 0.5-sec delay, 300 pulses (6 min). Assignments: SP (sugar phosphates, 3.2 ppm), Pi (inorganic phosphate, 1.0 ppm), PCr (phosphocreatine, -3.7 ppm), α-ATP (-6.1 ppm), α-ATP (-11.3 ppm), β-ATP (-19.8 ppm), external reference H_3PO_4 (-1.2 ppm).

B6D2f1 mice (20-25 grams) received single 10-kilorad doses of cobalt-60 gamma irradiation bilaterally at 1 krad/minute. This resulted in a progressive weight loss (30% total) and 100% mortality in 5-6 days. Six-minute spectral accumulations were collected for each mouse at rest at 24 hr preirradiation and at 2, 24, 48, 72, and 96 hr postirradiation. Comparing the six spectra for each mouse, the total integrated intensity and the intensities of each peak remained unchanged at 24 hr preirradiation and 2, 24, 48, 72, and 96 hr post-irradiation. Comparing the six spectra for each mouse, the total integrated intensity and the intensities of each peak remained constant. A progressive increase in the phosphocreatine and γ-adenosine triphosphate (γ-ATP) line widths were observed in the post-irradiation spectra. Although the concentrations

remained constant, the immobilization of these phosphate compounds (increase in line width) indicates a major change in the molecular environment. Emaciation and dehydration may be primarily responsible for this effect. Similar increases in the phosphocreatine and γ-ATP line widths were observed for mice deprived of food and water for 3 days.

It was expected that the more pronounced effects of radiation on the levels of these high-energy phosphate compounds would be exacerbated in fatigued mice. Swimming was selected as a method of forced exercise since it constitutes an intense form of physical effort and since exhaustion is readily discernible. Each mouse was required to swim to exhaustion (2-8 min) in a 3-liter beaker filled with water. Immediately after the first failure to resurface, the mouse was rescued and placed in the NMR tube. The beginning of the first 1-min spectral accumulation occurred 30 $\pm$ 6 sec after rescue. One-minute accumulations were collected continuously up to 15 min postswim. The levels of each phosphate compound (integrated intensity) during the postswim recovery intervals were compared with the preswim levels. To avoid the effects of nutritional deficiencies that accrue with time, irradiated mice were swim-fatigued within 9 hr postirradiation.

Compared to control mice, within 9 hr following 10 krad whole-body gamma irradiation, the swim times for irradiated mice to reach exhaustion shortened by 30%. The irradiated mice had the same reduced level and rate of recovery of phosphocreatine and ATP following swim exhaustion. They had slightly elevated sugar phosphate, and slightly reduced inorganic phosphate levels during the first 3 min following swim exhaustion. As shown in Figure 2, during the first 2 min of recovery, the phosphocreatine levels in irradiated mice were significantly lower than in control mice. At the given dose of radiation it appears that (a) the swim-induced fatigue was exacerbated, (b) enzymatic conversion of phosphocreatine to ATP by creatine kinase was unaffected and oxidative phosphorylation was unperturbed based on the recovery of phosphocreatine, and (c) anaerobic glycolysis was partially inhibited (3).

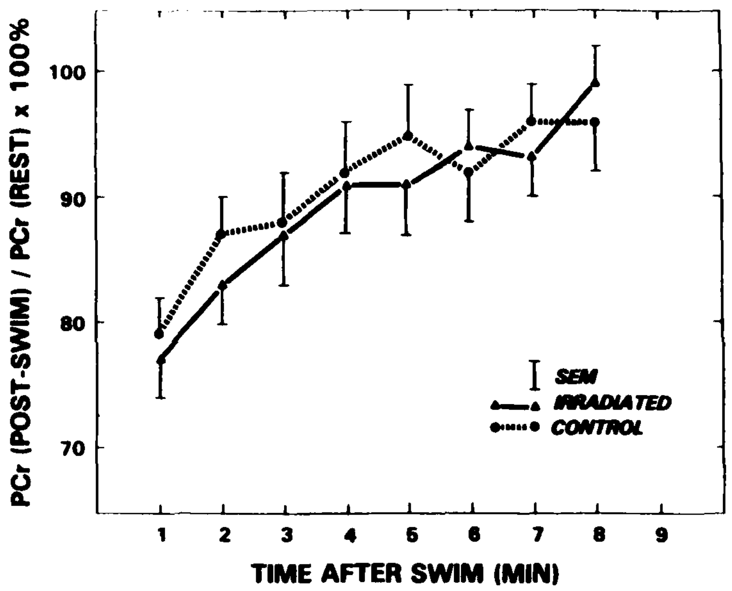

Figure 2. Post-swim levels of phosphocreatine for irradiated mice (n = 8) compared to control mice (n = 8). Points are means; error bars are SD.

REFERENCE

1. Haley, T. J., Flesher, A. M., Komesu, N., McCulloh, E. F., and McCormick, W. G. Effect of X-ray irradiation on muscle fatigue in rats. American Journal of Physiology 193: 355-359, 1958.

2. Kimeldorf, D. J., Jones, D. C., and Castanera, T. J. Effect of X-irradiation upon the performance of daily exhaustive exercise by the rat. American Journal of Physiology 174: 331-335, 1953.

3. Lyon, R. C., and McCreery, M. J. An in vivo study of radiation-induced fatigue in mice by phosphorus-31 nuclear magnetic resonance (NMR) spectroscopy. 7th International Congress of Radiation, Amsterdam, E3-06, 1983.

RADIATION-INDUCED CARDIOVASCULAR INJURY BY NUCLEAR MAGNETIC RESONANACE SPECTROSCOPY

Principal Investigator: M. J. McCreery
Associate Investigators: N. B. Joshi, A. L. Lunsford, C. E. Swenberg, and S. R. Yaffe

Nuclear magnetic resonance (NMR) spectroscopy is being used to study the metabolism of phosphate compounds in the functioning heart. Using isolated perfused heart, changes in the levels of adenosine 5'-triphosphate, creatine phosphate, and inorganic phosphate under different hemodynamic and pharmacologic conditions have been observed using phosphorus-31 NMR. The changes in intracellular pH of the heart were followed simultaneously in these experiments. The present studies were undertaken to investigate the radiation-induced perturbations to the production and utilization of high-energy phosphates in isolated perfused heart.

Hearts were perfused by Langendorff and by Morgan-Neely methods. Qualitatively, both preparations give similar results; however, the latter preparation is more versatile and has greater physiological relevance. The perfusion reservoirs, pressure columns, and the line between perfusion reservoir and heart are jacketed with water circulated at 37°C from a constant temperature bath. Krebs-Henseleit buffer (4.5% sodium chloride, 6.5% sodium bicarbonate, 19.1% magnesium sulphate, 5.75% potassium chloride, and 6.1% calcium chloride) with 2 millimolar (mM) pyruvate or 5 mM glucose were used to perfuse the heart. The perfusion buffer was oxygenated with a 95%-oxygen/5%-carbon dioxide mixture.

Ischemic heart conditions were created by clamping the perfusate inflow or by bubbling nitrogen gas through the perfusate reservoir. The isolated perfused heart was placed in an NMR tube (18 millimeters or 23 mm inside diameter) with a specially designed holder, and the NMR tube was then lowered into the NMR magnet to perform the measurements. The left atrium and aortic pressure was measured using a Gould pressure transducer and recorder. In the Langendorff method, the aortic pressure was kept at 100-120 centimeters (cm) of water, while in the Morgan-Neely method, the preload and afterload pressure were maintained at 10-20 cm and 80-100 cm of water, respectively. The gating pulse

to trigger the spectrometer from the pressure wave of the heart is accomplished with a WPI window discriminator and preset control.

Male rats of 300-400 grams were used in these experiments. Rats were irradiated to a fixed dose of 10 kilorads (krad) with cobalt-60 irradiation bilaterally at 1 krad/minute. They were anesthetized before the heart was excised. NMR measurements were performed using a Nicolet NT200, wide-bore pulsed NMR spectrometer operating at 80.99 megahertz for phosphorus-31.

NMR spectra were measured for control animals and for irradiated animals at 2, 24, and 48 hr post-irradiation. Typical NMR spectra for control and gamma-irradiated rat hearts are shown in Figure 1. Preliminary experiments indicate a progressive decline in total measurable phosphate levels in irradiated hearts. However, the creatine phosphate/adenosine 5'-triphosphate ratio showed an increase. These data suggest that the ionizing radiation perturbs the energy pathways of the heart. Experiments to confirm and extend these results are in progress.

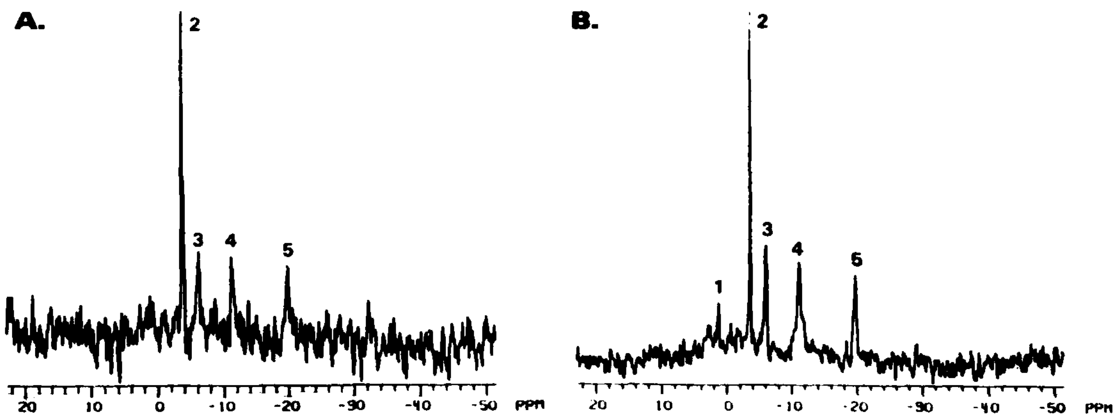

Figure 1. Phosphorus nuclear magnetic resonance spectra of Langendorff-perfused rat heart. A. Control. B. Cobalt-60-irradiated, 10 krads. Peak assignments: 1, inorganic phosphate; 2, creatine phosphate; 3, 4, 5 are, respectively, γ, α, and β peaks of adenosine 5'-triphosphate.

ELECTRON PARAMAGNETIC RESONANCE SPECTROSCOPY OF BONE AND TEETH

Principal Investigator: M. J. McCreery
Associate Investigators: A. J. Lunsford and C. E. Swenberg

It is well known that ionizing radiation induces paramagnetic centers in calcified tissues such as bones and teeth that can be detected by electron paramagnetic resonance (EPR) spectroscopy (1). Although short-lived radicals are produced in the cartilaginous phase of these tissues, the stable signals observed at room temperature are thought to derive from defects within their crystalline matrices (2). The major signal is an asymmetric singlet at $g = 2.0023$ whose origin is not known with certainty.

As part of our research program to assess the possibility of using the radiation-induced EPR signal intensity as a dosimeter, we have (a) measured the persistence of radiation-induced paramagnetic signals in in vivo bone, (b) measured the T_1 and T_m phase memory times for gamma-irradiated powdered hydroxyapatite, (c) theoretically calculated threshold atomic displacement probabilities for the constituents of bone, and (d) performed preliminary measurements of the EPR signal intensity at low electron irradiation (0.4 to 2.0 mega electronvolts, MeV) for different constituents of bone.

In Vivo Annealing of EPR Signal in Irradiated Rat Femurs

Eighteen male Sprague-Dawley rats, each weighing about 200 grams, were killed by halothane inhalation. The femurs from each animal were removed surgically and cleaned of most of the attached connective tissue and muscle. These bones were placed in labeled test tubes, sealed with parafilm, and irradiated with 10 kilorads of cobalt-60 gamma rays at a dose rate of 500 rads/minute. The exposure was performed bilaterally, making sure that the long axis of all bones was oriented perpendicular to the radiation field.

Dosimetric measurements were performed using ionization chamber techniques. After exposure, each of 15 irradiated right femurs were surgically implanted in the peritoneal cavity of a host rat under aseptic conditions. The corresponding left femur from each pair was placed aseptically into a sterile test tube, sealed, and placed in a constant-temperature bath at 37°C. The remaining six bones were put into labeled test tubes and placed in

a freezer at -10°C. The implanted bones and the corresponding 37°C contralateral bones were divided into five groups of three each for examination after the following time periods: 1 week, 2 weeks, 4 weeks, 6 weeks, and 8 weeks. The EPR spectra of the remaining six bones were measured the next day for control values and then returned to the freezer for storage. Each of these bones was also measured after each of the time periods to compare signal decay of the experimentally implanted bones with those stored at -10°C. The two remaining bones were kept at -10°C for the entire 8-week period and then analyzed as an additional control.

Results indicated that although there is some variance, the average value for the control bones does not indicate a change in amplitude within the 8-week period (Figure 1). A decrease in signal of the implanted bones relative to control during the same time period was observed. However, subjecting these data to a one-tailed t test showed that only the data after weeks 2, 4, and 8 are statistically less than their controls, using the criterion of p values less than 0.05. The percent decreases relative to controls after these elapsed times are 28%, 35%, and 61%, respectively. The variance of the data does not permit calculation of a meaningful rate constant of signal decay. Unlike previous studies, these results indicate a significant decrease in the radiation-induced EPR signal in bone, but this signal is still present after 8 weeks.

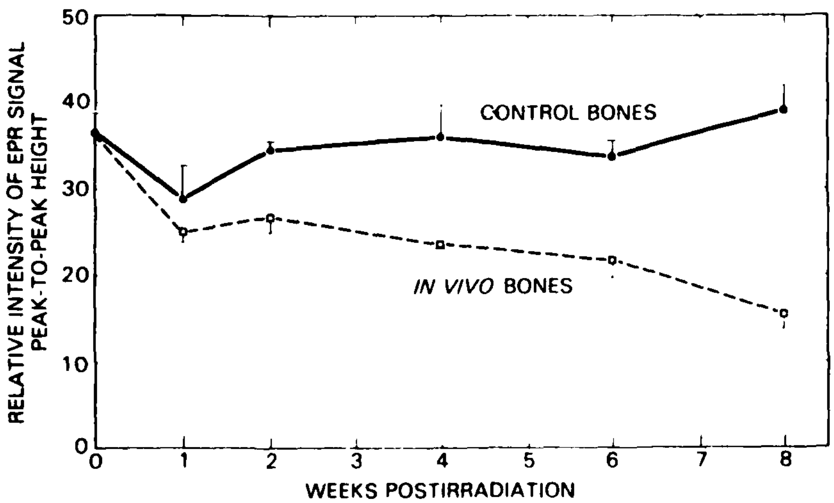

Figure 1. Mean values for four control bones (●) and three *in vivo* bones per group (○). Bars indicate standard errors. Spectrometer settings: sweep width, 100 gauss; field set, 3330 gauss; microwave frequency, 9 GHz; microwave power, 20 mW; modulation amplitude, 2 gauss at 100 kHz; time constant, 0.064 sec. Diphenylpicrylhydrazyl was used to calibrate the spectrometer.

The reason for the inconsistency of results among the reported studies is not clear; it may be the difference in experimental design. In the Slager et al. study, the implanted bone was grafted onto a dog radius as a cortical inlay. This would naturally stimulate bone metabolism, which is necessary for restructuring of the mineral deposit architecture and healing. An increased rate of decay of the radiation-induced radical defects would be expected. Koberle et al. irradiated rat tail vertebrae with 18,000 rads and found no change in signal amplitude within 21 days. However, this dose can cause significant necrosis of the vascular bed, so it is questionable how well these vertebrae were perfused during the experimental period. The implanted bones in our study were well perfused and were not physically damaged to stimulate new growth. Therefore, we believe that our results reflect more accurately the decay of radiation-induced signals in in vivo bone (3).

Spin Lattice and T_m Phase Memory Time of EPR Signal

Both the spin lattice relaxation time (T_1) and the phase memory time (T_m) of the main EPR signal at $g = 2.002$ have been measured for hydroxyapatite powder for two different gamma-irradiated samples (10 and 20 kilorads). The experiments were performed in collaboration with Dr. Michael Bowman, Department of Chemistry, Argonne National Laboratory. T_m was measured using the 90-180 Hahn sequence, and T_1 was measured by a 180 inverting pulse with magnetization monitored using a 90-180 echo. Results indicate that both T_1 and T_m were independent of total dose as expected, and T_1 = 9.0 microseconds (μsec) and T_m = 0.92 μsec. By operating in a pulse mode, at least 200 scans per second are possible; this should improve EPR signal to noise with shorter acquisition time for low doses of ionizing radiation.

Energy Threshold Response for Atomic Displacement

In order to improve understanding of the defects responsible for the radiation-induced EPR signal, a simple calculation has been performed to investigate if the displacement of any particular ion type in hydroxyapatite is the source of the room-temperature EPR signal. These calculations were performed in collaboration with Professor A. Damask, Department of Physics, Queens College, New York. As a function of electron energy bombardment, the atomic displacement cross section σ_i of each constituent (hydrogen, carbon,

oxygen, hydroxyl, phosphorus, and calcium) was calculated, and the expected EPR signal intensity was calculated, assuming a maximum transfer energy of 25 electronvolts. The calculations indicate that if no EPR signal is observed after a 0.4-MeV electron irradiation but a signal is present after a 2-MeV irradiation, then the EPR signal in hydroxyapatite must arise from displaced phosphorus or calcium ions and not from hydrogen, oxygen, or hydroxyl. This is because for the former, the number of ion displacements increases with dose whereas for the latter, the number does not increase. Using the Klein-Nishina equation, the total cross sections for hydrogen, oxygen, phosphorus, and calcium produced by cobalt and cesium gamma ray irradiation were collected. For an equal number of photons, differences in the $\sigma_K(Co)$ and $\sigma_K(Cs)$ for the displacement of different constituents are expected. Results of the analysis are summarized in Table 1. This table indicates that by comparing the EPR signals induced by different gamma sources, it should be possible to identify the ion(s) responsible for the EPR signal at g = 2.002. Experiments are being performed to test the validity of these calculations.

Table 1. Theoretical Atomic Displacement Cross Sections for Cobalt (Co) and Cesium (Cs) Irradiations for Hydroxyapatite

Element	$\sigma_K(Co)$	$\sigma_K(Cs)$	$\sigma_K(Co)/\sigma_K(Cs)$
Hydrogen	0.316×10^{-25} cm^2	0.132×10^{-25} cm^2	2.4
Oxygen	0.413×10^{-23} cm^2	0.770×10^{-24} cm^2	5.4
Phosphorus	0.153×10^{-23} cm^2	0.120×10^{-24} cm^2	12.8
Calcium	0.312×10^{-23} cm^2	0.117×10^{-24} cm^2	26.7

REFERENCES

1. Ostrowski, K., et al. Stable radiation-induced paramagnetic entities in tissue mineral and their use in calcified tissue research. In: Free Radicals in Biology, Volume IV. Pryor, W. A., ed. Academic Press, New York, 1980.

2. Ostrowski, K., and Dzodyic-Goclawska, A. Electron spin resonance spectroscopy in investigations in mineralized tissues. In: The Biochemistry and Physiology of Bone, Chapter 7. Bourne, G. M., ed. Academic Press, New York, 1976, pp. 303-327.

3. McCreery, M. J., Johnson, G. A., Swenberg, C. E., and Lunsford, A. E. Persistence of radiation-induced paramagnetic signals in in vivo bone. 7th International Congress of Radiation, Amsterdam, 1983, E3-07.

INDEX TO PRINCIPAL INVESTIGATORS

Alter, W. A., III 24,25
Amende, L. M. 47,53
Blake, P. K. 155,157,168
Bogo, V. 8,9
Braitman, D. J. 122,123
Buchanan, G. M. 92
Burghardt, W. F., Jr. 7
Casey, L. C. 78
Catravas, G. N. .. 21,24,25,26,34,38,40,42, 44,47,49,51,55,57,59,61
Chantry, K. H. 9
Chock, E. S. 51
Chock, S. P. 61
Christopher, J. P. 37,44
Cockerham, L. G. 119,120
Conklin, J. J. 68,74,76,77
Court, L. 21
Dalton, T. K. 11
Darden, J. H. 21
Daxon, E. E. 162
Devine, R. T. 149,158
Donlon, M. A. 47,49,51,53,55,57, 59,61,119,120
Dooley, M. A. .. 153,155,161,163,165,168
Dorval, E. D. 142
Doyle, T. F. 24,25,119,120
Dubois, A. 141
Durakovic, A. 131,133,135,138,142
Ege, G. N. 146
Eng, R. R. 144,147
Ferlic, K. P. 162
Fink, M. P. 68,74,76,78
Fiori, C. E. 51
Franz, C. G. 15
Freschi, J. E. 125
Gallin, E. K. 110,112,114
Giambarresi, L. I. 42
Gourmelon, P. 21
Gray, B. 99
Green, S. W. 114
Gruber, D. F. 68,74,76,96
Gunter-Smith, P. J. 117
Hagan, M. P. 100,102,103
Hale, M. L. 62,63
Hawkins, R. N. 24,25,121
Helgeson, E. A. 49,55
Hill, T. A. 8
Holahan, E. V. 103
Hunt, W. A. 7,11,12,14
Jackson, W. E. 15
Jacobs, A. J. 27,29,31
Jacocks, H. M., III 102
Kearsley, E. E. 168
Kelleher, D. L. 53
Ledney, G. D. 93
Levin, S. G. 15
Livengood, D. R. 107
MacVittie, T. J. 21,68,71,74,76,77,78
May, L. 59
McCarthy, K. F. 62,63
McClain, D. E. 57,59,61
McCreery, M. J. 170,178,182,184
Mestries, J. C. 21
Mickley, G. A. 9
Millar, D. B. 44
Monroy, R. L. 21,68,71,80,82
Moore, M. L. 161
Moran, A. 115
Mullin, M. J. 14
Murano, G. 77
Nold, J. 8
Past, M. R. 37
Patchen, M. L. 68,74,76,86
Pellmar, T. C. 128
Rabin, B. M. 12
Reddi, A. H. 62
Sessions, G. R. 9
Sheehy, P. A. 112,114
Speicher, J. 44
Steel, L. K. 26,34,38,40,55
Sweedler, I. K. 40
Swenberg, C. E. 175
Takenaga, J. K. 24
Vigneulle, R. M. 84
Walden, T. L. 26
Walker, R. I. 74,77
Weinberg, S. R. 88,89,90,91,98
Weiss, J. F. 27,29,31
Young, R. W. 15
Zeman, G. H. .. 149,151,153,155,157,158, 161,162,163,165,167,168